

Institute of Molecular Immunology, Helmholtz Center Munich

Acting director: Prof. Dr. med. Ralph Mocikat

**Chimeric co-stimulatory receptors as a strategy to
improve the performance of T cells in the tumor
environment**

Turning PD-1-mediated inhibition into activation

Dissertation to obtain the Doctorate in Natural Sciences

at the Faculty of Medicine

Ludwig-Maximilians-University Munich



submitted by

Ramona Schlenker

from Jena

2015

**Printed with permission of the Faculty of Medicine
Ludwig-Maximilians-University Munich**

Supervisor:	Prof. Dr. rer. nat. Elfriede Nößner
Co-supervisor:	Prof. Dr. rer. nat. Ludger Klein
Dean of the faculty:	Prof. Dr. med. dent Reinhard Hickel
Date of oral examination:	12.10.2015

To my parents

Stefanie & Reiner Schlenker

CONTENT

1	SUMMARY	1
2	ZUSAMMENFASSUNG	3
3	INTRODUCTION	5
3.1	Innate and adaptive immunity.....	5
3.1.1	CD8+ T cell characteristics and repertoire selection	5
3.1.2	T cell receptor and co-stimulatory signaling	6
3.2	T cell therapy for cancer	9
3.3	Tumor strategies to evade T cell cytotoxicity	12
4	OBJECTIVE OF THIS THESIS.....	15
5	MATERIAL	16
5.1	Consumables and equipment.....	16
5.2	Reagents, kits and bacteria	19
5.2.1	Reagents.....	19
5.2.2	Kits	21
5.2.3	Bacteria	21
5.3	Media and buffers.....	22
5.3.1	Basic media and buffers	22
5.3.2	Prepared media and buffers	22
5.4	Plasmids, primers and restriction enzymes	25
5.4.1	Plasmids.....	25
5.4.2	Primers.....	27
5.4.3	Restriction enzymes.....	28
5.5	Chimeric receptor sequences	29
5.5.1	Human chimeric receptor DNA sequences.....	29
5.5.2	Murine chimeric receptor DNA sequence	35
5.6	Antibodies for cell culture and flow cytometry analyses.....	36
5.6.1	Antibodies with anti-human specificities for cell culture.....	36
5.6.2	Antibodies with anti-human specificities for flow cytometry	36
5.6.3	Antibodies with anti-mouse specificities for cell culture	37
5.6.4	Antibodies with anti-mouse and anti-rabbit specificities for flow cytometry.....	37
5.7	Primary cells and cell lines	38
5.8	Blood samples	39

5.9	Patient samples	40
5.10	Mice	40
5.10.1	NSG mice	40
5.10.2	LoxP-TAg mice	41
6	METHODS	42
6.1	Molecular biology methods	42
6.1.1	Cloning of chimeric co-stimulatory receptors into pGEM and pMP71 vectors	42
6.1.2	Generation of in vitro transcribed RNA from pGEM plasmids	44
6.2	Cell culture techniques	45
6.2.1	Cultivation of human and murine cell lines and primary cells	45
6.2.2	Thawing, counting and freezing of cells	46
6.2.3	Isolation of peripheral blood mononuclear cells from human blood samples	46
6.2.4	Isolation of TILs from human renal cell carcinoma	47
6.2.5	Transduction of human T cells	47
6.2.6	Electroporation of human T cells and TILs	49
6.3	Functional assays	50
6.3.1	Loading of P815 with OKT3, anti-CD28 or PD-L1/Fc chimera	50
6.3.2	Co-culture of human T cells or TILs with target cells	50
6.3.3	Chromium release assays	51
6.3.4	Detection of cytokines by enzyme-linked-immunosorbent assays (ELISA)	52
6.3.5	Detection of cytokines by Bio-Plex analysis	53
6.4	Flow cytometry	54
6.4.1	Principle of flow cytometry	54
6.4.2	Staining of cell surface and intracellular markers	56
6.4.3	Staining combinations and gating strategies	57
6.4.4	Staining of phosphorylated signaling proteins	62
6.5	Cell sorting	64
6.5.1	Principle of cell sorting using FACS Aria IIIu	64
6.5.2	Sorting of T cells from human renal cell carcinoma TILs	64
6.6	Mouse models	66
6.6.1	Human melanoma xenograft NSG model	66
6.6.2	Hepatocellular carcinoma model	68
6.7	Statistical analyses	71
7	RESULTS	72
7.1	Design and expression of chimeric co-stimulatory receptors	72
7.1.1	Design of chimeric co-stimulatory receptors	72
7.1.2	Expression of chimeric receptors	74

7.2	PD-1:28 tm - and PD-1:cys28 tm -engineering of T cells enhanced TCR-mediated IL-2 and IFN- γ secretion	80
7.3	Ligation of PD-1:28 tm and PD-1:cys28 tm chimeric receptors increased TCR-mediated phosphorylation of extracellular signal regulated kinase and ribosomal protein S6.....	84
7.4	PD-1:28 receptors upgraded low-avidity T cells to approximate the cytokine response of high-avidity T cells	86
7.5	PD-1:28 receptors had no effect on tumor cell lysis	88
7.6	PD-1:28 tm reinstated IFN- γ secretion in unresponsive tumor-infiltrating lymphocytes from human renal cell carcinoma	89
7.7	PD-1:28 tm expressing T cells showed no aberrant cell expansion.....	91
7.8	PD-1:28 tm expression enhanced T cell proliferation in the microenvironment of a human melanoma xenograft.....	92
7.9	PD-1:28 tm did not affect survival in an autochthonous hepatocellular carcinoma mouse model but suppressed Th2+Th17 polarization of TILs	97
8	DISCUSSION.....	106
8.1	Design influences chimeric receptor expression	107
8.2	PD-1:28 chimeric receptors can enhance functionality of human T cells and restore tumor-inhibited TIL function.....	108
8.3	In vivo studies support the therapeutic potential of the PD-1:28 receptor..	111
8.4	Outlook.....	115
9	ABBREVIATIONS	116
10	REFERENCES	119
	ACKNOWLEDGEMENTS	128
	CURRICULUM VITAE.....	130
	PUBLICATIONS.....	131
	AFFIDAVIT.....	132

1 SUMMARY

Adoptive cell therapy using tumor-infiltrating lymphocytes (TILs) has yielded remarkable response rates in melanoma patients. This treatment cannot be easily applied to other tumor entities as isolation of TILs and their expansion is not always possible. The transfer of genetically engineered T cells can overcome the limitations of TIL therapy. However, clinical trials reported response rates lower than expected. The drawbacks of adoptive T cell therapy include short persistence and loss of function of transferred T cells. Co-stimulation can enhance T cell proliferation and survival and can restore cytotoxicity. As effector T cells are largely CD28 negative and most epithelial tumors do not express CD80 or CD86, T cells cannot receive co-stimulation in the tumor environment. In this thesis, a strategy was developed to facilitate co-stimulation of T cells in the tumor environment independent on CD28-CD80/86 interaction. Chimeric receptors were designed based on joining the PD-1 extracellular domain with the intracellular signaling domains of CD28 or 4-1BB. The chimeric receptors should initiate a co-stimulatory signal when ligated by PD-L1, which is highly expressed in most tumor environments.

The results demonstrate that T cells can be engineered to express the chimeric receptors whereby those receptors with the intracellular domain of CD28 were found to be better expressed than those with the 4-1BB signaling domain. PD-1:28 engineered T cells showed enhanced cytokine secretion (IL-2 and IFN- γ) and stronger TCR signaling (phosphorylation of ERK and RPS6) when stimulated with PD-L1 expressing target cells.

PD-1:28 engineering upgraded low-avidity T cells enabling them to secrete cytokine at levels comparable to high-avidity T cells when stimulated with PD-L1 positive target cells. This result is of specific interest for potential clinical application, since it suggests that PD-1:28 engineering of T cells might be a strategy to increase the anti-tumor activity of T cells without modifying the T cell receptor affinity and risking loss of specificity.

Furthermore it could be demonstrated that PD-1:28 engineering of anergic TILs from human renal cell carcinoma enabled them to secrete anti-tumoral IFN- γ indicating that PD-1:28-mediated co-signaling can overcome tumor-inflicted functional unresponsiveness.

Finally, using in vivo tumor models, it was observed that chimeric PD-1:28-expressing T cells proliferated more strongly in a human melanoma xenograft model and were resistant to the induction of a tumor-promoting Th2 cytokine profile in an autochthonous hepatocellular carcinoma model.

2 ZUSAMMENFASSUNG

Durch adoptiven Transfer von tumorinfiltrierenden Lymphozyten (TIL) können bemerkenswerte Ansprechraten in Melanompatienten erzielt werden. Diese Art der Therapie kann jedoch nicht bei allen Tumorentitäten angewandt werden, da die Isolierung von TIL und deren Expansion nicht immer möglich ist. Verwendet man T-Zellrezeptor-transgene T-Zellen, so kann man diese Einschränkungen umgehen, die erzielten Ansprechraten waren jedoch geringer als erwartet. Eine geringe Persistenz sowie der Funktionsverlust der transferierten T-Zellen können für den geringen Therapieerfolg verantwortlich sein. Kostimulation kann die Proliferation und das Überleben sowie die zytotoxische Aktivität von T-Zellen verbessern. Jedoch verlieren Effektor-T-Zellen ihre CD28 Expression und die meisten Karzinome exprimieren weder CD80 noch CD86. Ziel dieser Arbeit war es, eine Strategie zu entwickeln, die eine von der CD28-CD80/CD86-Interaktion unabhängige Kostimulation von T-Zellen im Tumormilieu ermöglicht. Dazu wurden chimäre Kostimulationsrezeptoren entwickelt, die aus der extrazellulären Domäne von PD-1 und der intrazellulären Signaldomäne von entweder CD28 oder 4-1BB bestehen. Diese chimären Rezeptoren sollten ein kostimulatorisches Signal in der T-Zelle auslösen, wenn die extrazelluläre PD-1-Domäne an PD-L1 bindet.

Es wurde beobachtet, dass chimäre Kostimulationsrezeptoren mit der CD28-Domäne besser exprimiert werden als solche mit der 4-1BB-Domäne. Weiterhin konnte gezeigt werden, dass T-Zellen, die PD-1:28 Rezeptoren exprimierten und mit PD-L1 positiven Zielzellen stimuliert wurden, mehr Zytokin (IL-2 und IFN- γ) sezernierten und die T-Zellrezeptor-Signalkaskade stärker aktivierten (erhöhte Spiegel an phosphoryliertem ERK und RPS6) als vergleichbare T-Zellen ohne PD-1:28.

Weiterhin wurde beobachtet, dass niedrig-avide T-Zellen durch PD-1:28 vergleichbar hohe Zytokinspiegel sezernieren konnten wie hoch-avide T-Zellen. Gentechnisches Engineering mit chimären Kostimulationsrezeptoren könnte also eine Strategie sein, um die Funktion von niedrig-aviden T-Zellen zu erhöhen, ohne die T-Zellrezeptoraffinität zu verändern und dadurch Spezifitätsverlust zu riskieren.

Weiterhin konnte gezeigt werden, dass Engineering von anergen TIL aus humanem Nierenzellkarzinom mit PD-1:28 die TIL dazu befähigte, IFN- γ zu sezernieren, wenn

sie mit PD-L1 positiven Zielzellen stimuliert wurden. Offensichtlich kann die Kostimulation über PD-1:28 Rezeptoren den tumor-induzierten Funktionsverlust von TIL überwinden.

Letztendlich konnten auch in In-vivo-Tumormodellen T-Zell-unterstützende Effekte von PD-1:28-vermittelter Kostimulation gezeigt werden. So wurde in einem Melanom-Xenograftmodell beobachtet, dass PD-1:28-exprimierende T-Zellen im Tumormilieu besser proliferieren. In einem autochthonen hepatozellulären Karzinommodell wurde gezeigt, dass der adoptive Transfer von PD-1:28-exprimierenden T-Zellen die Th2-Polarisierung von TIL im Tumormilieu verhindert.

3 INTRODUCTION

3.1 Innate and adaptive immunity

The immune system provides protection from toxins, infectious microorganisms and endogenous degenerated cells. Epithelial tissues form a barrier to separate the body from its environment. Antimicrobial substances within these epithelia are the first line of immune defense. If infectious microorganisms or toxins cross this barrier they are confronted by soluble and cellular components of the innate immune system. Soluble components, like the complement system, mark invaders as foreign to facilitate their recognition and elimination by cellular components. The main cellular components of innate immunity are natural killer cells, dendritic cells (DCs), macrophages and granulocytes. Granulocytes and macrophages phagocytize and digest microorganisms. NK cells can directly lyse infected or degenerated cells by disrupting their membranes and transferring lytic enzymes. The cross-talk between NK cells and DCs leads to a reciprocal enhancement of functionality. DCs are the connective element between innate and adaptive immunity. They induce the differentiation of naïve T cells into effector cells by presenting pathogen- or tumor-derived epitopes on major histocompatibility molecules (MHC). T cells together with B cells represent the cellular components of adaptive immunity. CD4⁺ T cells function as helper cells by producing stimulatory and regulatory cytokines. CD8⁺ T cells act as cytolytic T cells with the capacity of direct target cell elimination (1).

3.1.1 CD8⁺ T cell characteristics and repertoire selection

T cells derive from a lymphoid progenitor and complete their development in the thymus. Naïve T cells leave the blood stream through high endothelial venules and enter secondary lymphoid organs. Antigen presenting cells (APCs) residing in peripheral tissues also migrate to these organs and carry antigens from self-proteins, altered self-proteins, mutations or infectious encounters. CD8⁺ T cells recognize peptides presented on MHC class I molecules by APCs. MHC class I molecules consist of an α -chain non-covalently linked to β_2 -microglobulin and are expressed on all nucleated cells. MHC-I present peptides produced by the cell itself and are hence

very important for the elimination of virus-infected and degenerated cells. The recognition of the peptide-MHC complex (pMHC) is mediated through the T cell receptor (TCR). The TCR is a heterodimer consisting of an α - and a β -polypeptide chain. The variable region of the TCR determines its specificity and the constant region translates cognate pMHC binding into a stimulatory signal. The specificity of a T cell is determined by the amino acid sequence of the TCR's variable region (v-region). The complementarity determining regions (CDR) 1-3 within the v-region are implicated in antigen binding. Their amino acid sequence is assembled from different gene segments during the development of a T cell in the thymus. Only CD8⁺ T cells recognizing endogenous MHC class I molecules receive a survival signal (positive selection). In a second (negative) selection, CD8⁺ T cells recognizing self-derived epitopes are deleted from the repertoire. These selection processes lead to the development of a self-MHC-restricted T cell pool tolerant to self but capable of recognizing foreign harmful structures and degenerated or infected endogenous cells.

Ligation of the TCR by cognate pMHC initiates a signaling cascade leading to differentiation of naïve T cells into effector cells if in addition to the TCR signal (signal 1), a second co-stimulatory signal (signal 2) is provided. Additionally, the cytokine milieu (signal 3) shapes the strength and polarization of the differentiation.

Once activated, CD8⁺ effector T cells can exert various functions. By expression of Fas ligand, they can induce apoptosis in cells expressing the Fas receptor. Moreover, CD8⁺ effector T cells can permeabilize the cell membrane of target cells by perforin and release proteases into target cells. Those proteases activate caspases leading to apoptosis. Through secretion of cytokines such as interferons activated T cells can enhance MHC class I expression and inhibit viral replication (1).

3.1.2 T cell receptor and co-stimulatory signaling

The TCR is associated with CD3 proteins, which are essential to communicate the TCR/pMHC interaction to the cell interior. Immunoreceptor tyrosine-based activation motifs (ITAMs, YxxL) within the intracellular domains of all CD3 proteins (CD3 γ , CD3 δ , CD3 ϵ and CD3 ζ) translate pMHC binding into a stimulatory signal (figure 1). Tyrosine residues within the ITAMs are phosphorylated by leukocyte C-terminal Src kinase (Lck) and Fyn kinase when the TCR recognizes the presented epitope. CD3 ζ

binds to phosphorylated ITAMs and is activated by phosphorylation, which recruits “CD3 ζ associated protein of 70 kDa” (ZAP-70). ZAP-70 transmits the activatory signal to “linker for activation of T cells” (LAT) and “SH2 domain-containing leukocyte protein of 76 kDa” (SLP-76). Both LAT and SLP-76 in return activate various signaling molecules such as phospholipase C- γ (PLC- γ). PLC- γ cleaves phosphatidylinositol-3,4-bisphosphate (PIP₂) creating second messenger molecules inositol-1,4,5-trisphosphate (IP₃) and diacylglycerol. IP₃ induces calcium release by binding to the endoplasmic reticulum. The induced increase in calcium opens calcium release-activated calcium channels in the plasma membrane further enhancing the intracellular concentration of calcium through influx of calcium from the extracellular space. Calcium-calmodulin complexes form and activate the phosphatase calcineurin. Calcineurin dephosphorylates “nuclear factor of activated T cells” (NFAT). This transcription factor in concert with transcription factors AP1 and “nuclear factor of kappa light polypeptide gene enhancer in B cells” (NF κ B) promotes the transcription of cytokines including interleukin-2 (IL-2) and interferon- γ (IFN- γ). NF κ B is activated by translocation to the nucleus through protein kinase C- θ (PKC- θ), which is activated by the second messenger DAG. NF κ B induces transcription of cytokines and anti-apoptotic proteins such as Bcl-2 and Bcl-xL. AP-1 is generated by activation of “mitogen activated protein” (MAP) kinase pathway specifically “extracellular signal related kinase” (ERK), which requires DAG. ERK signaling, moreover, facilitates degranulation, a process that is required for cytotoxic activity (1, 2).

The second, co-stimulatory, signal required for optimal development of effector function, is mediated through the receptor CD28 on T cells. Co-stimulation converges with and enhances TCR signaling leading to superior effector function in addition to cell proliferation, protein translation and T cell survival (figure 1). CD28 is expressed on the surface of T cells as a homodimer. In humans, around 50% of naïve CD8+ T cells express CD28. During the differentiation from naïve into effector into terminally differentiated cells human CD8+ T cells lose CD28 expression (3).

The co-stimulatory ligands CD80 and CD86 have restricted expression patterns primarily limited to APCs. CD28 contains an intracytoplasmic signaling domain with the motifs YMNM, PRRP and PYAP. CD28 interaction with CD80 or CD86 leads to phosphorylation of the YMNM motif and recruitment of the p85 subunit of “phosphatidylinositol-4-phosphate 3-kinase” (PI3K) to the plasma membrane, which

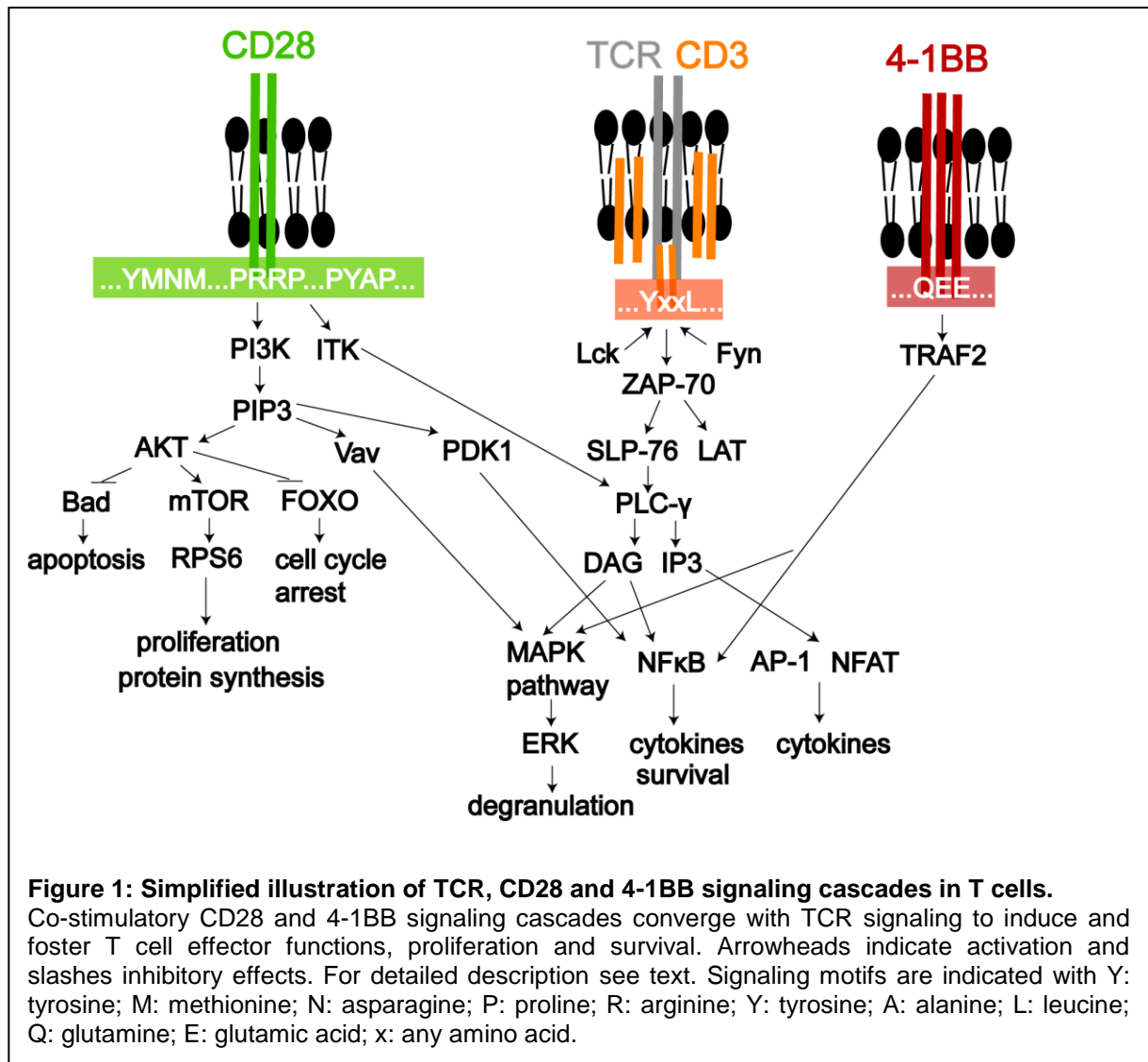
produces phosphatidylinositol-3,4,5-triphosphate (PIP3). PIP3 recruits pleckstrin homology domain containing proteins such as “phosphoinositide-dependent kinase 1” (PDK1), “protein kinase B” (AKT), and the guanine nucleotide exchange factor Vav. AKT activates the “mechanistic target of Rapamycin” (mTOR) signaling pathway leading to phosphorylation of “40S ribosomal protein S6” (RPS6). RPS6 is implicated in protein synthesis and T cell proliferation (4). Additionally, AKT inhibits the transcription factor “forkhead box protein” (FOXO), which transcribes genes leading to cell cycle arrest, and inhibits pro-apoptotic proteins such as “Bcl-2 associated agonist of cell death” (Bad) (5).

PDK1 enhances NFκB activity and Vav augments the MAPK pathway. Both PDK1 and Vav are additionally activated through the PYAP motif.

The “IL-2-inducible T cell kinase” (ITK) binds the CD28 motif PRPP and activates PLC-γ. The CD28 pathway converges with those TCR signals that lead to T cell proliferation and T cell effector functions such as cytokine secretion and degranulation (1, 5).

4-1BB (CD137) is another co-stimulatory receptor capable of augmenting TCR signaling. 4-1BB is a member of the tumor necrosis factor receptor (TNFR) superfamily and is absent in naïve T cells but induced following T cell stimulation (6). The expression peaks within 48-72 hours after activation. Signals transmitted through 4-1BB have been shown to have the greatest impact on sustaining immune responses - in contrast to CD28, which is required for initial activation of naïve T cells (6, 7).

The intracellular domain of 4-1BB contains the QEE motif, which, upon ligation with 4-1BBL, expressed on APCs, recruits TNFR associated factor 2 (TRAF2) (8, 9). TRAF2 activates MAPK pathways including ERK and activates nuclear translocation of NFκB (10). It thereby enhances cytokine production and T cell survival (figure 1).



3.2 T cell therapy for cancer

T cells with anti-tumor specificities are found within the tumor and can be isolated, cultivated *ex vivo* and re-infused into the patient (11). This so called adoptive therapy (ATT) with tumor-infiltrating lymphocytes (TILs) can yield durable remission in patients with metastatic cancer who are refractory to other cancer-related therapies (12). The clinical response has been shown to be closely linked to an anti-tumor activity of the TILs that are used for ATT (13). Shorter *ex vivo* cultivation of TILs and pre-conditioning patients before ATT using non-myeloablative lymphodepleting chemotherapy and radiation further enhanced response rates (13, 14). Lymphodepletion eliminates T and B cells and thereby reduces the competition of

transferred TILs with endogenous lymphocytes for cytokines. In addition, it reduces the amount of regulatory T cells, which might counteract the effect of TILs (15). In clinical trials with metastatic melanoma patients, response rates of up to 56% are reported (16). The drawbacks of TIL therapy are the requirement of specialized centers with the capability of T cell culture, the fact that tumor-reactive TILs cannot always be isolated and that some TILs cannot be sufficiently expanded.

The limitations of TIL availability can be overcome by the generation of tumor-reactive T cells using genetic engineering techniques. Thereby, peripheral T cells or other T cells are genetically engineered to express a tumor-specific TCR or chimeric antigen receptor. In one of the first clinical trials Morgan et al. reported in 2006 (17) that transfer of autologous T cells engineered with a TCR specific for “melanoma antigen recognized by T cells 1” (MART-1) achieved a response rate of 13%. An explanation for the rather low response rate compared to TIL therapy might be that transferred TIL populations are composed of T cells with specificities against various tumor antigens (18), while TCR-engineered T cells carry only one specificity, which narrows their anti-tumor capacity to those cells expressing the target antigen. In addition, the strength of the engineered TCR might not have been sufficient. The strength of the interaction between a single pMHC and one TCR is described by the so-called TCR affinity (19). However, as one T cell carries around 40,000 TCR molecules (20), T cell avidity seems to be the more suitable characteristic. Avidity is defined as the strength of the binding of multiple pMHCs and TCR molecules (19). In a clinical trial of metastatic melanoma patients receiving T cells engineered to express a MART-1 specific TCR it was observed that T cells of high avidity yielded higher response rates (30%) compared to T cells of lower avidity (13%) (21). The explanation for the better clinical responses might be stronger activation of the TCR signaling cascade (22) and more efficient recruitment of lytic granules to the target cell contact site (23) by high-avidity T cells. However, TCRs isolated from patients' T cells recognizing tumor-overexpressed self-antigens are often of low-affinity (24) as they derive from a repertoire that has gone through negative selection in the thymus where mostly low-avidity T cells egress from the thymus to the periphery. The affinity of a TCR can be increased by site-directed mutagenesis within the CDR of the TCR (25). This manipulation might pose the risk that a TCR can gain reactivity against new pMHC structures, including unwanted recognition of self-proteins. This is exemplified by recent observations where autologous PBLs transduced with an

affinity-enhanced MAGE-A3 reactive TCR caused neurological toxicities through cross-reactivity with MAGE-A12, expressed in the brain (26). In another clinical trial using T cells with a MAGE-A3 TCR, patients died from cardiac toxicities due to unpredicted cross-reactivity to cardiomyocyte-expressed protein titin (27).

Adoptive therapy using T cells engineered with chimeric antigen receptors (CARs) allows MHC-independent recognition of target structures. The extracellular antigen-binding domain is derived from the variable region of an antigen-specific antibody. The extracellular domain is linked via a spacer to the transmembrane and cytoplasmic domains of the CAR. CARs recognizing membrane-proximal epitopes require flexible hinge regions to allow antigen-binding (28). The most commonly used hinge regions are derived from the constant region (Fc-region) of antibodies such as IgG1 (29). However, the use of IgG Fc-derived hinge regions can cause severe adverse effects due to activation of NK cells, which secrete high amounts of inflammatory cytokines. This interaction can also induce an off-target activation of CAR-expressing T cells leading to lytic activity against NK cells and other cell types expressing IgG Fc receptors (30). Modifying IgG1-derived hinge regions to prevent activation of IgG Fc receptor positive cells (30) or the use of hinge regions derived from the extracellular domains of CD8 α (29) can prevent off-target activation. To translate antigen-binding into a T cell activating signal, CARs contain CD3 ζ -derived signaling domains. CARs could be expressed on human T cells and induced anti-tumor responses. However, CAR-engineered T cells showed only transient and rather poor activation (29). To increase the persistence and strengths of CAR-mediated T cell responses, so-called 2nd and 3rd generation CARs were designed. They contain additional signaling domains derived from co-stimulatory molecules such as CD28 and 4-1BB. T cells expressing CARs with 2 (2nd generation) or 3 (3rd generation) intracellular signaling domains secreted higher amounts of IL-2 as well as IFN- γ and proliferated to a greater extent (29). A mesothelin-directed CAR with CD3 ζ , CD28 and 4-1BB signaling domains mediated control of large mesothelioma xenograft tumors (31). In a xenograft model of pre-B-cell acute lymphoblastic leukemia, T cells expressing a CD19-directed CAR with CD3 ζ and 4-1BB domains achieved higher anti-leukemic effects and transferred T cells survived longer compared to T cells expressing a CD19-directed CAR with CD3 ζ and CD28 domains (32). High response rates of CAR-therapy were achieved in leukemia and lymphoma

patients. Kochenderfer et al. reported in 2012 (33) response rates of 75% among patients with B-cell malignancies treated with a CD19-directed CAR with CD3 ζ plus CD28 domains. In a clinical trial reported by Maude et al. 2014 (34), therapy of relapsed or refractory acute lymphoblastic leukemia patients with CD19-directed CARs containing CD3 ζ and 4-1BB signaling domains achieved a response rate of 90%. Transferred cells remained detectable in the patients up to 2 years.

The simultaneous triggering of CD3 ζ and co-stimulatory signals can be a benefit, however, if healthy tissues express target structures, co-stimulation might increase unwanted side effects. Morgan et al. (35) and Lamers et al. (36) reported severe side effects of CAR-engineered T cells due to activation by antigen positive healthy tissue. As 2nd and 3rd generation CARs are activated more strongly and at a lower threshold, antigen expression at low levels by healthy tissue is more likely to induce T cell activation compared to CARs containing a CD3 ζ signaling domain only. In addition, in contrast to antibodies, TCRs recognizing self-antigens have undergone negative selection in the thymus. Those T cells bearing TCRs with anti-self specificity are only of low avidity. Therefore, a safer approach might be to use T cells expressing low-avidity TCRs and deliver co-stimulatory signals to enhance their activity to elicit stronger anti-tumor response.

3.3 Tumor strategies to evade T cell cytotoxicity

Although significant response rates are achieved by ATT still only a fraction of patients responds and some tumor entities are largely refractory to this therapy (37). The strongest factor limiting the efficacy of immunotherapy is the tumor environment, which creates a milieu that counteracts immune response on multiple levels. By down-regulating MHC class I expression, tumor cells make themselves invisible for T cells. Myeloid-derived suppressor cells (MDSCs) secrete peroxynitrite, which alters TCR-peptide binding and thereby prevents T cell activation (38).

In addition to preventing recognition, the tumor environment can induce different types of immune cell unresponsiveness, including T cell tolerance such as exhaustion and anergy. Exhaustion develops when T cells are chronically stimulated. Exhausted T cells are unable to respond to stimulation and show only poor effector functions (39). T cell exhaustion is mediated through inhibitory receptors such as

“Programmed cell death protein 1” (PD-1). PD-1 is up-regulated on activated T cells and binds PD-L1, expressed on tumor cells, MDSCs and TILs. When PD-1 is ligated protein tyrosine phosphatase-1 and -2 (SHP-1, SHP-2) are recruited, which counteract TCR signaling. Through inhibition of PI3K and the MAPK pathway, PD-1 can directly attenuate T cell effector function and proliferation (40). Exhausted T cells were detected in melanoma (41), hepatocellular carcinoma (42), breast cancer, renal cell carcinoma and lung cancer patients (40). Anti-PD-1 antibody treatment achieved response rates of 18% in non-small-cell lung cancer, 28% in melanoma and 27% in renal cell carcinoma. 87% of responses in followed-up patients lasted >1 year (43). The anti-PD-1 antibody Nivolumab (Opdivo) was approved by the FDA in December 2014 for patients with unresectable or metastatic melanoma and in March 2015 for non-small cell lung cancer.

In addition to becoming exhausted, T cells can also acquire an anergic phenotype in the tumor environment. T cells become anergic when they receive TCR stimulation without proper co-stimulation or/and high co-inhibition mediated through “Cytotoxic T-lymphocyte-associated antigen 4” (CTLA-4; (44)). The anergic phenotype has been primarily described for CD4⁺ T cells. It is characterized by cell cycle arrest and reduced IL-2 response (45). The transcription factor NFAT and diacylglycerol kinase- α (DGK- α) are key mediators of anergy (46). Moreover, Zheng et al. (2012) (47) identified the transcription factor “Early growth response gene 2” (Egr2) as another regulator of anergy. They showed that deletion of Egr2 restored IL-2 production and proliferation.

Recently, it was described in human renal cell carcinoma that CD8⁺ T cells in the tumor microenvironment express high levels of DGK- α . Moreover, TILs showed reduced phosphorylation of ERK as well as JNK and were unresponsive to TCR stimulation with poor degranulation and IFN- γ secretion (48). IFN- γ and “tumor necrosis factor alpha” (TNF- α), secreted by cytotoxic T cells, are important cytokines for tumor control, not only because they can directly destroy tumor cells but additionally by elimination of tumor stroma (49, 50). Strong forces in the tumor microenvironment, including lactic acidosis, prevent T cells from secreting these cytokines (51). In addition to preventing Th1 cytokine secretion, Th2 cytokines and IL-10 are often induced, which can inhibit cytotoxic T cells and support MDSCs, which in turn inhibit maturation of DCs and foster angiogenesis (52).

The tumor environment cannot only induce a reduction of anti-tumoral cytokines but can also induce cytokines that are associated with tumor progression. MDSCs as well as “transforming growth factor beta” (TGF- β) can shift the balance towards tumor-promoting cytokines such as IL-4, IL-5 and IL-10.

Therefore, a major aim of immune therapy is to utilize a T cell product for ATT with strong anti-tumor reactivity, long-term persistence in the patient and the capacity to maintain an anti-tumor response despite tumor-mediated inhibition.

4 OBJECTIVE OF THIS THESIS

The loss of function and poor persistence of adoptive transferred T cells are major limitations of successful T cell therapy. In addition, TCRs isolated from cancer patients are mostly of low affinity. Higher response rates can be achieved with high-avidity T cells (21), but affinity-enhanced T cells pose increased risks of unwanted side effects (26). Therefore, there is a need for strategies to boost the response of low-avidity T cells without interfering with the TCR. Moreover, TILs showed deficits in signaling molecules (48) that might be reverted by co-stimulation. As co-stimulation is also reported to enhance T cell persistence and degranulation capacity (53), I hypothesized that it might be efficacious to engineer T cells or TILs for adoptive transfer with the capacity to receive co-stimulation in the tumor environment.

However, a large proportion of effector T cells are CD28 negative (54) and most carcinomas express only low levels of CD80 or CD86 (55, 56). Thus, co-stimulation cannot be provided via CD28-CD80/CD86 interaction. However, various tumors showed high expression of PD-L1 (57). Engineering T cells or TILs with a chimeric signaling receptor consisting of the extracellular domain of PD-1, the receptor for PD-L1, joined with the intracellular domain of a co-stimulatory molecule, CD28 or 4-1BB, might allow co-stimulation of transferred cells in the tumor environment. The extracellular PD-1 domain would bind PD-L1 presented on tumor cells and initiate co-stimulatory signaling in chimeric receptor expressing cells.

It was the main objective of this thesis to develop a chimeric receptor that can improve T cell function and proliferation. To this end, various chimeric co-stimulatory receptors were designed using different transmembrane and signaling domains. CD28- and 4-1BB-derived signaling domains were compared given that results from *in vivo* studies and clinical trials utilizing CD19-CAR T cells suggested superior activity of 4-1BB over CD28 (32, 34). To address the issue of improving low-avidity T cells, the effect of chimeric receptors on the functional performance of low-avidity T cells was assessed and compared to high-avidity T cells. The effects of chimeric signaling receptors on T cell performance was further assessed in several mouse models and in TILs of human renal cell carcinoma.

5 MATERIAL

5.1 Consumables and equipment

CONSUMABLES/EQUIPMENT	COMPANY
Balance PC 400 DeltaRange	Mettler, Gießen, GERMANY
BioPlex reader	BIO-RAD, Munich, GERMANY
Cell strainer 40 µm, 100 µm	Becton Dickinson, Heidelberg, GERMANY
Centrifuges Megafuge 2.0 R Rotanda 460R Centrifuge 5417 R Centrifuge 4K15	Heraeus Instruments, Hanau, GERMANY Hettich, Ebersberg, GERMANY Eppendorf, Hamburg, GERMANY Sigma Laboratory Centrifuges
Electrophoresis chamber and power supply	BIO-RAD, Munich, GERMANY
Electroporator Gene Pulser Xcell	BIO-RAD, Munich, GERMANY
Electroporation cuvettes, 4 mm	
Filter 0.45 µm	Millipore, Schwalbach, GERMANY
Flow cytometer and cell sorter LSR II BD FACSAria™ IIIu	Becton Dickinson, Heidelberg, GERMANY
Freezing vials 1.5 ml	Nunc, Wiesbaden, GERMANY
Incubator	Heraeus Instruments, Hanau, GERMANY
Integral water purification system Milli-Q®	Millipore, Schwalbach, GERMANY
Light microscope Leica DMIL	Leica Microsystems, Heidelberg, GERMANY
Luma plates TM96	Canberra-Packard, Dreieich, GERMANY
Magnetic cell separation columns LS columns, pre-separation columns	MiltenyiBiotec, Bergisch Gladbach, GERMANY
Multistepper	Eppendorf, Hamburg, GERMANY

CONSUMABLES/EQUIPMENT	COMPANY
Multi-well plates, polystyrene 24-well plates Tissue culture treated Non-tissue culture treated 96-well plates Tissue culture treated	Becton Dickinson Falcon, Heidelberg, GERMANY
Nanodrop ND-1000-Spektrophotometer	Peqlap Biotechnologie GmbH, Erlangen
Needles, 26G	NeoLab, Heidelberg, GERMANY
Neubauer counting chamber Depth 0.1 mm	Gesellschaft für Laborbedarf Würzburg, Würzburg, GERMANY
Nitrogen tank	Messer Griesheim, Krefeld, GERMANY
Parafilm®	Pechiney Plastic Packaging, Menasha, USA
Pasteur pipettes, glass	Josef Peske GmbH & Co KG, Munich, GERMANY
Petri dishes polystyrene 100 mm	Becton Dickinson Falcon, Heidelberg, GERMANY
Picture frame glasses for Neubauer counting chambers 20 x 26 mm, depth 0.4 mm	Hirschmann Laborgeräte, Eberstadt, GERMANY
Pipettes Single- and multi-channel	Eppendorf, Hamburg, GERMANY Thermo Scientific, Waltham, USA
Pipettor Pipetus®	Hirschmann Laborgeräte, Eberstadt, GERMANY
Pipette tips With/without filter 1-10 µl, 10-200 µl, 200-1000 µl	Eppendorf, Hamburg, GERMANY
Pipette tips for pipettor Disposable 10 ml, 25 ml Glass 2 ml, 5 ml, 10 ml, 20 ml	Greiner bio-one, Frickenhausen, GERMANY Hirschmann Laborgeräte, Eberstadt, GERMANY
Polymerisation chain reaction machine Flex Cycler	Analytik Jena, Jena, GERMANY
Rotator	VWR, Darmstadt, GERMANY
Scalpels	Braun, Tuttlingen, GERMANY
Scintillation counter TopCount NXT	Canberra-Packard, Dreieich, GERMANY
Scissors and tweezers for preparation	NeoLab, Heidelberg, GERMANY

CONSUMABLES/EQUIPMENT	COMPANY
Shaker Polymax 1040 Innova 4200	Heidolph New Brunswick Scientific, Edison, USA
Spectrophotometer	Tecan Group AG, Männedorf, SWITZERLAND
Sterile laminar flow hood	BDK Luft- und Reinraumtechnik GmbH, Sonnenbühl-Genkingen, GERMANY
Syringes 1 ml, 10 ml, 50 ml	Eppendorf, Hamburg, GERMANY
Syringes for multistepper 5 ml	Eppendorf, Hamburg, GERMANY
Thermomixer 5436	Eppendorf, Hamburg, GERMANY
Tissue culture flasks 75 cm ² , 175 cm ²	Greiner bio-one, Frickenhausen, GERMANY
Tubes Polypropylene 1.5 ml, 2 ml 15 ml, 50 ml	Eppendorf, Hamburg, GERMANY Becton Dickinson Falcon, Heidelberg, GERMANY
Tubes for flow cytometry, poly-propylene 1 ml 5 ml	Greiner bio-one, Frickenhausen, GERMANY Becton Dickinson Falcon, Heidelberg, GERMANY
Tubes for sterile filtration (0.2 µm) 50 ml	Becton Dickinson Falcon, Heidelberg, GERMANY
UV light imaging system InGenius	Syngene Bio Imaging, Cambridge, UK
Vortexer MS1 Minishaker	IKA Werke GmbH & Co KG, Staufen, GERMANY
Water bath	Köttermann Labortechnik, Uetze, GERMANY
Winged infusion set	Dispomed Witt oHG, Gelnhausen, GERMANY

5.2 Reagents, kits and bacteria

5.2.1 Reagents

REAGENT	COMPANY
7-Aminoactinomycin D (7-AAD)	Sigma-Aldrich, Taufkirchen, GERMANY
⁵¹ Cr Sodium chromate	Hartmann Analytic, Braunschweig, GERMANY
Ampicillin	Sigma-Aldrich, Taufkirchen, GERMANY
Acetic acid	Merck, Darmstadt, GERMANY
Accutase®	PAA Laboratories, Cölbe, GERMANY
Agarose, electrophoresis grade	GIBCO, Thermo Fisher Scientific, Schwerte, GERMANY
Ammonium chloride	Merck, Darmstadt, GERMANY
Beads for compensating fluorescence activated cell sorting (FACS) data	Becton Dickinson Pharmingen, Heidelberg, GERMANY
Biocoll® separating solution (Ficoll®)	Biochrom AG, Berlin, GERMANY
Bovine serum albumin (BSA)	Sigma-Aldrich, Taufkirchen, GERMANY
Carboxyfluorescein diacetate succinimidyl ester (CFDA-SE)	Invitrogen, Karlsruhe, GERMANY
CD3/CD28 mouse T-activator beads	Invitrogen, Karlsruhe, GERMANY
Collagenase IV	Sigma-Aldrich, Taufkirchen, GERMANY
Diethylpyrocarbonate (DEPC)	Sigma-Aldrich, Taufkirchen, GERMANY
Dimethyl sulfoxide (DMSO)	Sigma-Aldrich, Taufkirchen, GERMANY
Disodium hydrogen phosphate	Sigma-Aldrich, Taufkirchen, GERMANY
DNA ladder, 1kb	Thermo Fisher Scientific, Schwerte, GERMANY
DNA loading dye, 6x	Thermo Fisher Scientific, Schwerte, GERMANY
DNase I, type IV	Sigma-Aldrich, Taufkirchen, GERMANY
Ethanol, 99%	Merck, Darmstadt, GERMANY
Ethidium bromide 10 mg/ml	Roth, Karlsruhe, GERMANY
Ethylenediaminetetraacetic acid (EDTA), 0.5 M	Sigma-Aldrich, Taufkirchen, GERMANY
EDTA disodium	Roth, Karlsruhe, GERMANY
Fetal bovine serum (FBS)	GIBCO, Thermo Fisher Scientific, Schwerte, GERMANY
Human serum (23)	In-house production
L-glutamine	GIBCO, Thermo Fisher Scientific, Schwerte, GERMANY
Luria Broth and agar powder	Roth, Karlsruhe, GERMANY

REAGENT	COMPANY
Heparin-sodium	B. Braun, Melsungen, GERMANY
4-(2-hydroxyethyl)-1-piperazine-ethanesulfonic acid (HEPES)	Biochrom AG, Berlin, GERMANY
Ionomycin 0.5 mg/ml	Sigma-Aldrich, Taufkirchen, GERMANY
Isopropanol	Sigma-Aldrich, Taufkirchen, GERMANY
β -Mercaptoethanol	GIBCO, Thermo Fisher Scientific, Schwerte, GERMANY
Milk powder	Roth, Karlsruhe, GERMANY
Mucocit disinfectant cleaner	Mucocit disinfectant cleaner
Non-essential amino acids	GIBCO, Thermo Fisher Scientific, Schwerte, GERMANY
Paraformaldehyde (PFA)	Merck, Darmstadt, GERMANY
PCR MasterMix, 2x	Promega, Mannheim, GERMANY
Penicillin/streptomycin	GIBCO, Thermo Fisher Scientific, Schwerte, GERMANY
Percoll, density 1.13 g/ml	GE Healthcare, Freiburg GERMANY
Phorbol 12-myristate 13-acetate (58)	Sigma-Aldrich, Taufkirchen, GERMANY
Phosphoric acid, 1M	Sigma-Aldrich, Taufkirchen, GERMANY
Potassium hydrogen carbonate	Roth, Karlsruhe, GERMANY
Propidium iodide	Sigma-Aldrich, Taufkirchen, GERMANY
Recombinant human PD-L1 Fc chimera	R&D Systems, Wiesbaden, GERMANY
Recombinant human IL-2 Cross-reactive to mouse	Cancernova GmbH, Reute, GERMANY Chiron Novartis, USA
Recombinant human IFN- γ	Boehringer Ingelheim, Ingelheim, GERMANY
Recombinant murine IL-15	MiltenyiBiotec, Bergisch Gladbach, GERMANY
Recombinant fibronectin CH-296 RetroNectin [®]	Takara Bio Incorporation, Shiga, JAPAN
RNA ladder	Thermo Scientific, Schwerte, GERMANY
RNA loading dye, 2x	Thermo Scientific, Schwerte, GERMANY
Saponin	Merck, Darmstadt, GERMANY
Sodium acetate, 3 M	Sigma-Aldrich, Taufkirchen, GERMANY
Sodium pyruvate	GIBCO, Thermo Fisher Scientific, Schwerte, GERMANY
Sodium chloride	Sigma-Aldrich, Taufkirchen, GERMANY
Thy1.1 MicroBeads	MiltenyiBiotec, Bergisch Gladbach, GERMANY
TAE, 10x	GIBCO, Thermo Fisher Scientific, Schwerte, GERMANY

REAGENT	COMPANY
TransIT [®] -LT1 Reagent	Mirus Bio LLC, Madison, USA
Trypan blue	Sigma-Aldrich, Taufkirchen, GERMANY
Trypsin-EDTA	GIBCO, Thermo Fisher Scientific, Schwerte, GERMANY
Tween20	Sigma-Aldrich, Taufkirchen, GERMANY
Water Milli-Q [®] purified Nuclease-free	In-house production Promega, Mannheim, GERMANY

5.2.2 Kits

KIT	COMPANY
Cytokine Bio-Plex Human Th1, Th2 Murine Th1, Th2 + IL17	BIO-RAD, Munich, GERMANY
ELISA Kit, human/mouse IFN- γ , human/mouse IL-2	BD Biosciences, Heidelberg GERMANY
Gel Extraction Kit	Quiagen, Hilden, GERMANY
JetStar 2.0 preparation kit	Genomed GmbH, Löhne, GERMANY
MinElute [®] Reaction Cleanup Kit	Quiagen, Hilden, GERMANY
mMESSAGEmMACHINE Kit	Ambion [®] , Schwerte, GERMANY
RNeasy Mini Kit	Quiagen, Hilden, GERMANY

5.2.3 Bacteria

BACTERIA	COMPANY	APPLICATION
TOP10 and MACH1 <i>E.coli</i> (+ SOC medium)	Life Technologies, Schwerte, GERMANY	Transformation with Geneart, pGEM and pMP71 vectors

5.3 Media and buffers

5.3.1 Basic media and buffers

MEDIUM/BUFFER	COMPANY
AIM-V	Invitrogen, Karlsruhe, GERMANY
Dulbecco's modified eagle medium (DMEM)	GIBCO Invitrogen, Darmstadt, GERMANY
Dulbecco's phosphate buffered saline (PBS), 1x, 10x	GIBCO Invitrogen, Darmstadt, GERMANY
Freezing medium for TILs	IBIDI, Munich, GERMANY
Hank's buffered salt solution (HBSS) w/o and w Ca Mg	GIBCO Invitrogen, Darmstadt, GERMANY
Opti-MEM	GIBCO Invitrogen, Darmstadt, GERMANY
Phosflow Cytotfix Buffer [®]	BD Biosciences, Heidelberg GERMANY
Phosflow Perm Buffer III [®]	BD Biosciences, Heidelberg GERMANY
Roswell Park Memorial Institute (RPMI)-1640 medium	GIBCO Invitrogen, Darmstadt, GERMANY

5.3.2 Prepared media and buffers

MEDIUM/BUFFER	FORMULA
Cell freezing medium	RPMI-1640 + 1% L-glutamine + 1% non-essential amino acids + 1% sodium pyruvate + 20% DMSO } RPMI basic
Digestion buffer for human and murine tumors (except liver tumors)	RPMI-1640 + 0.1% BSA + 1% penicillin/streptomycin + 10 mM HEPES + 218 U/ml collagenase IV + 435 KunitzU/ml DNase I, type IV

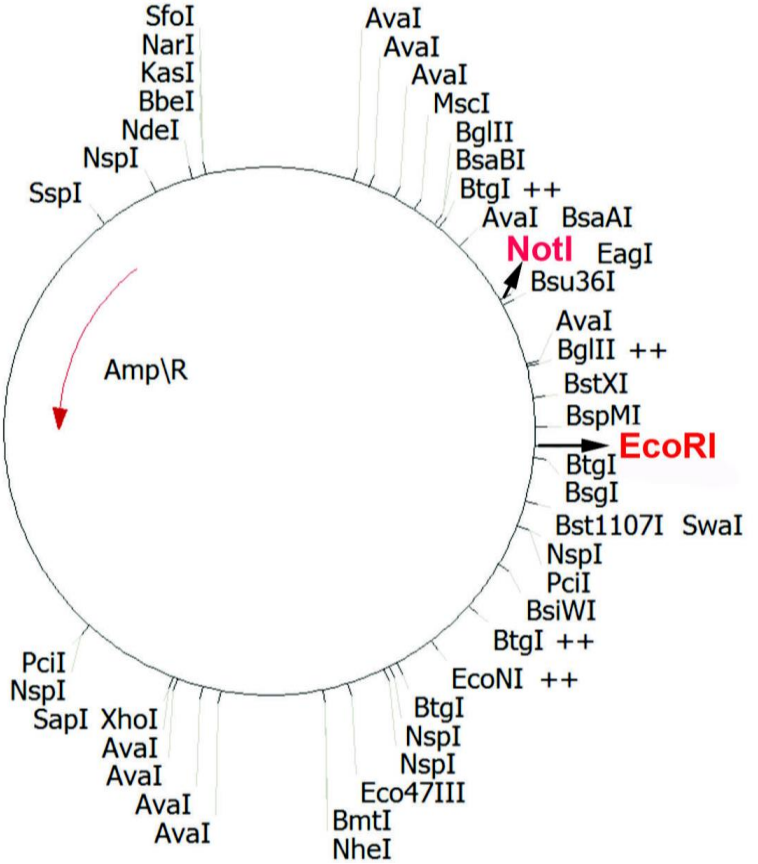
MEDIUM/BUFFER	FORMULA
Digestion buffer for murine liver tumors	RPMI-1640 + 0.1% BSA + 1% penicillin/streptomycin
Digestion buffer for murine liver tumors	RPMI-1640 + 0.1% BSA + 1% penicillin/streptomycin + 10 mM HEPES + 800 U/ml collagenase IV
Enzyme-linked-immunosorbent assay (ELISA) buffers Coating buffer, pH 9.5 Washing buffer	Milli-Q [®] purified water + 8.4 g sodium hydrogen carbonate + 3.56 g sodium carbonate PBS + 0.05% Tween20
Erythrocyte lysis buffer pH 7.2-7.4	Milli-Q [®] purified water + 0.15 M ammonium chloride + 1 mM potassium hydrogen carbonate + 0.1 mM EDTA disodium
Human embryonic kidney cell 293 medium (HEK medium)	DMEM + 1% L-glutamine + 1% non-essential amino acids + 1% sodium pyruvate + 12% FCS
LB Medium	500 ml Milli-Q [®] water + 12.5 LB powder + 100 µg/ml Ampicillin
Magnetic cell separation buffer (MACS buffer)	PBS + 0.5% FCS + 2 mM EDTA
Murine embryonic kidney cell 293 medium (mHEK medium)	DMEM + 1% L-glutamine + 1% non-essential amino acids + 1% sodium pyruvate + 12% FCS + 0.05% β-mercaptoethanol

MEDIUM/BUFFER	FORMULA
Fluorescence activated cell sorting (FACS) buffer	PBS + 2 mM EDTA + 2% HS + 0.1% sodium azide
FACS permeabilization buffer (0.1%; 0.35%)	PBS + 0,1 or 0.35 % saponin + 2% HS
FACS fixation buffer	PBS + 1% PFA
Human tumor-infiltrating lymphocyte medium (TIL medium)	AIM-V + 1% L-glutamine + 10% HS
Medium for human T cells (TCM)	RPMI basic + 10% HS
Medium for murine T cells and the murine hepatocellular carcinoma cell line 434 (MTM)	RPMI basic + 12% FCS + 0.05% β -mercaptoethanol
Percoll 100 x 80% 40%	90% Percoll in 10x PBS 1x PBS + 80% 100x Percoll 1x PBS + 40% 100x Percoll + 250 IU Heparin
Transfection buffer pH 6,76	100 ml Milli-Q [®] purified water + 50 mg disodium hydrogen phosphate + 74 mg potassium chloride + 1.6 g sodium chloride + 1 g HEPES
Tumor cell medium (RCC medium)	RPMI basic + 12% FBS

5.4 Plasmids, primers and restriction enzymes

5.4.1 Plasmids

PLASMIDS	CHARACTERISTICS/ SOURCE
<p>pGEM vectors: pGEM-EGFPA120</p> <p>T7 Promoter</p>	<p>Kindly provided by Slavoljub Milosevic, Medigene GmbH, Martinsried, GERMANY</p> <p>Coding for green fluorescent protein, the vector's backbone contains a T7 polymerase binding site for the generation of in vitro transcribed (ivt) RNA and a poly-A-tail of 120 base pairs</p> <p>Sequences of the chimeric signaling receptors PD-1:8tm:28, PD-1:cys28tm, PD-1:28tm, PD-1trunc, PD-1:BBtm, PD-1tm:BB-pGEM</p>

PLASMIDS	CHARACTERISTICS/ SOURCE
<p>pMP71 vectors: pMP71 backbone</p>  <p>PD-1:28tm-pMP71</p> <p>T58 (b23m-p-a7m)-pMP71, D115 (b8m-p-a22m)-pMP71</p>	<p>Kindly provided by Wolfgang Uckert, Max Delbrück Center Berlin, GERMANY Vector for retroviral transduction combining the MPSV-LTR promoter-enhancer sequences and improved 5' untranslated sequences derived from MESV MPSV: murine myeloproliferative sarcoma virus; LTR: long terminal repeats; MESV: murine embryonic stem cell virus</p> <p>Sequence of the chimeric signaling receptor PD-1:28tm cloned into the pMP71 backbone, kindly provided by Matthias Leisegang, Max Delbrück Center Berlin, GERMANY</p> <p>Kindly provided by Matthias Leisegang, Max Delbrück Center Berlin, GERMANY Sequences of the HLA-A2 restricted, tyrosinase-specific TCRs T58 and D115 cloned into the pMP71 backbone</p>

5.4.2 Primers

PRIMERS	SEQUENCE 5'->3'	COMPANY
Primers for cloning chimeric receptors into the pGEM-vector PD-1:8 tm :28 PD-1:cys28 tm , PD-1:28 tm , PD-1trunc, PD-1:BB tm , PD-1 tm :BB PD-1:8 tm :28 PD-1:cys28 tm , PD-1:28 tm , PD-1trunc PD-1:BB tm , PD-1 tm :BB	Forward ATAAAGCTTATGCAGATTCCTCAGGCC Forward ATAGTCGACACCGGTGCCACC Reverse ATAGAATTCTCAGGATCTGTAGGCGGCG Reverse ATAGGTACCGAATTCGGATCCTC Reverse ATAGGTACCGAATTCGGATCCTTAGAGCTC	Metabion, Planegg, GERMANY
Primers for cloning the PD-1:28 tm chimeric receptor into the pMP71-vector	Forward ATAGCGGCCGCGCCACCATGCAGATTCCTC Reverse ATAGAATTCTCAGCTTCTGTAGGCGGCG	Metabion, Planegg, GERMANY
Primer for sequencing Geneart plasmids	ATACACTATAGGGCGAATTGGCG	Metabion, Planegg, GERMANY
Primer for sequencing pGEM plasmids	AATACGACTCACTATAG	Provided by MWG Eurofins, Ebersberg, GERMANY
Primer for sequencing pMP71 plasmids	TGAAAATTAGCTCGACAAAGTTAAGTAATAG TCCCTC	Metabion, Planegg, GERMANY

5.4.3 Restriction enzymes

ENZYMES & BUFFERS	RECOGNITION SITES 5'->3'	COMPANY
<p>Enzymes for cloning PD-1:8tm:28 into the pGEM-vector: HindIII-high fidelity (CutSmart Buffer) EcoRI-high fidelity (CutSmart Buffer)</p> <p>Enzymes for cloning PD-1:cys28tm, PD-1:28tm, PD-1trunc, PD-1:BBtm, PD-1tm:BB into the pGEM-vector: HincII (CutSmart Buffer) EcoRI-high fidelity (CutSmart Buffer)</p>	<p>AAGCTT GAATTC</p> <p>GTCGAC GAATTC</p>	<p>New England Biolabs, Frankfurt am Main, GERMANY</p>
<p>Enzymes for cloning PD-1:28tm and mPD-1:28tm into the pMP71-vector: NotI-high fidelity (CutSmart Buffer) EcoRI-high fidelity (CutSmart Buffer)</p>	<p>GCGGCCGC GAATTC</p>	<p>New England Biolabs, Frankfurt am Main, GERMANY</p>
<p>Ligation of inserts and vector backbones T4 Ligase (T4 Ligase Buffer)</p>	<p>Not applicable</p>	<p>New England Biolabs, Frankfurt am Main, GERMANY</p>
<p>Linearization of pGEM plasmids: SpeI-high fidelity (CutSmart Buffer)</p>	<p>ACTAGT</p>	<p>New England Biolabs, Frankfurt am Main, GERMANY</p>

5.5 Chimeric receptor sequences

5.5.1 Human chimeric receptor DNA sequences

PD-1:8tm:28

5' -> 3'

ATGCAGATTCTCAGGCCCCCTGGCCCGTGGTCTGGGCTGTGCTGCAGCTGGG
 ATGGCGCCTGGCTGGTTCCTGGACAGCCCCGACAGACCCTGGAACCCCCCTA
 CCTTCAGCCCTGCCCTGCTGGTGGTGACAGAGGGCGACAACGCCACCTTCACC
 TGTAGCTTCAGCAACACCAGCGAGAGCTTCGTGCTGAACTGGTACAGAATGAGC
 CCCAGCAACCAGACCGACAAGCTGGCCGCCTTCCCCGAGGACAGAAGCCAGC
 CCGGCCAGGACTGCCGGTTCAGAGTGACCCAGCTGCCCAACGGCCGGGACTT
 CCACATGAGCGTGGTGC GCGCCAGACGGAACGACAGCGGCACATACCTGTGC
 GGCGCCATCAGCCTGGCCCCCAAGGCCAGATCAAAGAGAGCCTGCGGGCCG
 AGCTGAGAGTGACCGAGAGAAGGGCCGAGGTGCCACAGCCCACCCCAGCCC
 ATCTCCAAGACCTGCCGGCCAGTTCAGACCCTGGTGTTCGTGCCCGTGTTCCCT
 GCCCGCTAAGCCCACCACAACCCCTGCCCTAGGCCTCCTACCCCAGCCCCTA
 CAATCGCCAGCCAGCCCCTGTCTCTGCGGCCTGAGGCTTGTAGACCTGCCGCT
 GGCGGAGCCGTGCACACCAGAGGGCTGGACTTCGCCTGCGATATCTACATCTG
 GGCCCCTCTGGCCGGCACCTGTGGCGTGCTGCTGCTGTCCCTGGTGATCACCC
 TGTACTGCAACCACCGGAACAGAAGCAAGCGGAGCCGGCTGCTGCATAGCGA
 CTACATGAACATGACCCCCAGACGGCCTGGCCCCACCAGAAAGCACTACCAG
 CCCTACGCCCTCCCCGGGACTTCGCCGCCTACAGATCC**TGA**

ATG start codon

TGA stop codon

PD-1 domains

CD8α domains

CD28 domains

pGEM vector:

AAGCTT**ATG**...**TGA****GAATTC**

AAGCTT HindIII restriction site

GAATTC EcoRI restriction site

PD-1:cys28tm

5' -> 3'

ATGCAGATTCTCAGGCCCTTGGCCTGTTCGTGTGGGCTGTGCTCCAGCTGGG
ATGGCGGCCTGGCTGGTTTCTGGACAGCCCCGACAGACCCTGGAACCCCCCTA
CATTTTCCCCTGCCCTGCTGGTTCGTGACCGAGGGCGACAATGCCACCTTCACCT
GTAGCTTCAGCAACACCAGCGAGAGCTTCGTGCTGAACTGGTACAGAATGAGC
CCCAGCAACCAGACCGACAAGCTGGCCGCCTTCCCCGAGGATAGATCTCAGCC
CGGCCAGGACTGCCGGTTCAGAGTGACCCAGCTGCCCAACGGCCGGGACTTC
CACATGTCTGTTCGTGCGGGCCAGACGGAACGACAGCGGCACATATCTGTGCGG
CGCCATCAGCCTGGCCCCCAAGGCCAGATCAAAGAGAGCCTGAGAGCCGAG
CTGAGAGTGACCGAGAGAAGGGCCGAAGTGCCTACCGCCCACTGTCCCAGCC
CTCTGTTTCCTGGCCCTAGCAAGCCCTTCTGGGTGCTGGTGGTTCGTGGGCGGA
GTGCTGGCCTGTTACAGCCTGCTCGTGACCGTGGCCTTCATCATCTTTTGGGT
GCGCAGCAAGCGGAGCCGGCTGCTGCACAGCGACTACATGAACATGACCCC
CAGACGGCCAGGCCCCACCAGAAAGCACTACCAGCCTTACGCCCTCCCAGA
GACTTCGCCGCCTACAGAAGCTGA

ATG start codon

TGA stop codon

PD-1 domains

CD28 domains

pGEM vector:

GTTCGAC...**ATG**...**TGA****GAATTC**

GTTCGAC HincII restriction site

GAATTC EcoRI restriction site

PD-1:28tm

5' -> 3'

ATGCAGATTCTCAGGCCCTTGGCCTGTTCGTGTGGGCTGTGCTCCAGCTGGG
ATGGCGGCCTGGCTGGTTTCTGGACAGCCCCGACAGACCCTGGAACCCCCCTA
CATTTTCCCCTGCCCTGCTGGTTCGTGACCGAGGGCGACAATGCCACCTTCACCT
GTAGCTTCAGCAACACCAGCGAGAGCTTCGTGCTGAACTGGTACAGAATGAGC
CCCAGCAACCAGACCGACAAGCTGGCCGCCTTCCCCGAGGATAGATCTCAGCC
CGGCCAGGACTGCCGGTTCAGAGTGACCCAGCTGCCCAACGGCCGGGACTTC
CACATGTCTGTTCGTGCGGGCCAGACGGAACGACAGCGGCACATATCTGTGCGG
CGCCATCAGCCTGGCCCCCAAGGCCCAGATCAAAGAGAGCCTGAGAGCCGAG
CTGAGAGTGACCGAGAGAAGGGCCGAAGTGCCCTACCGCCCACCCTAGCCCATC
TCCAAGACCTGCCGGCCAGTTCTGGGTGCTGGTGGTTCGTGGGCGGAGTGCTG
GCCTGTTACAGCCTGCTCGTGACCGTGGCCTTCATCATCTTTTGGGTGCGCAG
CAAGCGGAGCCGGCTGCTGCACAGCGACTACATGAACATGACCCCCAGACG
GCCAGGCCCCACCAGAAAGCACTACCAGCCTTACGCCCTCCCAGAGACTTC
GCCGCCTACAGAAGCTGA

ATG start codon

TGA stop codon

PD-1 domains

CD28 domains

pGEM vector:

GTTCGAC...**ATG**...**TGAGAATTC**

GTTCGAC HincII restriction site

GAATTC EcoRI restriction site

pMP71 vector:

GCGGCCGC...**ATG**...**TGAGAATTC**

GCGGCCGC NotI restriction site

GAATTC EcoRI restriction site

PD-1trunc

5' -> 3'

ATGCAGATTCTCAGGCCCTTGGCCTGTCGTGTGGGCTGTGCTCCAGCTGGG
ATGGCGGCCTGGCTGGTTTCTGGACAGCCCCGACAGACCCTGGAACCCCCCTA
CATTTTCCCCTGCCCTGCTGGTTCGTGACCGAGGGCGACAATGCCACCTTCACCT
GTAGCTTCAGCAACACCAGCGAGAGCTTCGTGCTGAACTGGTACAGAATGAGC
CCCAGCAACCAGACCGACAAGCTGGCCGCCTTCCCCGAGGATAGATCTCAGCC
CGGCCAGGACTGCCGGTTCAGAGTGACCCAGCTGCCCAACGGCCGGGACTTC
CACATGTCTGTCGTGCGGGCCAGACGGAACGACAGCGGCACATATCTGTGCGG
CGCCATCAGCCTGGCCCCCAAGGCCCAGATCAAAGAGAGCCTGAGAGCCGAG
CTGAGAGTGACCGAGAGAAGGGCCGAAGTGCCCTACCGCCCACCCTAGCCCATC
TCCAAGACCTGCCGGCCAGTTCCAGACACTGGTTCGTGGGAGTCGTGGGCGGA
CTGCTGGGATCTCTGGTGCTGCTCGTGTGGGTGCTGGCCGTGATCTGTAGCAG
AGCCGCCAGAGGCACCATCGGCTTGA

ATG start codon

TGA stop codon

PD-1 domains

pGEM vector:

GTTCGAC...ATG...TGA**GAATTC**

GTTCGAC HincII restriction site

GAATTC EcoRI restriction site

PD-1:BBtm

5' -> 3'

ATGCAGATTCTCAGGCCCTTGGCCTGTCGTGTGGGCTGTGCTCCAGCTGGG
ATGGCGGCCTGGCTGGTTTCTGGACAGCCCCGACAGACCCTGGAACCCCCCTA
CATTTTCCCCTGCCCTGCTGGTTCGTGACCGAGGGCGACAATGCCACCTTCACCT
GTAGCTTCAGCAACACCAGCGAGAGCTTCGTGCTGAACTGGTACAGAATGAGC
CCCAGCAACCAGACCGACAAGCTGGCCGCCTTCCCCGAGGATAGATCTCAGCC
CGGCCAGGACTGCCGGTTCAGAGTGACCCAGCTGCCCAACGGCCGGGACTTC
CACATGTCTGTTCGTGCGGGCCAGACGGAACGACAGCGGCACATATCTGTGCGG
CGCCATCAGCCTGGCCCCCAAGGCCAGATCAAAGAGAGCCTGAGAGCCGAG
CTGAGAGTGACCGAGAGAAGGGCCGAAGTGCCCTACCGCCCACCCTAGCCCATC
TCCAAGACCTGCCGGCCAGATTATCTCATTCTTCCTGGCCCTGACCTCTACCGC
CCTGCTGTTTCTGCTGTTCTTTCTGACCCTGCGGTTTCAGCGTCGTGAAGCGGG
GCAGAAAGAAGCTGCTGTACATCTTCAAGCAGCCCTTCATGCGGCCCGTGCA
GACCACCCAGGAAGAGGACGGCTGCTCCTGCCGGTTTCCCGAGGAAGAAGA
GGGGGGCTGCGAGCTCTAA

ATG start codon

TAA stop codon

PD-1 domains

4-1BB domains

pGEM vector:

GTTCGAC...**ATG**...**TAA****GAATTC**

GTTCGAC HincII restriction site

GAATTC EcoRI restriction site

PD-1tm:BB

5' -> 3'

ATGCAGATTCTCAGGCTCCTTGGCCTGTCGTGTGGGCCGTGCTCCAGCTGGG
ATGGCGGCCTGGATGGTTCCTGGACAGCCCCGACAGACCCTGGAACCCCCCTA
CATTTTCCCCTGCCCTGCTGGTTCGTGACCGAGGGCGACAATGCCACCTTCACCT
GTAGCTTCAGCAACACCAGCGAGAGCTTCGTGCTGAACTGGTACAGAATGAGC
CCCAGCAACCAGACCGACAAGCTGGCCGCCTTCCCCGAGGATAGATCTCAGCC
CGGCCAGGACTGCCGGTTCAGAGTGACCCAGCTGCCCAACGGCCGGGACTTC
CACATGTCTGTTCGTGCGCGCCAGACGGAACGACAGCGGCACATATCTGTGCGG
CGCCATCAGCCTGGCCCCCAAGGCCAGATCAAAGAGAGCCTGAGAGCCGAG
CTGAGAGTGACCGAGAGAAGGGCCGAAGTGCCTACCGCCCACCCTAGCCCATC
TCCAAGACCTGCCGGCCAGTTCCAGACACTGGTTCGTGGGAGTCGTGGGCGGC
CTGCTGGGATCTCTGGTGCTGCTCGTGTGGGTGCTGGCCGTGATCA**AAGCGGG**
GCAGAAAGAAGCTGCTGTACATCTTCAAGCAGCCCTTCATGCGGCCCGTGCA
GACCACCAGGAAGAGGACGGCTGCTCCTGCCGGTTTCCCGAGGAAGAAGA
GGGGGGCTGCGAGCTCTAA

ATG start codon

TAA stop codon

PD-1 domains

4-1BB domains

pGEM vector:

GTTCGAC...**ATG**...**TAA****GAATTC**

GTTCGAC HincII restriction site

GAATTC EcoRI restriction site

5.5.2 Murine chimeric receptor DNA sequence

mPD-1:28tm

5' -> 3'

ATG TGGGTCCGCCAGGTGCCATGGTCCTTCACCTGGGCCGTGCTGCAGCTGTC
CTGGCAGAGCGGCTGGCTGCTGGAAGTGCCCAACGGCCCTTGGAGAAGCCTG
ACCTTCTACCCCGCCTGGCTGACCGTGTCTGAGGGCGCCAACGCCACCTTCAC
CTGTAGCCTGAGCAATTGGAGCGAGGACCTGATGCTGAACTGGAACAGACTGA
GCCCCAGCAACCAGACCGAGAAGCAGGCCCGCCTTCTGCAACGGCCTGAGCCA
GCCTGTGCAGGACGCCAGATTCCAGATCATCCAGCTGCCCAACAGACACGACT
TCCACATGAACATCCTGGACACCCGCAGAAACGACAGCGGCATCTACCTGTGC
GGCGCCATCAGCCTGCACCCCAAGGCCAAGATCGAGGAAAGCCCTGGCGCCG
AGCTGGTGGTGACAGAGAGAATCCTGGAAACCAGCACTAGATAACCCAGCCCC
AGCCCTAAGCCCGAGGGCAGATTCCAGGGCATGTTCTGGGCTCTGGTGGTGGT
GGCCGGCGTGCTGTTTTGTTACGGCCTGCTCGTGACCGTGGCCCTGTGCGTGA
TCTGGACCAACAGCAGAAGAAACAGACTGCTGCAGAGCGACTACATGAACAT
GACCCCCAGAAGGCCTGGCCTGACCAGAAAGCCCTACCAGCCTTACGCCCT
GCCAGAGACTTCGCCGCCTACAGACCT TGA

ATG start codon

TGA stop codon

PD-1 domains

CD28 domains

pMP71 vector:

GCGGCCGC...**ATG**...**TAA****GAATTC**

GCGGCCGC NotI restriction site

GAATTC EcoRI restriction site

5.6 Antibodies for cell culture and flow cytometry analyses

5.6.1 Antibodies with anti-human specificities for cell culture

SPECIFICITY	SPECIES/ ISOTYPE	CLONE	COMPANY	CONCENTRATION
CD3	Mouse IgG2a	OKT3	In-house production	5 µg/ml (T cell activation) 5 µg/1 x 10 ⁶ P815 (P815 loading for co-culture)
CD28	Mouse IgG1	CD28.2	BD	1 µg/ml (T cell activation) 5 µg/1 x 10 ⁶ P815 (P815 loading for co-culture)
PD-1 (CD279)	Mouse IgG1	EH12.2H7	BioLegend	20 µg/ml (blocking experiments)
PD-L1 (CD274)	Mouse IgG2b	29E.2A3	BioLegend	20 µg/ml (blocking experiments)

5.6.2 Antibodies with anti-human specificities for flow cytometry

SPECIFICITY	FLUORO- CHROME	SPECIES/ ISOTYPE	CLONE	COMPANY	DILUTION
CD3ε	PB	Mouse IgG1	SK7	BioLegend	1:17
	PE-Cy7	Mouse IgG1	SK7	BioLegend	1:20
CD4	APC-eF780	Mouse IgG1	RPA-T4	eBioscience	1:25
CD8α	PB	Mouse IgG1	RPA-T8	BD	1:25
	V500	Mouse IgG1	RPTAT8	BD	1:25
CD11c	APC	Mouse IgG1	B-Ly6	BD	1:5
CD45	PE-Cy7	Mouse IgG1	HI30	BioLegend	1:50
HLA-A2	Unconjugated	Mouse IgG1	HB54	In-house production	undiluted
Isotype	FITC	Mouse IgG1	MOPC21	BD	1:10
PD-1	APC	Mouse IgG1	MIH4	eBioscience	1:25
	PE	Mouse IgG1	MIH4	eBioscience	1:25
PD-L1 (CD274)	FITC	Mouse IgG1	M1H1	BD	1:5

SPECIFICITY	FLUOROCROME	SPECIES/ISOTYPE	CLONE	COMPANY	DILUTION
p-ERK (pT202/pY204)	Unconjugated	Rabbit IgG	D13.14.4E	Cell Signaling	1:300
p-RPS6 (pS235/236)	APC	Rabbit IgG	D57.2.2E	Cell Signaling	1:50
Tyrosinase	Unconjugated	Mouse IgG2a	T311	Upstate Biotechnology	1:50

A647: Alexa 647

APC-eF780: Allophycocyanin – eFluor 780

P: Phosphorylated

PE: Phycoerythrin

PerCP-Cy5.5: Peridinin-chlorophyll – Cyanine 5.5

T: Threonine

V500: Violet 500

APC: Allophycocyanin

FITC: Fluorescein isothiocyanate

PB: Pacific Blue

PE-Cy7: Phycoerythrin – Cyanine 7

S: Serine

Y: Tyrosine

5.6.3 Antibodies with anti-mouse specificities for cell culture

SPECIFICITY	SPECIES/ISOTYPE	CLONE	COMPANY	CONCENTRATION
CD3	Armenian hamster IgG1	145-2C11	BD	1 µg/ml (T cell activation)
CD28	Syrian hamster IgG2	37.51	BD	0.1 µg/ml (T cell activation)

5.6.4 Antibodies with anti-mouse and anti-rabbit specificities for flow cytometry

SPECIFICITY	FLUOROCROME	SPECIES/ISOTYPE	CLONE	COMPANY	DILUTION
CD3	APC-Cy7	Armenian Hamster IgG	145-2C11	Biolegend	1 :50
CD4	A700	Rat IgG2a	RM4-5	BD	1:100
CD8	BV421	Rat IgG2a	53-6.7	BioLegend	1:100
CD19	V450	Rat IgG2a	1D3	eBioscience	1:100
CD45	PE-Cy7	Rat IgG2b	30-F11	BD	1:100
H2-D ^b	PE	Mouse IgG2b	KH95	BD	1:100

SPECIFICITY	FLUOROCROME	SPECIES/ISOTYPE	CLONE	COMPANY	DILUTION
Large and small T antigens	FITC	Mouse IgG2a	Pab108	BD	1 :50
Mouse IgG1	FITC	Rabbit IgG	Poly-clonal	Dako	1:20
Mouse IgG2a	A647	Rabbit IgG	Poly-clonal	Invitrogen	1:500
PD-1	PerCP-Cy5.5	Rat IgG2a	29F.1A12	BioLegend	1:100
PD-L1	PE	Rat IgG2a	MIH5	BD	1:50
Rabbit IgG	A647	Goat IgG	Poly-clonal	Invitrogen	1:500
TCR β constant region	PB	Armenian Hamster IgG	H57-597	BioLegend	1:25
Thy1.1	A647	Mouse IgG1	OX7	BioLegend	1:100

A647: Alexa 647

APC-Cy7: Allophycocyanin – Cyanine 7

PB: Pacific blue

PerCP-Cy5.5: Peridinin-chlorophyll – Cyanine 5.5

V450: Violet 450

A700: Alexa 700

BV421: Brilliant violet 421

PE-Cy7: Phycoerythrin – Cyanine 7

5.7 Primary cells and cell lines

CELL LINE	CHARACTERISTICS	CULTURE MEDIUM	SOURCE
HEK293 A2	Transduced to express HLA-A2	RCC medium	Kindly provided by Matthias Leisegang, Max Delbrück Center Berlin, GERMANY
HEK GaLV	Retroviral packaging cell line expressing gag, pol and env genes	HEK medium	Kindly provided by Wolfgang Uckert, Max Delbrück Center Berlin, GERMANY
HEK/Tyr	Transduced to express HLA-A2 and tyrosinase	RCC medium	Kindly provided by Matthias Leisegang, Max Delbrück Center Berlin, GERMANY
HEK/Tyr/PD-L1	Transduced to express HLA-A2, tyrosinase and PD-L1	RCC medium	Kindly provided by Matthias Leisegang, Max Delbrück Center Berlin, GERMANY

CELL LINE	CHARACTERISTICS	CULTURE MEDIUM	SOURCE
FM3	Melanoma cell line	RCC medium	Kindly provided by Perthor Straten, Herlev Hospital, Herlev, DENMARK
FM55	Melanoma cell line	RCC medium	Kindly provided by Perthor Straten, Herlev Hospital, Herlev, DENMARK
FM86	Melanoma cell line	RCC medium	Kindly provided by Perthor Straten, Herlev Hospital, Herlev, DENMARK
SKMel23	Melanoma cell line	RCC medium	Monica C. Panelli, NIH, Bethesda, USA
P815	Murine mastocytoma cell line	RCC medium	ATCC, Rockville, Maryland, USA
PlatE	Retroviral packaging cell line expressing gag, pol and env genes	HCC medium	Kindly provided by Wolfgang Uckert, Max Delbrück Center Berlin, GERMANY
TCR-I TCR-I/mPD-1:28 tm	T cells of TCR-I transgenic mice, MOCK- or mPD-1:28 tm - transduced TCR-I recognizes epitope I of simian virus large T antigen (SAINNYAQKL)	MTM	Kindly provided by Matthias Leisegang, Max Delbrück Center Berlin, GERMANY
434	Murine hepatocellular carcinoma cell line	HCC medium	Kindly provided by Gerald Willimsky, Max Delbrück Center Berlin, GERMANY

5.8 Blood samples

Drawing of blood samples from healthy donors was performed by trained personnel and approved by the local Ethics Committee. Donors gave their consent.

5.9 Patient samples

Clear cell renal cell carcinoma tissues and blood samples were kindly provided by the Urologische Klinik Dr. Castringius, Planegg, Germany. Tissue collection was approved by the local Ethics Committee and patients gave their consent. Tumors were classified according to the TNM system published by the UICC 2010.

PATIENT ID	TNM STATUS
RCC102	pT3a N0 M0 G2
RCC105	pT3a N0 M0 G3
RCC106	pT1a N0 M0 G2
RCC110	pT1b N0 M0 G2
RCC112	pT1a N0 M0 G2

5.10 Mice

The animal experiments were approved by the local authorities according to the legal regulations for animal experiments.

5.10.1 NSG mice

NOD/scid IL2Rg^{null} (NSG) mice were bred on the genetic background of non-obese diabetic (NOD) mice characterized by reduced innate immunity. NSG mice carry the *prkdc*^{scid} mutation, a loss-of-function mutation in the PRKDC gene, leading to defective repair of DNA strand breaks during V(D)J recombination in the development of B and T cells. This severe combined immunodeficiency (scid) is characterized by a major reduction of T and B cells. Additionally, NSG mice carry a null mutation in the IL-2 receptor gamma chain (IL2Rg^{null}) blocking NK cell differentiation. The impairment of innate immunity and absence of adaptive immunity render NSG mice a good model system for adoptive T cell therapy of human tumor xenografts.

NSG mice were obtained from Charles River.

5.10.2 LoxP-TAg mice

LoxP-TAg mice were bred on the background of C57BL/6 mice. They are transgenic for the oncogene simian virus large T antigen (TAg) that is separated from its β -actin/ β -globin promoter by a stop cassette preventing TAg expression (59). I.v. injection of adenovirus coding for Cre recombinase (Ad.Cre) leads to deletion of the stop cassette in the liver due to the tropism of adenovirus. Eight to 24 weeks after Ad.Cre injection, mice develop multinodular hepatocellular carcinoma (60, 61).

6 METHODS

6.1 Molecular biology methods

6.1.1 Cloning of chimeric co-stimulatory receptors into pGEM and pMP71 vectors

Chimeric co-stimulatory constructs were ordered at Geneart, Life Technologies, delivered as a lyophilized powder and dissolved in nuclease-free water at a concentration of 0.5 µg/µl.

For amplification TOP10 or MACH1 *E.coli* were chemically transformed with the Geneart constructs. Bacteria were thawed on ice, 1 µl of plasmid was added to the bacteria and incubated for 30 minutes on ice. Heat shock for 30 seconds at 42°C caused uptake of the DNA by the bacteria. They were placed on ice for 2 minutes, 350 µl of SOC medium was added and the bacteria incubated with gentle agitation at 37°C for 1 hour. 20 µl of transformed bacteria were plated on agar-coated Petri dishes containing 100 µg/ml Ampicillin. The plates were incubated over night at 37°C. After incubation separate colonies were picked using a pipette tip and added to a 10 ml tube containing 4 ml LB medium. The bacteria were incubated over night with agitation at 37°C. 200 µl of densely grown cultures were added to 300 ml of LB medium and again incubated over night with agitation at 37°C. Plasmid DNA was isolated using the Jetstar preparation kit. The bacteria cultures were centrifuged at 3400 g for 10 minutes at room temperature, the supernatant discarded and the pellet re-suspended in 10 ml re-suspending buffer E1 and transferred to a 50 ml tube. 10 ml of lysis buffer E2 was added and the collection tube inverted 10 times, thereafter 10 ml precipitation buffer E3 was added and the tube inverted again for 10 times. The suspension was centrifuged at 5000 g for 10 minutes at room temperature and the supernatant applied through a 70 µm filter onto an equilibrated column. The column was filled up with washing buffer E5 and the flow-through discarded. The column was placed on top of a 50 ml collection tube and the DNA eluted by adding 15 ml of elution buffer E6. 10.5 ml isopropanol was added to the DNA, mixed and centrifuged at 5000 g for 45 minutes at 4°C. The supernatant was discarded, the pellet dehydrated with 1 ml 75% ethanol, air-dried and re-suspended in nuclease-free

water. The concentrations of the plasmid DNAs were determined by quantification of UV absorbance at 260 nm using NanoDrop[®] spectrophotometer. UV absorbances at 230 nm and 280 nm were also detected to determine DNA purity. 260/280 and 260/230 ratios were above 1.8 indicating no contamination with proteins or salts, respectively. The plasmid DNAs were sent to Eurofins MWG for sequencing.

To clone the chimeric co-stimulatory receptors into the pGEM and pMP71 vector backbones 5-9 µg of plasmid DNA were mixed with the appropriate forward and reverse primers (see 5.4.2 Primers, final concentration 1.5 pmol/µl), 5% DMSO and 1x PCR Master Mix. Nuclease-free water was added to yield a final volume of 100 µl. Chimeric signaling receptor DNAs were amplified using the following program:

# OF CYCLES	STEP	TEMPERATURE	DURATION
1	Denaturation	94°C	5 minutes
35	Denaturation	94°C	5 minutes
	Annealing	62°C	30 seconds
	Polymerisation	72°C	1 minute
1	Final extension	72°C	5 minutes
	Hold	4	Infinite

The PCR products were run on a 1% agarose gel (in 1x TAE) containing ethidium bromide at 130 V for 45 minutes. To determine the size of the products, 1 kb DNA ladder was run simultaneously. The PCR products were cut out and purified using the Gel Extraction Kit from Qiagen. 1 ml of QG buffer was added to the gel pieces, incubated for 10 minutes in a water bath at 50°C. The liquid gel-buffer-mix was loaded onto a column and centrifuged for 30 seconds at 20000 g. The column was washed with 750 µl PE buffer and centrifuged for 30 seconds at 20000 g. To remove remaining buffer, the column was centrifuged twice for 1 minute at 20000 g. The column was placed on top of a 1.5 ml tube and DNA eluted by adding 45 µl of nuclease-free water onto the column. The column was incubated for 1 minute at room temperature and centrifuged for 30 seconds at 20000 g. This step was repeated to yield a final volume of 90 µl.

The pGEM and pMP71 vectors as well as the chimeric signaling receptor PCR products were digested using the appropriate enzymes (see 5.4.3 Enzymes). 10 µg of vector were mixed with CutSmart buffer (1:10) and 60 units of either EcoRI-high

fidelity (HF) and NotI-HF (pMP71) or EcoRI-HF and HindIII-HF or HincII (pGEM). Nuclease-free water was added to the vector-enzyme-mix to yield a final volume of 106 μ l. The vectors were digested for 1 hour at 37°C. The digested vectors were applied to a 1% agarose gel containing ethidium bromide at 130 V for 45 minutes. The vector backbones were cut out and purified using the Gel Extraction Kit from Quiagen (see above).

PCR products of chimeric signaling receptors were mixed with CutSmart buffer (1:10) and 60 units of either EcoRI-HF and NotI-HF (pMP71) or EcoRI-HF and HindIII-HF or HincII (pGEM). PCR products were digested for 1 hour at 37°C, applied to a 1% agarose gel containing ethidium bromide at 130 V for 45 minutes, cut out of the gel and purified using the MinElute[®] Reaction Cleanup Kit from Quiagen (procedure see purification above).

Vectors and PCR products were ligated by mixing 7 μ l of vector and 1 μ l of DNA coding for chimeric signaling receptors plus 400 units T4 ligase and T4 ligase buffer (1:10). The ligation mix was incubated ~ 16 hours at 16°C. TOP10 or MACH1 *E.coli* were transformed with 1 μ l of the ligation and plasmids were obtained from bacteria cultures (see above).

6.1.2 Generation of in vitro transcribed RNA from pGEM plasmids

pGEM plasmids coding for the chimeric signaling receptors were linearized by incubating 40 μ g of pGEM plasmid with 80 units SpeI-HF and CutSmart buffer (1:10). Nuclease-free water was added to a final volume of 100 μ l. The SpeI-HF recognition site is located behind a poly-A tail of ~ 116 bp. This poly-A tail is meant to increase the stability of in vitro transcribed (ivt) RNA. The linearization mix was incubated ~ 16 hours at 37°C. Then, 4 mM EDTA, 48 mM sodium acetate and 67% ethanol (all final concentration) were added to the DNA, incubated for 45 minutes at -20 °C and centrifuged for 15 minutes at 20000 g and 4°C.

Ivt-RNA was generated from linearized pGEM plasmids using the mMESSEGE mMACHINE Kit from Ambion. 3 μ g of linearized DNA was mixed with NTP/CAP (1x, 7-methyl guanosine cap and nucleotides), reaction buffer (1x) and T7 polymerase (1:10). Nuclease-free water was added to a final volume of 40 μ l. The mix was incubated for 2 hours at 37°C. DNase was added (1:20) and incubated for 30 minutes at 37°C. Ivt-RNA was purified using the RNeasy Mini Kit from Quiagen.

350 μ l RLT buffer and 250 μ l 100% ethanol were added to the ivt-RNA and loaded onto a column. The column was centrifuged at 20000 g for 30 seconds and washed 3 times with 500 μ l PE buffer. For the first 2 washing steps the column was centrifuged at 20000 g for 30 seconds and for the last washing step at 20000 g for 2 minutes. The column was placed onto a 1.5 ml tube and the ivt-RNA eluted by adding 40 μ l nuclease-free water onto the column. The column was incubated for 1 minute at room temperature and centrifuged for 1 minute at 20000 g. Concentrations of the ivt-RNAs were determined by quantification of UV absorbance at 260 nm using NanoDrop[®] spectrophotometer. The ivt-RNAs were run on 1% agarose gels (in 1 x TAE, DEPC-water) for quality control.

6.2 Cell culture techniques

6.2.1 Cultivation of human and murine cell lines and primary cells

All primary cells and cell lines were handled under sterile conditions and were grown at 37°C and 6.5% CO₂.

The human melanoma cell lines SKMel23, FM3, FM55 and FM86 as well as the murine mastocytoma cell line P815 were grown in T75 cm² tissue culture flasks with RCC medium until confluent and passaged 1:3-1:8 by detaching adherent cells with 2 x trypsin/EDTA.

HEK/Tyr and HEK/Tyr/PD-L1 were grown in T75 cm² tissue culture flasks with RCC medium until confluent and passaged 1:3 by detaching adherent cells by pipetting up and down.

The murine hepatocellular carcinoma cell line 434 and the retroviral packaging cell line PlatE were grown in T75 cm² culture flasks with MTM medium until confluent and passaged 1:8 by detaching adherent cells with 2 x trypsin/EDTA or by pipetting up and down, respectively.

The retroviral packaging cell line HEK GaLV was grown in T75 cm² culture flasks with HEK medium until confluent and passaged 1:8 by detaching adherent cells by pipetting up and down.

Human T cells of healthy donors were cultivated at 1-1.5 x 10⁶ cells/ml in T cell medium supplemented with 50 U/ml IL-2 and split every 2-3 days. They were cultivated in 24-well plates or in T75 cm² culture flasks.

Murine T cells were cultivated at $1-1.5 \times 10^6$ cells/ml in MTM medium supplemented with 50 U/ml IL-2. They were cultivated in 24-well plates or in T75 cm² culture flasks.

6.2.2 Thawing, counting and freezing of cells

For thawing, freezing vials containing frozen cells were placed in a water bath at 37°C. The suspension was transferred to a 15 ml tube containing FCS and centrifuged at 472 g for 5 minutes at room temperature. TILs were centrifuged at 300 g for 10 minutes. The supernatant was discarded and cell pellet re-suspended in the appropriate medium.

Cell numbers were determined using Neubauer counting chambers. To allow discrimination of viable and dead cells, cell suspensions were diluted with trypan blue (1:2 in PBS). Trypan blue is excluded from viable cells but passes the cell membrane of dead cells. TILs and peripheral blood mononuclear cells isolated from blood were counted in trypan blue (1:2 in PBS) containing 3% acetic acid to exclude erythrocytes.

The following formula was applied to determine cell numbers:

Cell number/ml = mean of cells counted in 4 big quadrants x dilution factor x chamber factor (10^4)

For long-term storage, cell pellets were re-suspended in ice-cold FCS and mixed with equal amounts of ice-cold cell freezing medium. Cells were frozen in 1 ml aliquots in freezing vials and stored at -80 °C until transfer to the gas phase of liquid nitrogen tanks.

6.2.3 Isolation of peripheral blood mononuclear cells from human blood samples

Syringes were supplemented with 10 IU heparin-sodium/ml blood. Blood samples were diluted 1:2 with RPMI-1640, layered over 20 ml Ficoll[®] 50 ml tubes and centrifuged without break for 20 minutes at 840 g and room temperature. Peripheral blood mononuclear cells (PBMCs) gather in the interphase between plasma and ficoll. PBMCs were transferred to 50 ml tubes, diluted 1:2 with RPMI-1640 and centrifuged at 758 g with break for 12 minutes at room temperature. The cell pellet was re-suspended in T cell medium, counted and used in experiments or frozen.

6.2.4 Isolation of TILs from human renal cell carcinoma

Human renal cell carcinoma (RCC) tissues were obtained from patients who underwent nephrectomy. Tumor and healthy tissues were dissected by pathologists and infiltrating lymphocytes were directly isolated. To this end, tissue samples (average size 4 cm x 2 cm x 1.5 cm) were placed in Petri dishes and cut into small pieces using scalpel and scissors. Dehydration of the tissue was prevented by adding HBSS (containing Ca^{2+} , Mg^{2+}). The cut tissue was transferred to a 50 ml tube and centrifuged with HBSS (containing Ca^{2+} , Mg^{2+}) for 2 minutes at 472 g and room temperature. This washing step was repeated until the supernatants appeared bloodless. Those supernatants contained cells, which did not deeply infiltrate into the tumor and are called tumor circulating lymphocytes (TCLs). To obtain TILs, the tissue was then digested for 30 minutes on a shaker at room temperature in digestion medium (6 ml buffer/ml tissue pellet). After centrifugation for 5 minutes at 472 g and room temperature the supernatant was placed on ice and the cell pellet re-suspended in HBSS without Ca^{2+} and Mg^{2+} and centrifuged as before. The supernatant was placed on ice and the pellet re-suspended in 5 mM EDTA in HBSS without Ca^{2+} and Mg^{2+} (6 ml/ml tissue pellet). After incubation for 30 minutes on a shaker at room temperature, the suspension was centrifuged as before, the supernatant placed on ice, the pellet re-suspended in HBSS (containing Ca^{2+} , Mg^{2+}) and centrifuged again. The supernatant was placed on ice, the tissue digested a second time in digestion buffer as described above. The suspension was centrifuged and the pellet transferred to a Petri dish. The tissue was squeezed between two Petri dishes until homogenous and filtered through a 70 μm filter. All supernatants were centrifuged at 472 g for 10 minutes at room temperature. All pellets were pooled but the ones containing TCLs separately from those containing TILs.

6.2.5 Transduction of human T cells

The transduction of human T cells comprised a 14 days-lasting protocol with day 0 being the day of PBMCs activation. The transduction was performed in a laboratory of S2 standard. All centrifugation steps of T cells or PBMCs were performed at 472 g and room temperature for 5 minutes, unless otherwise stated.

Day -1

The retroviral packaging cells HEK GaLV were seeded at 1.5×10^6 cells per Petri dish (100 mm) in 10 ml HEK medium.

Tissue culture treated 24-well plates were coated with 5 $\mu\text{g/ml}$ anti-human CD3 and 1 $\mu\text{g/ml}$ anti-human CD28 antibodies in 500 μl PBS per well. Plates were sealed with Parafilm[®] and kept at 4°C until the next day.

Day 0

470 μl of DMEM medium was mixed with 30 μl of TransIT[®]-LT1 transfection reagent and incubated for 5 minutes at room temperature. 12.5 μg of plasmid coding for the transgenes (TCR-T58 or -D115, chimeric co-stimulatory receptors) were added to the medium-transfection reagent-mix and incubated for 15 minutes at room temperature. The medium of HEK GaLV cells was replaced by RPMI basic supplemented with 10% FCS and the DNA-transfection-mix was added dropwise to the HEK GaLV cells.

The antibody mix on the 24-well plates was replaced with 2% BSA (in PBS). After incubation for 30 minutes at room temperature the plates were washed once with PBS. PBMCs of healthy donors were thawed, re-suspended in TCM supplemented with 100 U/ml IL-2 and seeded at 1×10^6 cells in 1 ml per well in antibody coated 24-well plates. Cultivation of PBMCs in anti-CD3 and anti-CD28 antibody coated wells with medium containing IL-2 induced activation and proliferation of T cells, a prerequisite for successful transduction.

Day 1

Non-tissue culture treated 24-well plates were coated with 10 $\mu\text{g/ml}$ RetroNectin[®] in 500 μl PBS per well. Plates were sealed with Parafilm[®] and kept at 4°C until the next day.

Day 2

RetroNectin[®] on the 24-well plates was replaced with 2% BSA (in PBS). After incubation for 30 minutes at room temperature the plates were washed once with PBS. The virus-containing medium of the HEK GaLV cells was harvested and centrifuged at 200 g for 10 minutes at 32°C. The supernatant was added to the RetroNectin[®] coated plates at 1 ml/well, plates were sealed with Parafilm[®] and

centrifuged for 90 minutes at 3200 g at 32°C. The plates for the second transduction were kept at 4°C.

Activated T cells were harvested and seeded at 0.5×10^6 cells in 1 ml per well in TCM supplemented with 100 U/ml IL-2 in virus-coated plates. As a control some T cells were seeded on plates coated with HEK GaLV medium not containing virus particles. These T cells are referred to as MOCK.

Day 3

T cells were split 1:4 into virus-coated plates from day 2 and provided with 750 μ l TCM and a final concentration of 100 U/ml IL-2.

Day 6

Transduced T cells were harvested, re-suspended in TCM supplemented with 100 U/ml IL-2 and seeded at $1-1.5 \times 10^6$ cell/ml in T75 cm² culture flasks.

Day 8

Transduced T cells were provided with fresh TCM supplemented with 100 U/ml IL-2.

Day 10 and day 13

Transduced T cells were provided with fresh TCM supplemented with 50 U/ml IL-2.

Day 15

Transduced T cells were harvested and used in experiments or frozen at $5-10 \times 10^6$ cells per vial.

6.2.6 Electroporation of human T cells and TILs

Electroporation cuvettes and Opti-MEM were cooled and ivt-RNA was thawed on ice. For experiments with T cells only, a 24-well plate was prepared with 1 ml/well TCM supplemented with 50 U/ml IL-2 and pre-warmed in the incubator. For experiments with TILs a 24-well plate was prepared with 1 ml/well TIL medium and pre-warmed in the incubator.

Human activated T cells MOCK-transduced or transduced to express the tyrosinase specific TCRs T58 or D115 were thawed, re-suspended in Opti-MEM and adjusted to

a concentration of $1.8 \times 10^6/200 \mu\text{l}$. T cells sorted from TILs (see 6.5.2) were re-suspended in $400 \mu\text{l}$ Opti-MEM. Sorting yielded cell number between $0.4\text{-}0.8 \times 10^6$. $200 \mu\text{l}$ of cells were transferred to an electroporation cuvette, incubated for 10 seconds on ice, $20 \mu\text{g}$ (unless otherwise stated) ivt-RNA coding for the co-stimulatory receptors was added and the cuvette was incubated for 10 seconds on ice. The cuvette was placed in the electroporator and the cells were pulsed with 900 V for 2.3 ms . The cuvette was removed from the electroporator and $200 \mu\text{l}$ of TCM supplemented with 50 U/ml IL-2 (for experiments with T cells only) or $200 \mu\text{l}$ of TIL medium was added to the cuvette. The cuvette was tilted and the cells poured into the 24-well plates with pre-warmed medium. The cuvette was rinsed 3 times with the appropriate medium. Electroporated cells were incubated 3-4 hours before use in experiments.

6.3 Functional assays

6.3.1 Loading of P815 with OKT3, anti-CD28 or PD-L1/Fc chimera

P815 cells were detached with accutase, centrifuged at 472 g for 5 minutes at room temperature, re-suspended in Opti-MEM, counted and loaded at $5 \mu\text{g}/1 \times 10^6$ cells with each OKT3 and PD-L1/Fc chimera. P815 were incubated on a shaker for 30 minutes at room temperature, washed once with Opti-MEM, re-suspended in TIL medium, counted and used in experiments.

6.3.2 Co-culture of human T cells or TILs with target cells

Target cells were detached by trypsination (melanoma cell lines), accutase (P815) or pipetting up and down (HEK/Tyr, HEK/Tyr/PD-L1), centrifuged at 472 g for 5 minutes at room temperature, re-suspended in either TCM (experiments with transduced T cells) or TIL medium (experiments with TILs) and counted.

Transduced and electroporated T cells, TILs and PBMCs were harvested or thawed, re-suspended in either TCM (experiments with transduced T cells) or TIL medium (experiments with TILs) and counted. Transduced and electroporated T cells as well as PBMCs used in experiments with TILs served as controls and were cultivated in TIL medium.

Transduced and electroporated T cells were cultivated in 96-well plates at 0.025×10^6 cells in 100 μl with 0.05×10^6 target cells in 100 μl TCM with or without 20 $\mu\text{g/ml}$ blocking antibodies to PD-1 and PD-L1.

TILs and transduced and electroporated T cells as well as PBMCs used in the same experiment were cultivated in 96-well plates at 0.1×10^6 cells in 50 μl with 0.1×10^6 target cells in 50 μl TIL medium. As a control effector and target cells were cultivated alone. Co-culture supernatants were harvested after ~ 16 hours and stored at -20°C until analysis by ELISA or Bio-Plex.

6.3.3 Chromium release assays

The lytic activity of T cells was assessed by cell mediated lysis assays. Target cells labeled with radioactive $^{51}\text{Chromium}$ release $^{51}\text{Chromium}$ when they are lysed by T cells. The amount of lysed cells is calculated from the amount of radioactivity in the co-culture supernatant.

One $\times 10^6$ target cells were re-suspended in 100 μl FCS and labeled with 50 μCi $^{51}\text{Chromium}$ for 1 hour at 37°C . Target cells were washed twice with CML medium.

T cells were added 50 $\mu\text{l/well}$ in CML medium to 96-well plates at the respective effector:target cell ratio. $^{51}\text{Chromium}$ -labeled target cells were added to T cells at 2000 cells in 50 $\mu\text{l/well}$. T and target cells were co-cultured at 37°C . To determine the maximal amount of radioactivity, 50 μl of $^{51}\text{Chromium}$ -labeled target cells were directly pipetted to a filter plate (Luma plate). After 4 hours of co-culture 50 μl of the supernatant were pipetted to the filter plate. Target cells cultivated alone served as an indicator of spontaneous lysis.

The filter plates were allowed to dry overnight. The scintillator within in the plates is excited by the Gamma radiation of released $^{51}\text{Chromium}$ and emits light that was detected by the scintillation counter TopCount. The following formula was applied to calculate specific cell lysis:

$$\% \text{ cell lysis} = \frac{\text{measured } ^{51}\text{Cr-release} - \text{spontaneous } ^{51}\text{Cr-release}}{(\text{max. } ^{51}\text{Cr-release}/2) - \text{spontaneous } ^{51}\text{Cr-release}} \times 100$$

6.3.4 Detection of cytokines by enzyme-linked-immunosorbent assays (ELISA)

Culture and co-culture supernatants were analyzed for IL-2 and IFN- γ by “sandwich” ELISA. Capture antibodies against IL-2 or IFN- γ are bound to 96-well plates and bind cytokines within the samples to be analyzed. Bound cytokine can be detected by a second biotin-labeled antibody recognizing a different epitope of the cytokine. The biotin-labeled antibody is bound by peroxidase-conjugated avidin which in turn converts the substrate 3,3',5,5'-tetramethylbenzidine and hydrogen peroxide into a colored product, which is detected by a spectrophotometer set to 405 nm. The color intensity of the product is proportional to bound cytokine. A standard cytokine solution is diluted serially and the standard curve is plotted as the standard cytokine concentration against detected optical density. The concentrations (pg/ml) of cytokine within the samples tested can be interpolated from the standard curve.

IL-2 and IFN- γ ELISAs were performed according to the manufacturer's protocol. 96-well plates were coated with 50 μ l/well capture antibody (1:250 in coating buffer) at 4°C for ~ 16 hours. The plates were washed 5 times with 300 μ l/well washing buffer, blocked with 1% milk powder (in Milli-Q[®] purified water) for 1 hour at room temperature and washed again 3 times. 50 μ l culture and co-culture supernatants as well as serially diluted standard were incubated on the plates for 1 hour at room temperature, the plates were washed 5 times and 100 μ l detection antibody plus peroxidase-conjugated avidin (both 1:250 in 1% milk powder) were incubation on the plates for 1 hour at room temperature. To remove unbound enzyme the plates were washed 5 times. 50 μ l/well of substrate were added to the plates and incubated for 15 minutes at room temperature. The reaction was stopped by adding 50 μ l/well 1 M phosphoric acid. The optical density of the samples was detected using the “ELISA reader sunshine” and concentration of cytokine calculated by the software Tecan. Culture and co-culture supernatants of human and murine transduced T cells were acquired as duplicates. Co-culture supernatants of human TILs were acquired as single measurements due to insufficient cell yield.

The transduced TCRs T58 and D115 are only functional in CD8⁺ T cells. To compensate for varying transduction efficiencies and CD8⁺/CD4⁺ T cell ratios, the percentage of TCR+CD8⁺ T cells within the cell suspension was analyzed by flow

cytometry (FC) and used to calculate the amount of produced cytokine by a cell population being 100% TCR+CD8+:

$$\text{cytokine produced by } 100 \% \text{ TCR+CD8+ T cells} = \frac{\text{cytokine concentration measured}}{\% \text{ TCR+CD8+ T cells detected by FC}} \times 100$$

6.3.5 Detection of cytokines by Bio-Plex analysis

Co-culture supernatants of human TCR-transduced chimeric receptor-electroporated T cells and target cells as well as of murine TILs/splenocytes and target cells or PMA/I were analyzed for cytokine content by Bio-Plex. Capture antibodies coupled to beads containing fluorescent dyes bind cytokines within the sample. Biotinylated detection antibodies bind a different epitope of the cytokines and react with streptavidin-PE conjugates. The fluorescent dyes within the beads allow distinction of different beads and thus facilitate the simultaneous detection of various cytokines.

Cytokine Bio-Plex was performed according to the manufacturer's protocol. Cytokine standard was dissolved in 500 μl of the according culture medium (TCM or MTM) and incubated for 30 minutes at 4°C. 128 μl of the dissolved standard were mixed with 72 μl culture medium and serially diluted. 100 μl of assay buffer were pipetted onto the filter plates and flushed through the filter with a vacuum pump. 50 μl of 1:10 diluted fluorescently dyed beads conjugated with antibodies recognizing specific cytokines were added to the plates which were immediately washed twice with 100 μl washing buffer. 50 μl of standard solutions (in duplicates) and 50 μl of samples (single measurements) were added to the plates and incubated for 30 minutes on a shaker at room temperature. The plates were washed as described above, 25 μl /well of biotinylated detection antibody (1:10 in detection antibody diluent) were added and incubated 30 minutes on a shaker at room temperature. The plates were washed as described, 50 μl /well of streptavidin-PE (1:100 in assay buffer) were added and incubated for 10 minutes on a shaker at room temperature. The plates were washed as described and 125 μl /well of washing buffer were added and the amount of cytokine detected using Bio-Plex-Array-Reader. The fluorescent dyes within the beads allow identification of detected cytokine and the signal emitted by PE is translated in concentration of cytokine (pg/ml).

The amount of cytokines secreted by human TCR-transduced chimeric signaling receptor-electroporated T cells was calculated as cytokine produced by a cell population being 100% TCR+CD8+ (see section 6.3.4).

6.4 Flow cytometry

6.4.1 Principle of flow cytometry

Flow cytometry allows the detection of physical properties as well as surface and intracellular marker expression of cells or particles. Cells or particles within the suspension to be analyzed are separated in a laminar flow and pass through laser beams individually. The emitted light provides information on the size of cells (forward scatter) and their granularity (sideward scatter). In addition, the expression of surface and intracellular markers can be analyzed with the help of fluorochrome-conjugated antibodies. The photons emitted by different fluorochromes are detected and digitalized by photomultiplier tubes. Filters separating the photons of different fluorochromes allow simultaneous analysis of various markers.

In this thesis the cytometer LSRII by BD was used for flow cytometry analysis of cells. The LSRII contains 4 different lasers (355 nm, 405 nm, 488 nm and 633 nm) allowing simultaneous detection of 18 fluorochromes. Table 1 shows characteristics of used fluorochromes, lasers and filters.

Table 1: Characteristics of used fluorochromes, lasers and filters for detection at the LSRII.

FLUORO-CHROME	EXCITATION MAXIMUM (NM)	EMISSION MAXIMUM (NM)	LASER	LASER WAVE-LENGTH (NM)	DETECTION FILTER (NM)
7-AAD	543	655	Blue laser	488	630/30
A647	650	668	Red laser	633	660/20
A700	696	719	Red laser	633	660/20
APC	650	660	Red laser	633	660/20
APC-eF780	650	780	Red laser	633	780/60
APC-Cy7	650	785	Red laser	633	780/60
BV421	407	421	Violet laser	405	450/50
FITC	494	520	Blue laser	488	530/30
PB	401	452	Violet laser	405	450/50
PE	496	578	Blue laser	488	575/26
PE-Cy7	496	785	Blue laser	488	780/60
PerCP-Cy5.5	482	695	Blue laser	488	695/40
PI	535	617	UV laser	355	610/20
V450	404	448	Violet laser	405	450/50
V500	415	500	Blue laser	488	525/20

7-AAD: 7-Actinomycin

A700: Alexa 700

APC-Cy7: Allophycocyanin – Cyanine 7

BV421: Brilliant violet 421

PB: Pacific blue

PE-Cy7: Phycoerythrin – Cyanine 7

PI: Propidium iodide

V500: Violet 500

A647: Alexa 647

APC: Allophycocyanin

APC-eF780: Allophycocyanin – eFluor 780

FITC: Fluorescein isothiocyanate

PE: Phycoerythrin

PerCP-Cy5.5: Peridinin-chlorophyll – Cyanine 5.5

V450: Violet 450

If more than one fluorochrome is detected, the fluorescence spillover of one fluorochrome into the detector of another one has to be compensated. To this end, along with the analyzed samples beads labeled with only one fluorochrome have to be acquired. Those so-called CompBeads[®] are polystyrene microparticles binding any κ light chain bearing immunoglobulin of mouse, rat or hamster origin. In addition, there are negative CompBeads[®] with no binding capacity. Both types of beads were

mixed 1+1 and stained with 1 fluorochrome labeled antibody that was used in the respective staining combination. CompBeads[®] were acquired for all fluorochromes used and with the same PMT settings as the labeled samples. Data acquired with the LSRII was analyzed using FlowJo[®] software.

6.4.2 Staining of cell surface and intracellular markers

All centrifugation steps were performed at 472 g for 5 minutes at room temperature. However, TILs were centrifuged at 300 g for 10 minutes at room temperature. Incubation was performed in the dark and on ice unless otherwise stated.

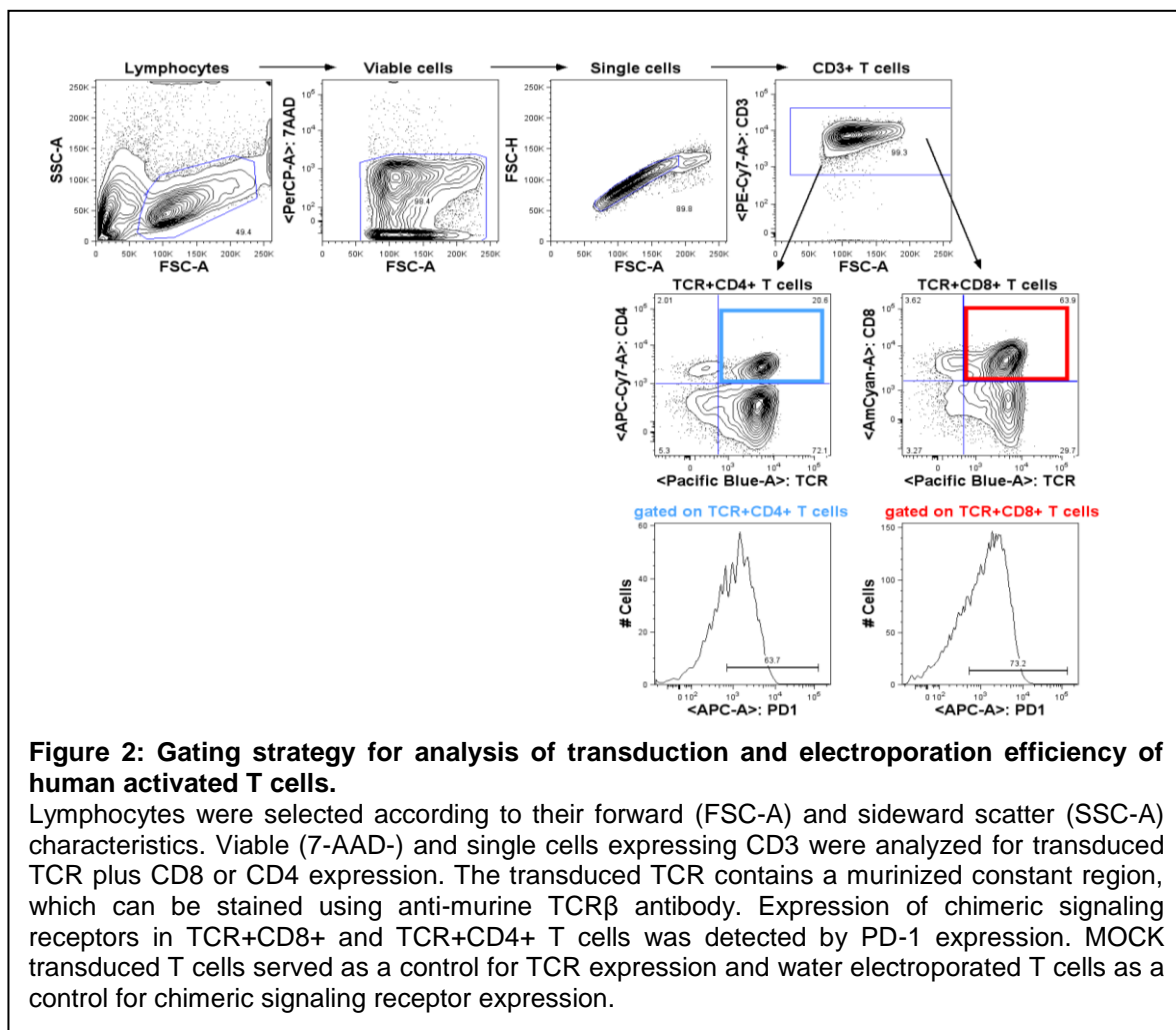
Cells ($0.05-0.2 \times 10^6$) were transferred into 1 ml FACS tubes, washed with 500 μ l FACS buffer and the supernatant removed leaving 50 μ l in the tube. Antibodies to surface markers (see 6.4.3 Staining combinations) and 7-AAD discriminating live and dead cells were added and incubated for 30 minutes. Cells were washed as described above and acquired on the LSRII. When intracellular markers were included in the analysis it was proceeded as follows: For fixation cells were re-suspended with 500 μ l 1% paraformaldehyde and incubated for 20 minutes. After centrifugation cells were permeabilized with 0.1% saponin, incubated for 30 minutes, centrifuged, incubated with 0.35% saponin for 30 minutes and centrifuged again. The supernatant was removed leaving 50 μ l in the tube. Antibodies to intracellular markers were added and incubated for 30 minutes. Cells were washed with 500 μ l 0.1% and 0.35% saponin and when staining included non-labeled primary antibodies incubated with secondary antibodies for 30 minutes. Finally, cells were washed with 500 μ l 0.35% saponin and acquired on the LSRII.

6.4.3 Staining combinations and gating strategies

6.4.3.1 Analysis of transduction and electroporation efficiency of human T cells and TILs

Table 2: Staining combination for analysis of transduction and electroporation efficiency of human activated T cells

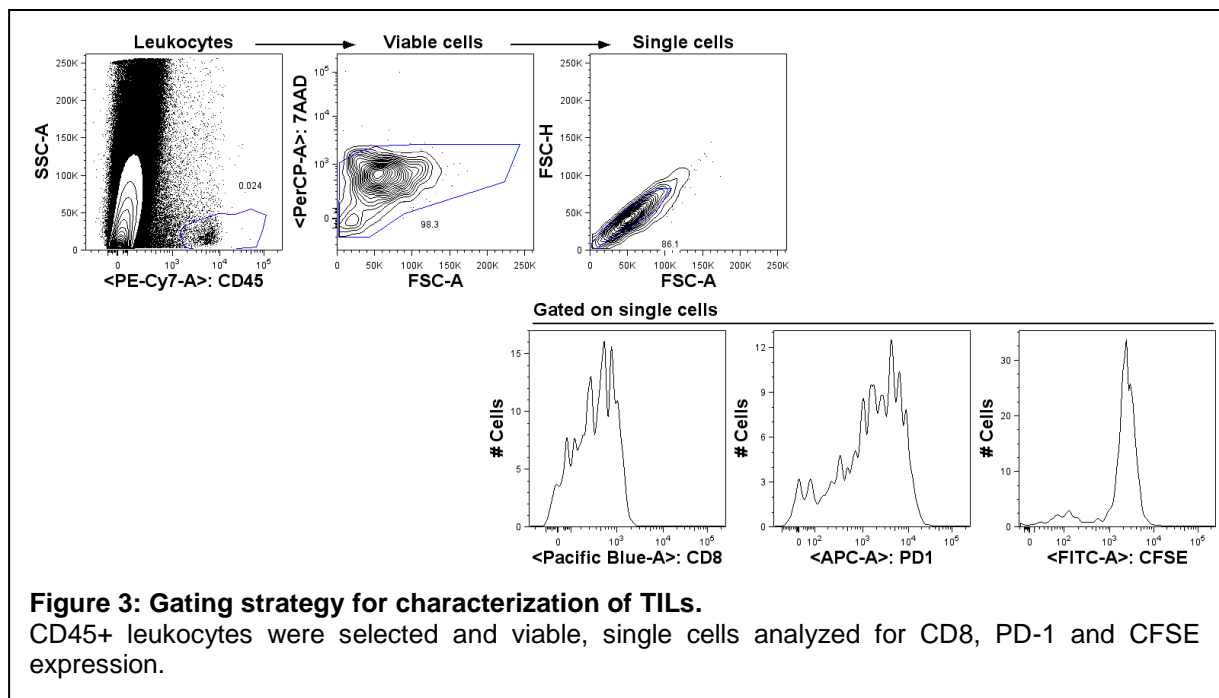
MARKER/FEATURE	FLUOROCHROME	STAINING
CD3	PE-Cy7	Cell surface
CD4	APC-eF780	Cell surface
CD8	V500	Cell surface
Murine TCR β -chain	PB	Cell surface
PD-1	APC	Cell surface
Viability	7-AAD	Cell surface



6.4.3.2 Analysis of T cells isolated from melanoma xenografts in NSG mice

Table 3: Staining combination for analysis of T cells isolated from human melanoma xenografts

MARKER/FEATURE	FLUOROCHROME	STAINING
CD4	APC-A780	Cell surface
CD8	PB	Cell surface
CD45	PE-Cy7	Cell surface
PD-1	APC	Cell surface
Proliferation	CFSE	Intracellular
Viability	7-AAD	Cell surface



6.4.3.3 Analysis of transduction efficiency of murine T cells and characterization of murine TILs and splenocytes

Table 4: Staining combination for analysis of transduction efficiency and T cell phenotype

MARKER/FEATURE	FLUOROCHROME	STAINING
Bcl-2	FITC	Intracellular
CD3	APC-Cy7	Intracellular
CD4	A700	Intracellular
CD8	BV421	Intracellular
CD62L	PE-Cy7	Cell surface
PD-1	PerCP-Cy5.5	Intracellular
Thy1.1	A647	Intracellular

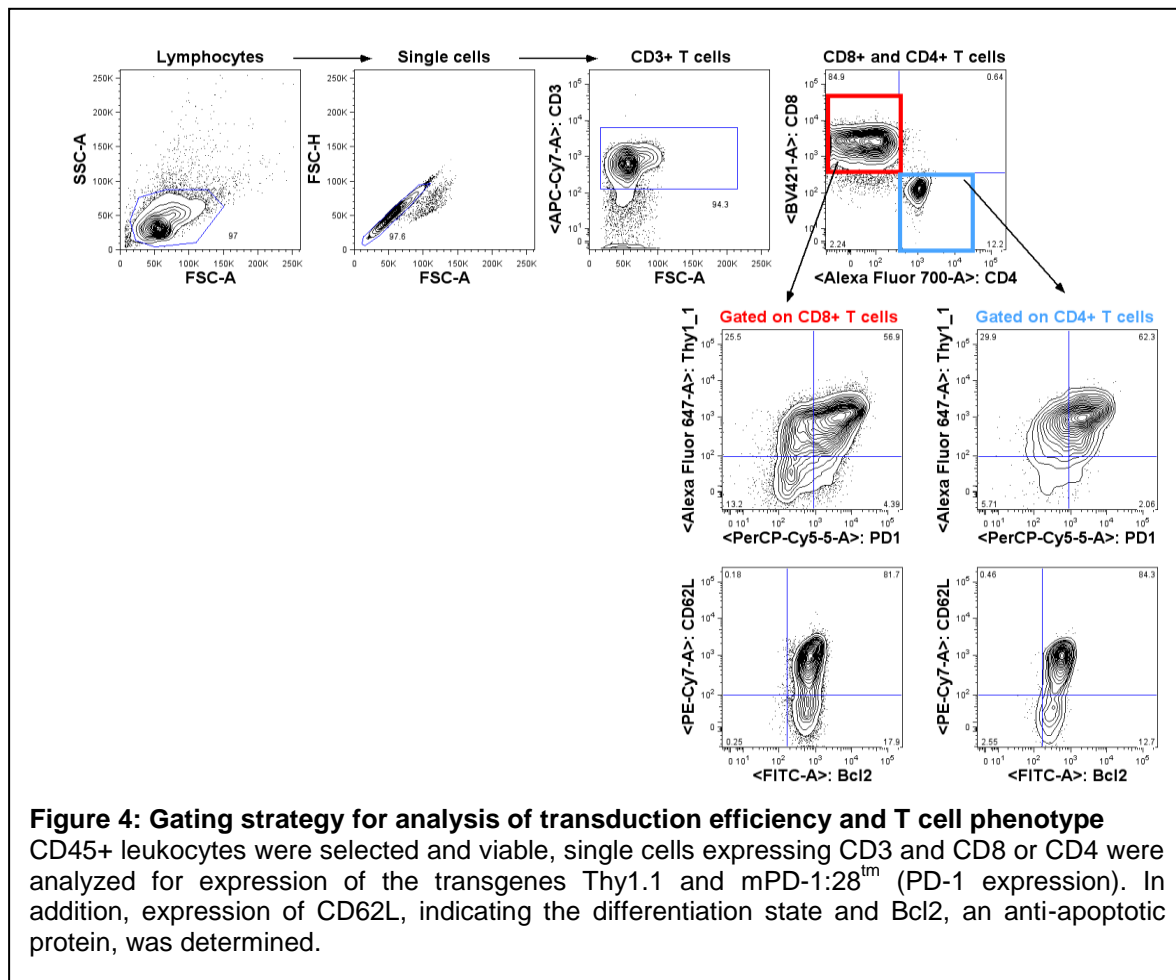
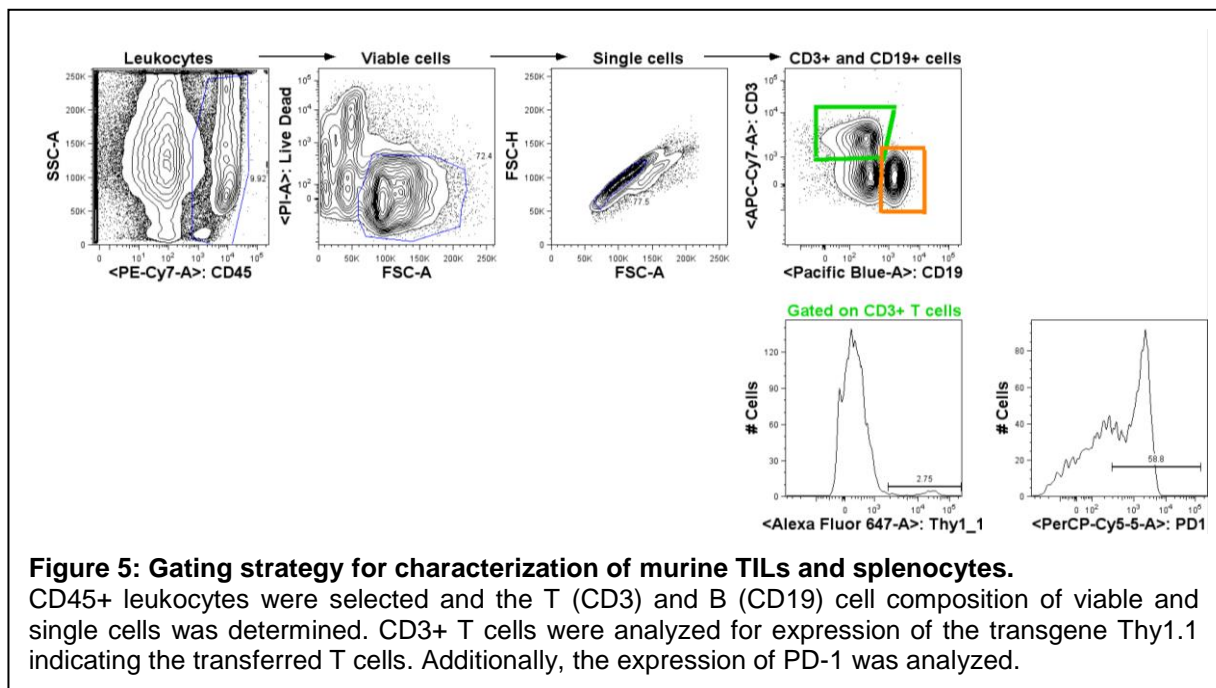


Table 5: Staining combination for characterization of murine TILs and splenocytes

MARKER/FEATURE	FLUOROCHROME	STAINING
CD3	APC-Cy7	Cell surface
CD19	V450	Cell surface
CD45	PE-Cy7	Cell surface
PD-1	PerCP-Cy5.5	Cell surface
Thy1.1	A647	Cell surface
Viability	PI	Cell surface



6.4.3.4 Characterization of tumor and transduced HEK293 cells

Table 6A-C: Staining combinations for melanoma, HEK/Tyr and HEK/Tyr/PD-L1 cells

A

MARKER/FEATURE	FLUOROCHROME	STAINING
HLA-A2	unconjugated	Cell surface
Mouse IgG	FITC	Cell surface
Viability	7-AAD	Cell surface

B

MARKER/FEATURE	FLUOROCHROME	STAINING
PD-L1	FITC	Cell surface
Viability	7-AAD	Cell surface

C

MARKER/FEATURE	FLUOROCHROME	STAINING
Tyrosinase	unconjugated	Intracellular
Mouse IgG2a	A647	Intracellular
Viability	7-AAD	Cell surface

Table 7A-C: Staining combinations the hepatocellular carcinoma cell line 434.

A

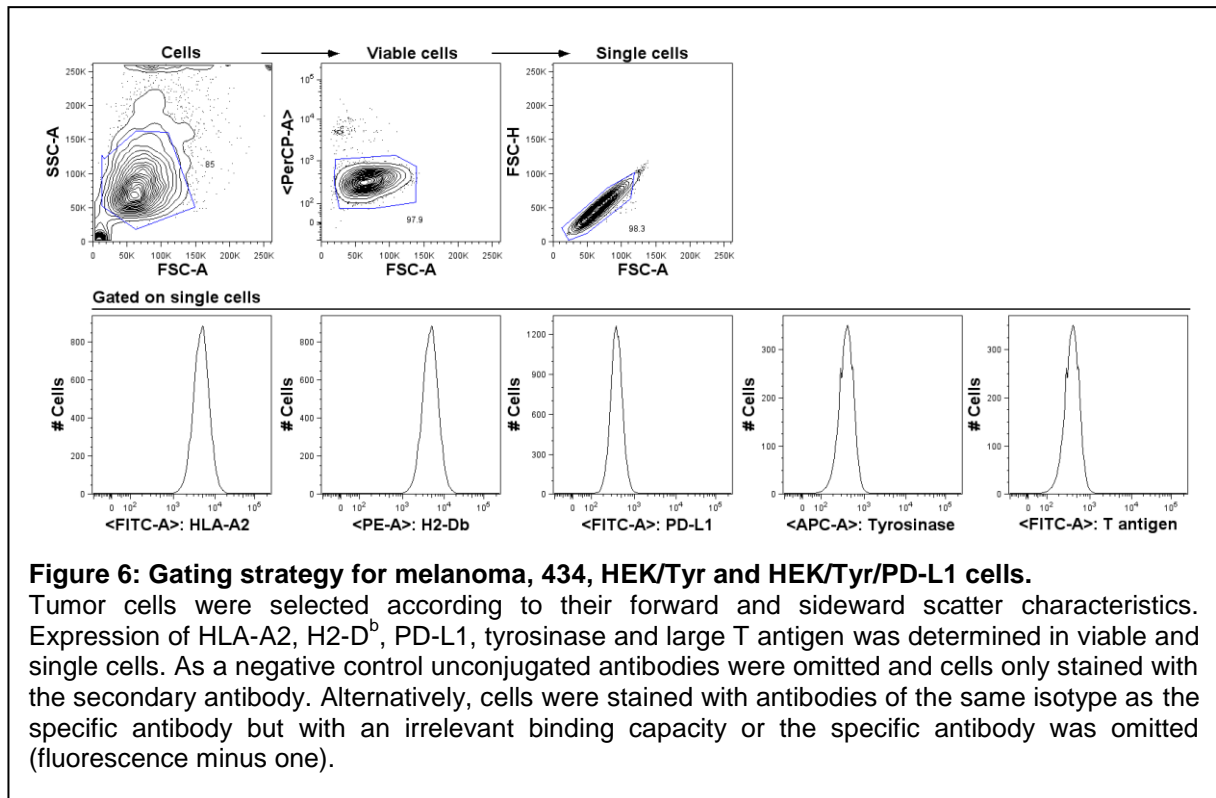
MARKER/FEATURE	FLUOROCHROME	STAINING
H2-D ^b	PE	Cell surface
Viability	7-AAD	Cell surface

B

MARKER/FEATURE	FLUOROCHROME	STAINING
PD-L1	PE	Cell surface
Viability	7-AAD	Cell surface

C

MARKER/FEATURE	FLUOROCHROME	STAINING
Large T antigen	FITC	Cell surface
Viability	7-AAD	Cell surface



6.4.4 Staining of phosphorylated signaling proteins

TCR-T58-transduced, chimeric signaling receptor-electroporated T cells were harvested, re-suspended in RPMI basic and 0.2×10^6 cells were transferred into 1 ml FACS tubes. The cells were centrifuged and supernatant removed leaving 50 μ l in the tube. Antibodies to CD45 and CD8 as well as 7-AAD (table 8) were added and incubated for 20 minutes at room temperature. Cells were washed with 500 μ l RPMI basic and stimulated with 0.2×10^6 HEK/Tyr/PD-L1 cells in 200 μ l RPMI basic for 30 minutes at 37°C. The reaction was stopped by adding 400 μ l Phosflow Cytfix Buffer[®]. After incubation for 15 minutes at 37°C, cells were centrifuged, re-suspended in 500 μ l Phosflow Perm Buffer III[®], incubated for 30 minutes on ice and centrifuged again. The cells were washed with 500 μ l FACS buffer and the supernatant removed leaving 50 μ l in the tube. Antibodies to p-ERK and p-RPS6 were added and incubated for 30 minutes on ice. Cells were washed with 500 μ l FACS buffer as described above. The samples stained for p-RPS6 were placed on ice. An A647-conjugated secondary antibody was added to the samples stained for p-ERK, incubated for 30 minutes on ice and then washed with 500 μ l FACS buffer. The supernatant was removed and the samples acquired at the LSRII.

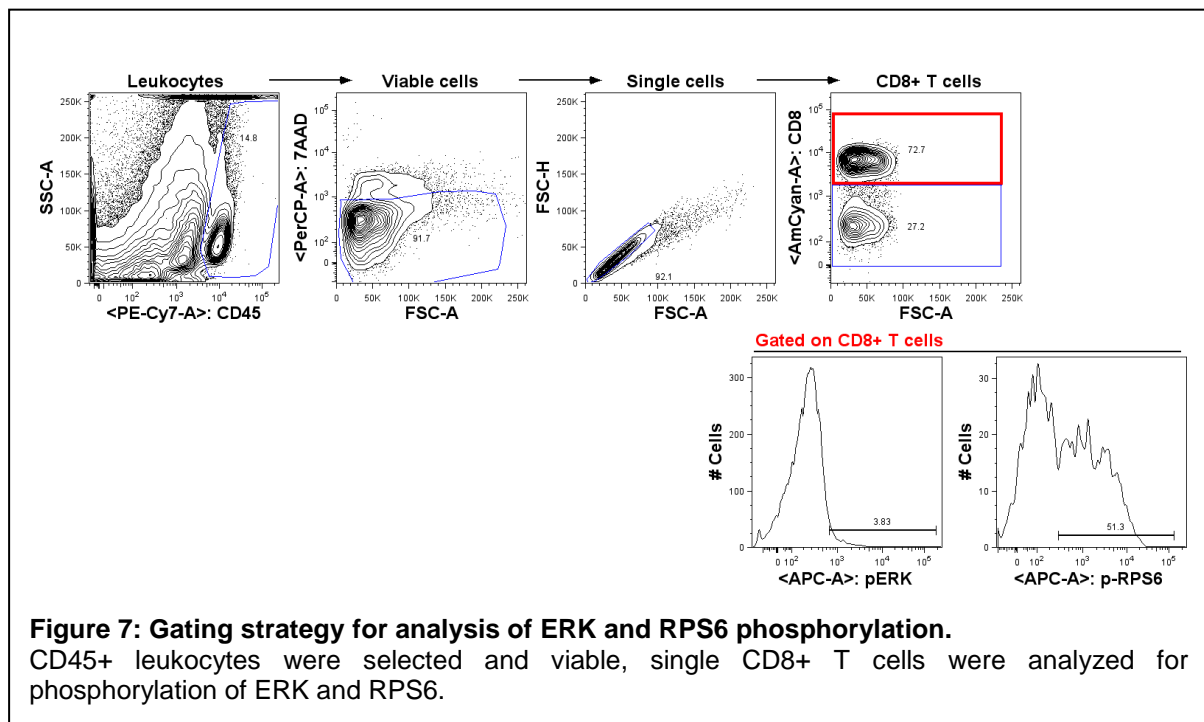
Table 8A-B: Staining combinations for analysis of phosphorylated proteins.

A

MARKER/FEATURE	FLUOROCHROME	STAINING
CD8	V500	Cell surface
CD45	PE-Cy7	Cell surface
p-ERK (pT202/pY204)	unconjugated	Intracellular
Rabbit IgG	A647	Intracellular
Viability	7-AAD	Cell surface

B

MARKER/FEATURE	FLUOROCHROME	STAINING
CD8	V500	Cell surface
CD45	PE-Cy7	Cell surface
p-RPS6 (pS235/236)	A647	Intracellular
Viability	7-AAD	Cell surface



6.5 Cell sorting

6.5.1 Principle of cell sorting using FACS Aria IIIu

The cell suspension to be sorted was stained with fluorochrome-conjugated antibodies and analyzed for fluorochrome signals (see section 6.4.1 Principle of flow cytometry). Once the photons emitted by the fluorochromes have been detected cells can be selected according to marker expression. After passing the laser beam cells are separated and independently charged. Individual drops then pass an electrical field, are attracted to their opposite polarity and collected.

6.5.2 Sorting of T cells from human renal cell carcinoma TILs

RCC tissue suspensions were transferred into 5 ml tubes, washed with 2 mM EDTA (in PBS) and the pellet re-suspended in 30 μ l 2 mM EDTA. Tissue suspensions were stained with fluorochrome-conjugated antibodies (see table 9), sorted with the FACS Aria IIIu applying the gating strategy depicted in figure 8 into 1.5 ml tubes supplied with TIL medium. CD11c-CD3⁺/CD3⁻ cells were sorted applying “purity” (highest cell yield) or “single cell” (highest purity) mode. Characteristics of used fluorochromes, lasers and filters are depicted in table 10. Sorted CD11c-CD3⁺/⁻ cells were centrifuged at 300 g for 10 minutes at room temperature, re-suspended in the appropriate medium, counted and used in experiments.

Table 9: Staining combination for sorting CD11c-CD3⁺/⁻ RCC-TILs

MARKER/FEATURE	FLUOROCHROME	STAINING
CD3	PB	Cell surface
CD11c	APC	Cell surface
CD45	PE-Cy7	Cell surface
Viability	APC-Cy7 (“Near IR”)	Cell surface

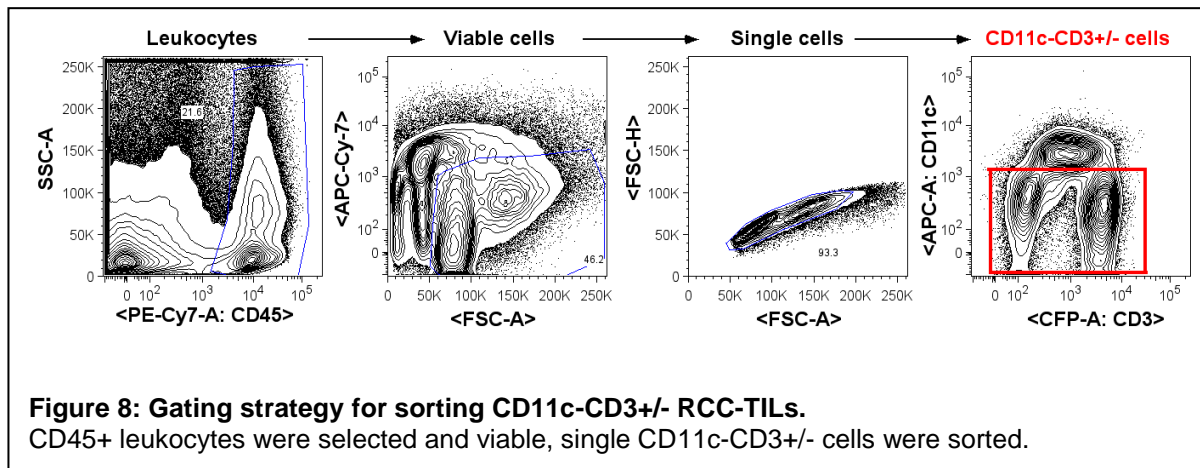


Table 10: Characteristics of used fluorochromes, lasers and filters for detection at the FACS Aria IIIu.

FLUORO-CHROME	EXCITATION MAXIMUM (NM)	EMISSION MAXIMUM (NM)	LASER	LASER WAVE-LENGTH (NM)	DETECTION FILTER (NM)
APC	650	660	Red laser	633	660/20
Near IR fluorescence reactive dye	750	775	Red laser	633	780/60
PB	401	452	Violet laser	405	450/40
PE-Cy7	496	785	Blue laser	561	780/60

APC: Allophycocyanin

PB: Pacific blue

PE-Cy7: Phycoerythrin – Cyanine 7

6.6 Mouse models

The animal experiments were approved by the local authorities according to the legal regulations for animal experiments.

6.6.1 Human melanoma xenograft NSG model

To select optimal experimental settings, 2×10^6 HLA-A2+ tyrosinase+ human melanoma cells SK-Mel23 were injected s.c. into age-matched 9 weeks old, female mice. When tumors were palpable, 2×10^6 TCR-D115 T cells were injected in 200 μ l PBS i.v. per mouse. Blood, lungs, spleens and tumors were isolated and cell suspensions obtained as described in section 6.6.1.1-2.

For assessing the impact of PD-1:28tm expression on T cell performance in vivo, age-matched, 7-11 weeks old, male mice were injected s.c. with 5×10^6 HLA-A2+ tyrosinase+ human melanoma cells SK-Mel23. TCR-D115 and TCR-D115/PD-1:28tm T cells were labeled with 0.15 μ M CFDA-SE for 8 minutes at 37°C. The reaction was stopped with FCS and cells were washed twice with PBS. Intracellular esterases remove acetate groups of CFDA-SE and thereby convert it to the fluorescent carboxyfluorescein succinimidyl ester (CFSE). With each cell division the fluorescence intensity of CFSE is halved allowing monitoring of T cell proliferation.

When tumors reached a size of 802 mm³ (SEM = 83), 6×10^6 CFSE labeled TCR-D115 or TCR-D115/PD-1:28tm T cells were injected in 50 μ l PBS per mouse i.t.. Tumors were harvested 4 hours, 1, 2, 4, 6 and 10 days after ATT and single cell suspensions were prepared for flow cytometry analysis.

For studying the effect of PD-1:28tm expression on tumor size, age-matched, 12 weeks old, male mice were injected s.c. with 5×10^6 HLA-A2+ tyrosinase+ human melanoma cells SK-Mel23. When tumors were palpable (mean = 78 mm³, SEM = 5), 6×10^6 TCR-D115 or TCR-D115/PD-1:28tm or TCR-T58 or TCR-T58/PD-1:28tm T cells (n = 4 mice per group) or PBS (n = 3 mice) were injected in 50 μ l PBS per mouse i.t.. Tumor size (mm³) was calculated using the formula for determining ellipsoid volumes: $\pi/6 \times \text{length} + \text{width} + \text{height}$.

6.6.1.1 Isolation of adoptively transferred T cells from murine lung, spleen and blood

Mice were sacrificed, spleens and lungs isolated and dispersed through a 40 µm filter with the plunger of a 10 ml syringe into a 50 ml tube. The filter was rinsed twice with RPMI-1640 and the cells centrifuged at 472 g for 5 minutes at room temperature. The cell pellet was re-suspended in 2 ml erythrocyte lysis buffer and incubated for 2 minutes at room temperature. Adding 20 ml of PBS stopped the lysis reaction. Cells were centrifuged as before, washed once with PBS, counted and analyzed by flow cytometry.

Blood samples were taken by cardiac puncture of sacrificed mice with 26G needles and heparin-rinsed syringes. Blood samples were centrifuged at 472 g for 5 minutes at room temperature and the cell pellet re-suspended in 3 ml erythrocyte lysis buffer. After incubation for 5 minutes at room temperature, 20 ml of PBS were added and centrifuged as before. Cells were washed once with PBS, counted and analyzed by flow cytometry.

6.6.1.2 Isolation of TILs from melanoma xenografts grown in NSG mice

Mice were sacrificed, s.c. grown tumors isolated, placed in a Petri dish and cut to small pieces using scalpel and scissors. Tumor pieces were transferred to a 50 ml tube, filled up to 20 ml with HBSS (containing Ca^{2+} , Mg^{2+}) and centrifuged at 472 g for 2 minutes at room temperature. The supernatant was placed on ice and the pellet re-suspended in digestion buffer at 1 ml buffer/ml pellet and incubated for 30 minutes on a shaker at room temperature. The suspension was centrifuged at 472 g for 5 minutes at room temperature, the supernatant placed on ice and the pellet washed with HBSS without Ca^{2+} and Mg^{2+} . The supernatant was placed on ice and the pellet re-suspended in 5 mM EDTA in HBSS without Ca^{2+} and Mg^{2+} (6 ml/ml tissue pellet). After incubation for 5 minutes on a shaker at room temperature, the suspension was centrifuged as before, the supernatant placed on ice and the pellet dispersed through a 40 µm filter with the plunger of a 10 ml syringe. The filter was rinsed twice with HBSS (containing Ca^{2+} , Mg^{2+}). All supernatants were centrifuged at 472 g for 10 minutes at room temperature, all pellets were pooled, counted and analyzed by flow cytometry.

6.6.2 Hepatocellular carcinoma model

Age-matched 6 weeks old, male LoxP-TAg mice were injected with adenovirus coding for Cre recombinase (Ad.Cre) to activate the oncogenic process. 11.5 weeks after injection, splenocytes were isolated and transduced to express Thy1.1 or Thy1.1 plus mPD-1:28tm (Thy1.1/mPD-1:28tm) as described in section 6.6.2.1. Recipient mice received radiation (5 Gy) 1 day before ATT. Five x 10⁶ transduced splenocytes were injected in 100 µl PBS r.o. into recipient mice (18-27 weeks old, male) who had received Ad.Cre 15 weeks before for induction of oncogenesis. 11 mice received Thy1.1 splenocytes, 12 mice Thy1.1/mPD-1:28tm splenocytes and 12 mice did not receive ATT. Mice were sacrificed when tumors reached a size of 1.5 cm. Single cell suspensions of spleens and tumors were prepared as described in sections 6.6.1.1 and 6.6.2.2.

6.6.2.1 Isolation, transduction and bead-based sorting of murine splenocytes

The transduction of murine splenocytes comprised a 5 days-lasting protocol with day 0 being the day of splenocytes activation. The transduction was performed in a laboratory of S2 standard. All centrifugation steps of splenocytes were performed at 400 g and room temperature for 10 minutes, unless otherwise stated.

Day -2

The packaging cells PlatE were seeded at 1 x 10⁶ cells in 4 ml mHEK medium/well in a tissue culture treated 6-well plate.

Day -1

18 µg of plasmid coding for the transgenes (Thy1.1 or mPD-1:28tm) and 15 µl of sodium chloride were mixed and filled up to a total volume of 150 µl with Milli-Q[®] water. 150 µl of transfection buffer were added dropwise to the DNA-mix and incubated for 15 minutes.

Day 0

Six LoxP-TAg mice (15 weeks after Ad.Cre) with multi-nodular HCC were sacrificed, spleens removed and dispersed through a 40 µm filter with the plunger of a 10 ml syringe into a 50 ml tube. The filter was rinsed twice with RPMI-1640 and the cells centrifuged at 472 g for 5 minutes at room temperature. The cell pellet was re-suspended in 2 ml erythrocyte lysis buffer and incubated for 2 minutes at room temperature. Adding 20 ml of PBS stopped the lysis reaction. Cells were centrifuged as before, washed once with PBS, re-suspended in MTM supplemented with 10 IU/ml IL-2, 1 µg/ml anti-CD3 and 0.1 µg/ml anti-CD28 antibodies and seeded at 0.5×10^6 /ml in T125 cm² culture flasks.

Day 1

Non-tissue culture treated 24-well plates were coated with 12.5 µg/ml RetroNectin[®] in 500 µl PBS per well and incubated at 37°C for 30 minutes. RetroNectin[®] was replaced with 2% BSA (in PBS). After incubation for 30 minutes at room temperature the plates were washed once with PBS. The virus-containing medium of the PlatE cells was harvested, replaced by fresh mHEK and the PlatE cells were placed back into the incubator. The virus supernatant was filtered through a 0.45 µm filter and added to the RetroNectin[®] coated plates at 1 ml/well. The plates were centrifuged at 3000 g and 4°C for 90 minutes.

Activated splenocytes were harvested and seeded in virus coated plates at 1.8×10^6 cells in 1 ml per well in MTM supplemented with 10 IU/ml IL-2 and 0.4×10^6 CD3/CD28 beads/ml. The plates were centrifuged at 800 g and 32°C for 30 minutes. Splenocytes were either seeded on plates coated with virus coding for Thy1.1, Thy1.1 plus mPD-1:28tm (Thy1.1/mPD-1:28tm, virus supernatants mixed 1+1) or on plates coated with virus-free medium (MOCK control).

Day 2

The virus-containing medium of the PlatE cells was harvested, filtered through a 0.45 µm filter, supplemented with 10 IU/ml IL-2 and added to splenocytes at 1ml/well. The plates were centrifuged at 800 g and 32°C for 30 minutes. After incubation for 6 hours at 37°C the splenocytes were harvested and seeded at 5 ml/harvested well in MTM supplemented with 50 ng/ml IL-15 in T75 cm² tissue culture flasks.

Day 5

Transduced splenocytes were harvested and Thy1.1 and Thy1.1/mPD-1:28tm cells were separated for Thy1.1. Magnetic beads and buffers for separation were cooled on ice. Cells were re-suspended in MACS buffer at 93×10^6 cells/ml and passed through pre-separation columns to remove cell clumps. Anti-Thy1.1 magnetic beads were added to the cells at 1 μ l beads/ 1×10^6 cells and incubated on ice for 20 minutes. Cells were washed with MACS buffer, re-suspended in MACS buffer at 1 ml/ 150×10^6 cells. LS separation columns were placed in the magnetic field of a MACS separator, equilibrated with 3 ml MACS buffer and 500 μ l of the cell suspension were added per column. Columns were rinsed 3 times with 3 ml MACS buffer, removed from the separator, placed on a 15 ml collection tube and cells were flushed out by pushing a plunger into the column. Cells were centrifuged, re-suspended in 1 ml MACS buffer and underwent a second separation step.

The magnetic separation achieved a purity of 81% for Thy1.1 transduced splenocytes and 83% of Thy1.1/mPD-1:28tm transduced splenocytes. Splenocytes were injected r.o. at 5×10^6 cells in 100 μ l PBS per LoxP-TAg mouse.

6.6.2.2 Isolation of TILs from hepatocellular carcinoma grown in LoxP-TAg mice

Mice were sacrificed and the liver was rinsed through the vena portae hepatis with PBS until it appeared bloodless. The liver tumors were isolated from surrounding healthy tissue and dispersed through a 100 μ m filter with the plunger of a 10 ml syringe into a 50 ml tube. The filter was rinsed twice with RPMI-1640 and the suspension centrifuged at 472 g for 10 minutes at room temperature. The supernatant was discarded, the pellet re-suspended in 10 ml digestion buffer and incubated for 20 minutes in a water bath at 37°C. The suspension was centrifuged as before, the supernatant discarded and the pellet re-suspended in 4 ml 40% Percoll and layered over 4 ml 80% Percoll in a 15 ml tube. The suspension was centrifuged at 800 g without break for 20 minutes at room temperature. The interphase containing TILs was transferred to a 15 ml tube, 8 ml of erythrocyte lysis buffer was added and the suspension centrifuged at 472 g for 10 minutes at room temperature.

The pellet was re-suspended in MTM, counted and used in experiments or analyzed by flow cytometry.

6.6.2.3 Co-culture of murine T cells, splenocytes and TILs with target cells and stimulation with phorbol-12-myristate-13-acetate and ionomycin

434 cells were detached by trypsination, centrifuged at 472 g for 5 minutes at room temperature, re-suspended in MTM and counted.

TILs and splenocytes were isolated, re-suspended in MTM and counted. They were cultivated at 0.1×10^6 cells in 100 μ l with 0.1×10^6 434 cells in 100 μ l. In addition, TILs and splenocytes were stimulated with 50 ng/ml phorbol-12-myristate-13-acetate (PMA) and 500 ng/ml ionomycin (I). As a control effector and target cells were cultivated alone. Supernatants were harvested after ~ 16 hours.

Transduced T cells were harvested, re-suspended in MTM and counted. They were cultivated at 0.005×10^6 cells in 100 μ l with 0.005×10^6 434 cells in 100 μ l. As a control effector and target cells were cultivated alone. Co-culture supernatants were harvested after ~ 24 hours.

Supernatants were stored at -20 °C until analysis by Bio-Plex or ELISA.

6.7 Statistical analyses

Statistical tests were performed using Graph Pad Prism 6 software. The significance level was set to 0.05.

The Mann-Whitney U test (Wilcoxon rank sum test) is a nonparametric test for the comparison of unpaired groups.

The Wilcoxon matched-pairs signed rank test is a nonparametric test for the comparison of paired groups.

7 RESULTS

7.1 Design and expression of chimeric co-stimulatory receptors

7.1.1 Design of chimeric co-stimulatory receptors

The rationale of this dissertation was to develop strategies for endowing T cells with the capacity to receive co-stimulation in the tumor environment independent from the classical co-stimulatory molecule CD28. As effector T cells are largely CD28 negative and the majority of tumors do not express CD80 or CD86, co-stimulation cannot be mediated through a classical CD28/CD80 or CD28/CD86 interaction in the tumor environment. Therefore, the intracellular signaling domain of a co-stimulatory molecule, CD28 or 4-1BB, was joined with an extracellular protein domain whose ligand is present in the tumor environment. A protein commonly expressed by a variety of tumor entities is PD-L1 (57). The receptor of PD-L1 is PD-1. The physiological PD-1/PD-L1 interaction results in an inhibitory signal. A chimeric co-stimulatory receptor consisting of the extracellular domain of PD-1 and the intracellular domain of CD28 or 4-1BB may possibly support T cells not only by facilitating co-stimulation but also by alleviating the native inhibitory PD-1 signal through ligand competition. Different receptors were designed and compared for surface expression and function (figure 9). The PD-1:8tm:28 receptor encompasses the entire extracellular domain of PD-1 (amino acids (AA) 1-170) followed by the CD8 α sequence encoding the membrane proximal extracellular region, the complete transmembrane and the membrane proximal intracellular region (AA 128-210). The domain derived from CD8 α was meant to function as a hinge region to improve flexibility and ligand binding of the intended chimeric protein. The PD-1:8 sequence was followed by the sequence coding for the entire intracellular domain of CD28 (AA 180-220) encompassing the signaling motifs YMNM, PRRP and PYAP. The PD-1:cys28tm chimeric receptor was adapted from a publication by Prosser et al. (62). Here, the extracellular sequence of PD-1 (AA 1-155) was followed by the sequence of CD28 encoding AA 141-220 of CD28 including a section of the extracellular and the complete transmembrane and intracellular domains of CD28. The CD28 sequence included the cysteine residue at position 141, which may be

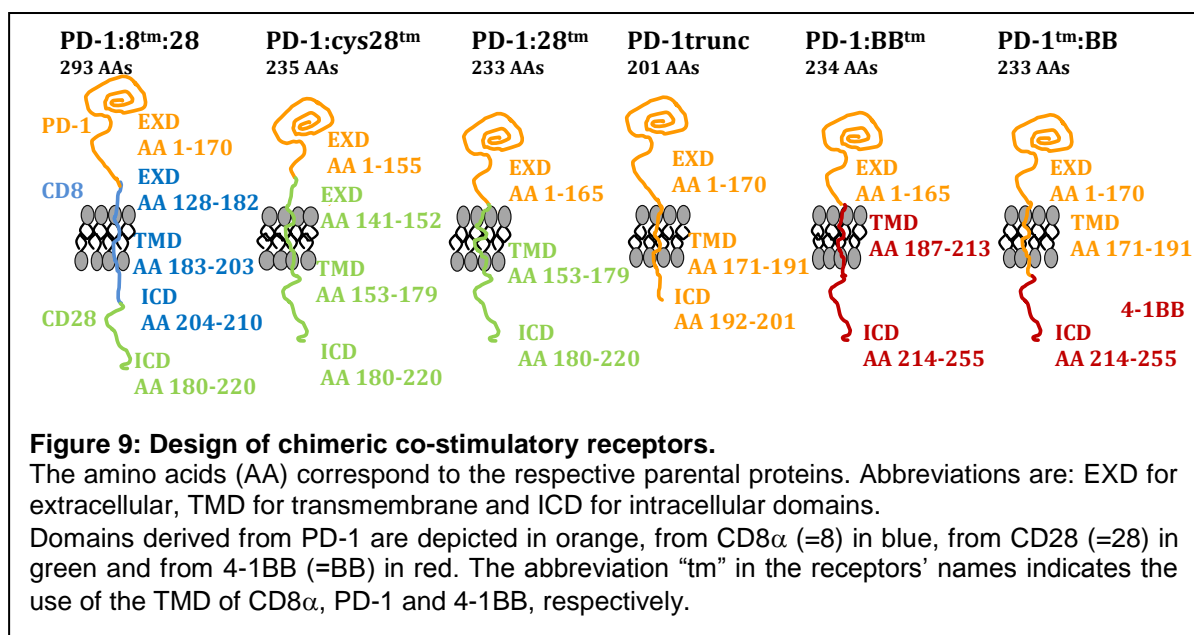
important to allow dimerization of the PD-1:cys28tm receptor as it is seen for the native CD28 protein (62). The native PD-1 is a monomeric receptor and thus, the chimeric PD-1:28 receptor is unlikely to dimerize if the CD28 encoded extracellular cysteine is absent.

The PD-1:28tm receptor was adapted from Ankri et al. (63). The extracellular sequence spanning AA 1-165 of PD-1 was followed by the sequence encoding the complete transmembrane and intracellular domains of CD28. In contrast to PD-1:cys28tm the extracellular cysteine from CD28 is absent.

The PD-1trunc receptor encodes for the extracellular and transmembrane domains of PD-1 and lacks any intracellular signaling domain; thus, no signal transduction will occur. This allows determining whether alleviating the inhibitory signaling of the native PD-1 will have an impact on the anti-tumor T cell function.

In addition to the CD28 co-stimulatory domain the co-stimulatory domain of 4-1BB was chosen as it has been proposed that the 4-1BB signaling cascade is particularly effective to support secondary T cell responses (64). The PD-1:BBtm receptor contains the same extracellular domain as PD-1:28tm, i.e. AA 1-165 of PD-1, yet joined to the transmembrane and intracellular domains (AA 187-255) of 4-1BB, including the signaling motif QEE.

Moreover, a PD-1tm:BB was designed using the extracellular plus transmembrane sequences of PD-1 (AA 171-191) and only the intracellular domain of 4-1BB (AA 214-255).



7.1.2 Expression of chimeric receptors

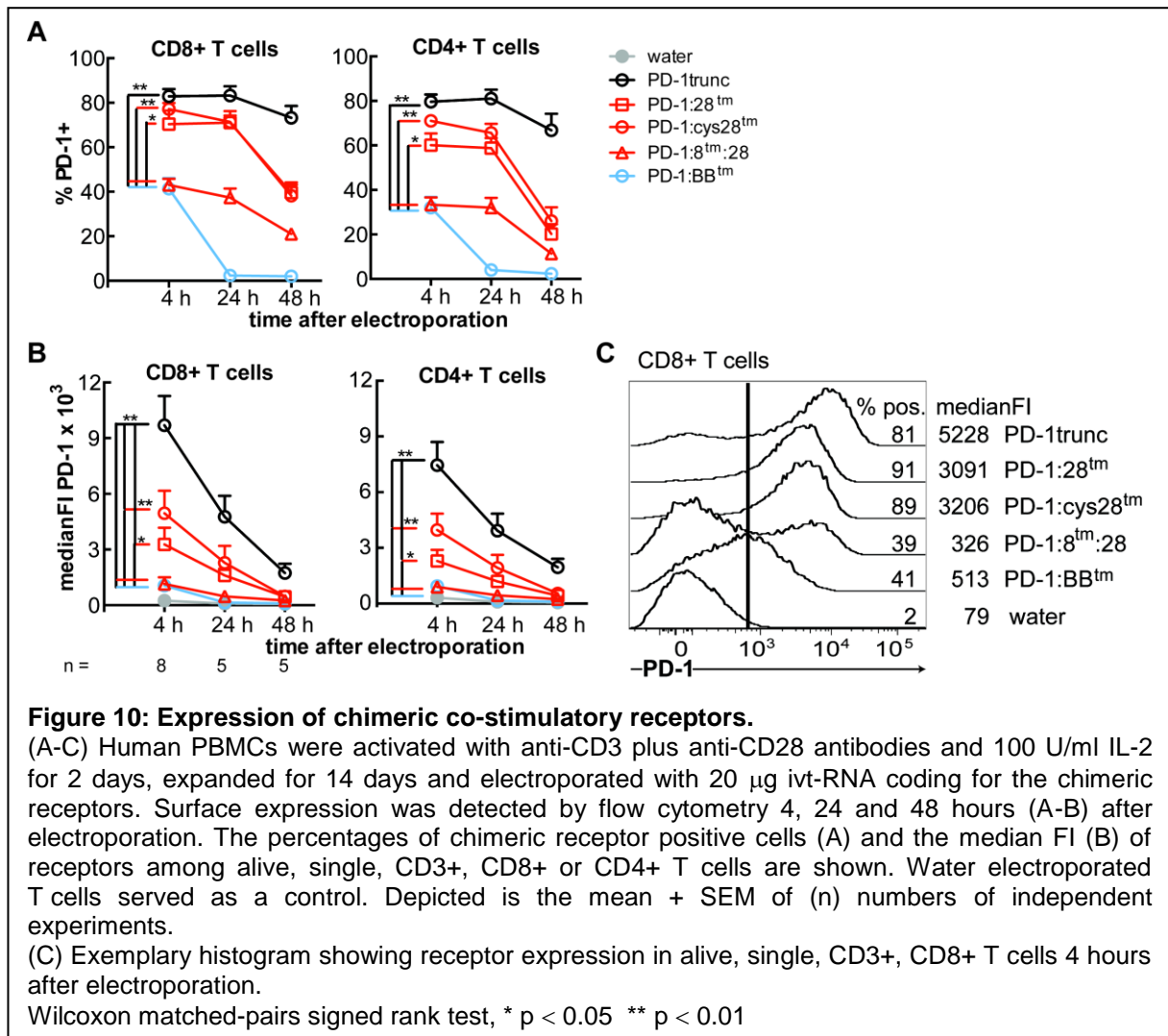
To determine whether T cells can express the chimeric receptors, human activated T cells were electroporated with ivt-RNA coding for the receptors. Four, 24 and 48 hours after electroporation T cells were analyzed for surface expression of chimeric receptors by flow cytometry using an anti-PD-1 antibody recognizing the extracellular domain of PD-1. Alive, single, CD3⁺ CD8⁺ or CD3⁺ CD4⁺ T cells were gated and analyzed for the percentage of T cells expressing the chimeric receptor. The intensity of receptor expression was deduced from the median fluorescence intensity (median FI). As depicted in table 11 and figure 10, 4 hours after electroporation, the PD-1trunc receptor was most efficiently expressed in terms of both percentage of positive cells and the median FI. At 4 hours after electroporation, there was no significant difference in percentage of T cells expressing PD-1trunc and both PD-1:cys28tm and PD-1:28tm. In contrast, the PD-1:8tm:28 receptor containing the transmembrane domain of CD8 α showed significantly lower surface expression compared to PD-1trunc ($p < 0.01$), PD-1:cys28tm or PD-1:28tm (both $p < 0.05$). The PD-1:BBtm receptor was expressed on significantly less cells and with lower intensity compared to PD-1:28tm ($p < 0.05$), PD-1:cys28tm or PD-1trunc ($p < 0.01$). The pattern was similar for CD8⁺ and CD4⁺ T cells.

Table 11: Percentages of surface PD-1 positive cells and median FI of PD-1 (mean \pm SEM) 4 hours after electroporation.

	CD8 ⁺ T cells		CD4 ⁺ T cells	
	%+	median FI	%+	median FI
PD-1trunc	83 \pm 3	9692 \pm 1584	80 \pm 3	7450 \pm 1251
PD-1:cys28 tm	77 \pm 3	4951 \pm 1216	71 \pm 2	3960 \pm 888
PD-1:28 tm	70 \pm 6	3276 \pm 904	60 \pm 5	2300 \pm 604
PD-1:8 tm :28	43 \pm 3	1146 \pm 364	33 \pm 3	900 \pm 298
PD-1:BB tm	41 \pm 5	1058 \pm 231	32 \pm 5	317 \pm 84

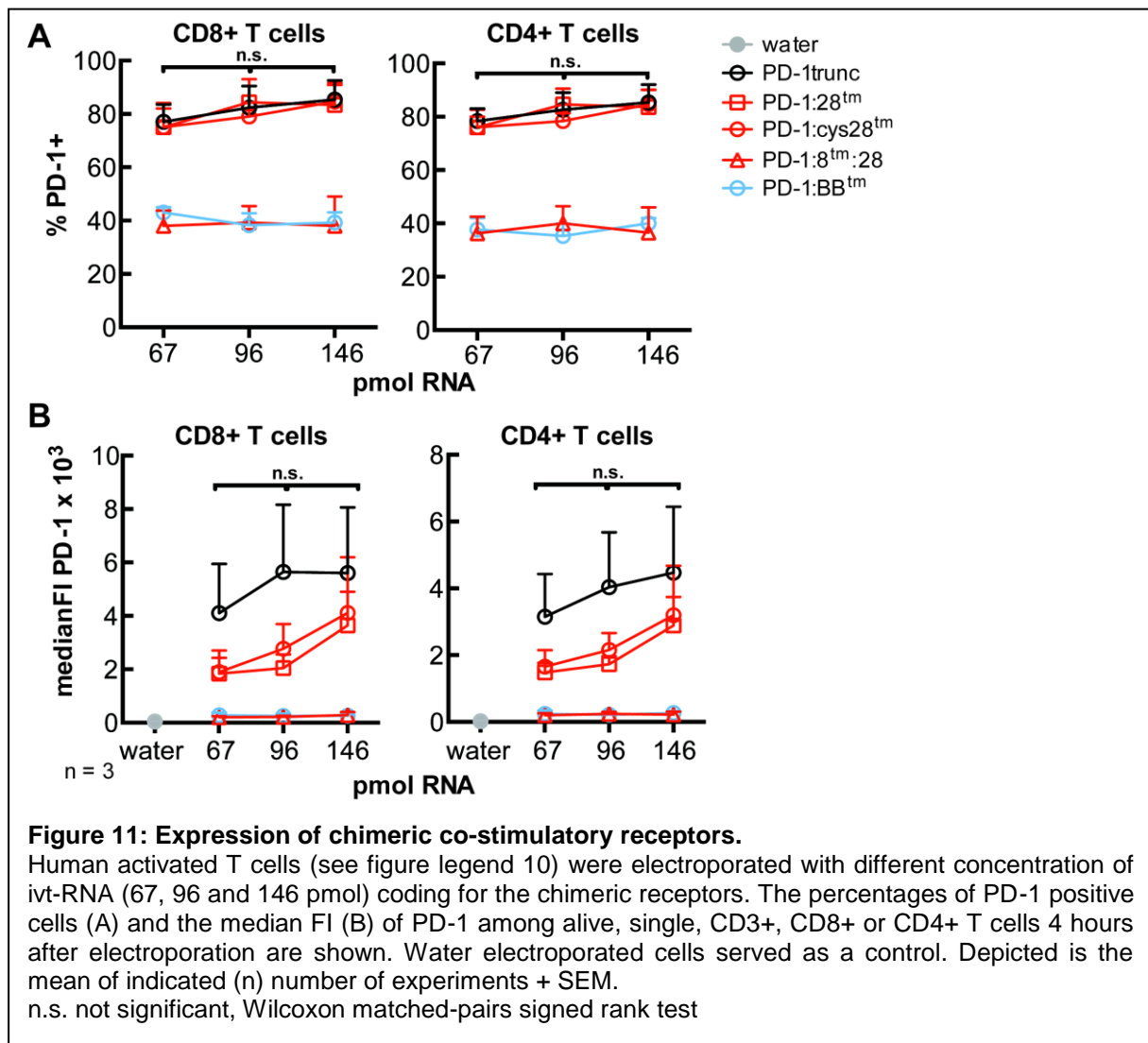
Concerning the kinetics of surface expression over 48 hours (figure 10), it was observed that PD-1trunc, PD-1:cys28tm, PD-1:28tm and PD-1:8tm:28 stayed stable for 24 hours regarding the percentage of positive cells, while the median FI decreased

on both CD8+ and CD4+ T cells. Compared to the other receptors, the PD-1:BBtm construct was the only one not expressed beyond 24 hours.



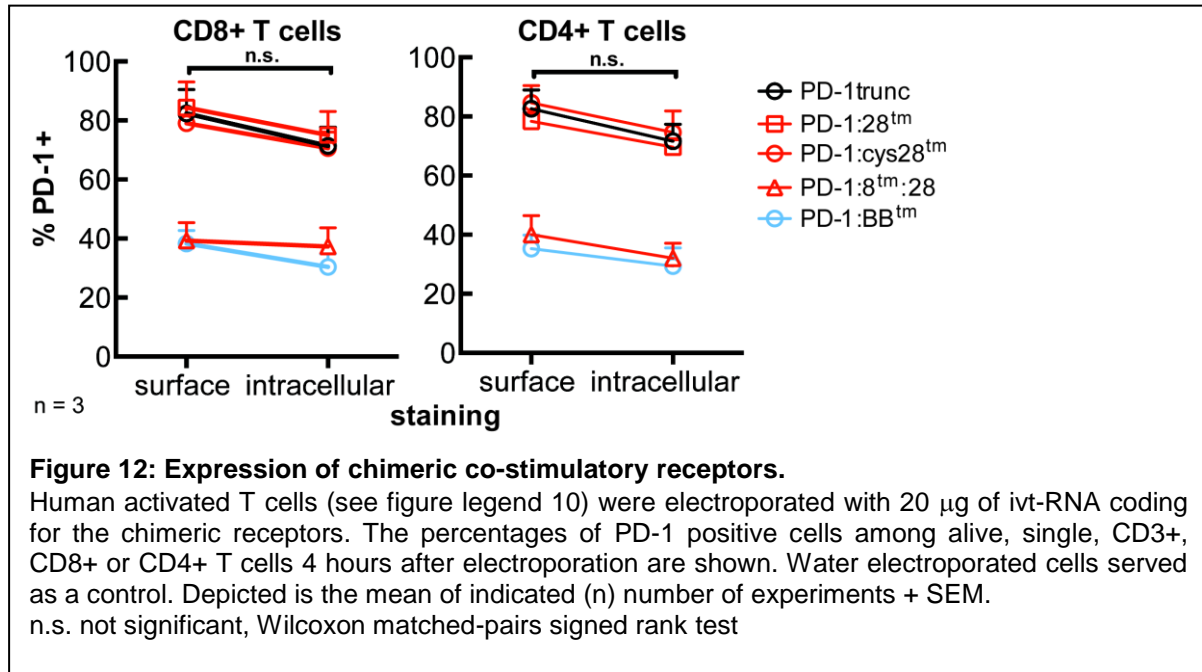
To explore whether the observed differences in surface expression between the receptors were due to differences in base-pair-lengths of the constructs, all receptors were tested at equimolarity of electroporated ivt-RNA. The previously used 20 μ g of ivt-RNA amounted to molar concentrations of 97 pmol for PD-1trunc, 83 pmol for PD-1:cys28tm and PD-1:BBtm, 84 pmol for PD-1:28tm and 66 pmol for PD-1:8tm:28. Three equimolar conditions (67, 96 and 146 pmol) were tested. As depicted in figure 11, the differences in receptor surface detection remained with lower percentages of positive cells for PD-1:8tm:28 and PD-1:BBtm. Moreover, the percentage of positive

T cells was similar across the concentration range tested while the median FI slightly increased with increasing concentrations (not significant).

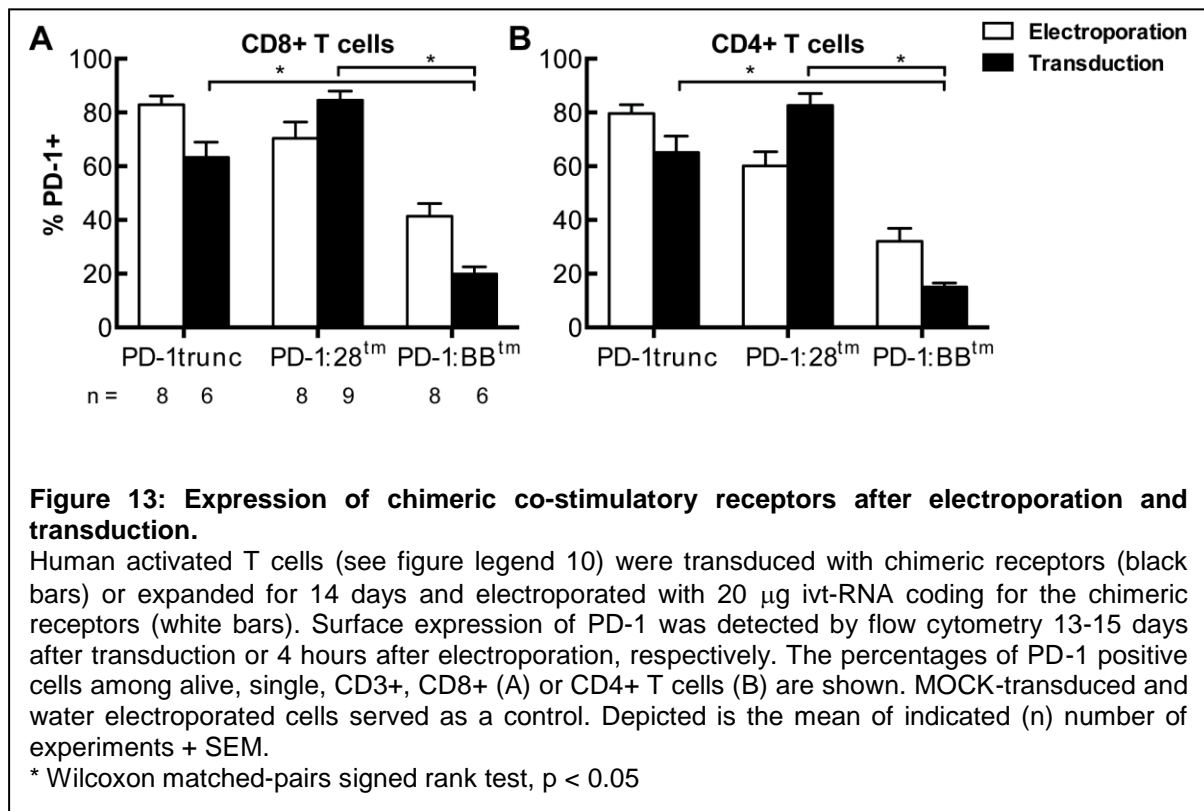


In a next step it was tested whether the differences in surface presence were due to lower translation or intracellular retention of chimeric proteins. Therefore, T cells were stained for chimeric receptors on the cell surface and intracellularly. As shown in figure 12, there was no difference in the percentage of positive cells between cells that were surface stained and cells that were stained after cell permeabilization detecting surface plus intracellular receptor expression. Thus, the observed differences in surface expression were not caused by impaired trafficking of the chimeric proteins to the cell surface.

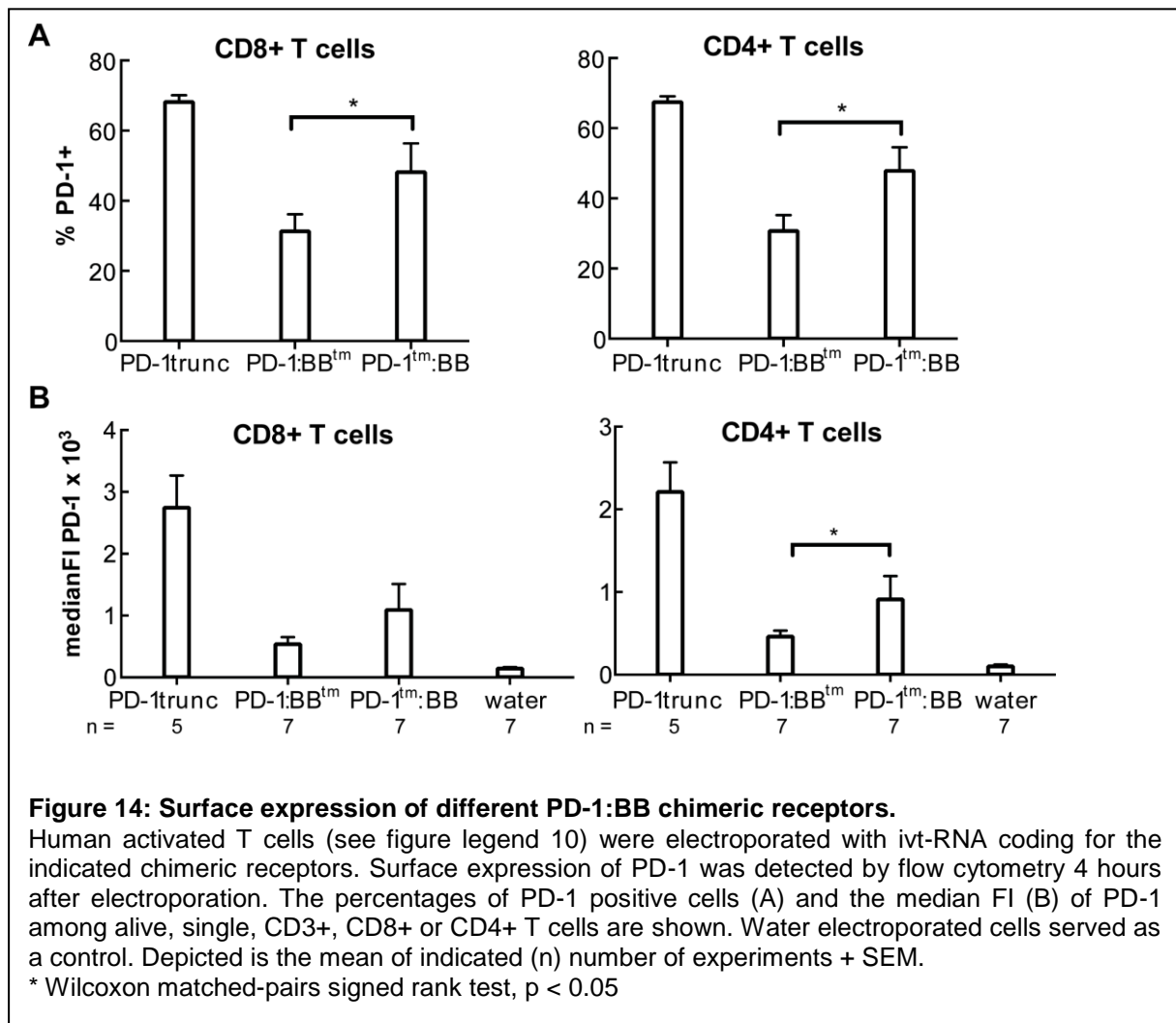
The percentage of receptor positive T cells and the median FI of PD-1:8tm:28 and PD-1:BBtm remained low when stained intracellularly. Thus, no intracellular pool of receptors seemed to exist.



To assess if the weak expression of PD-1:BBtm compared to PD-1trunc and PD-1:28tm is due to transient expression from ivt-RNA, chimeric co-stimulatory receptor sequences were cloned into the pMP71 vector for retroviral transduction. Retroviral transduction leads to integration of transferred DNA into the cell's genome. This process should result in stable expression of the transduced sequences. T cells were stained with anti-PD-1 antibodies to detect chimeric receptor surface expression 13-15 days after transduction. As depicted in figure 13, expression profiles of chimeric co-stimulatory receptors after transduction were similar to those observed after electroporation and the transduced PD-1:BBtm construct was still significantly less expressed compared to PD-1trunc and PD-1:28tm ($p < 0.05$).



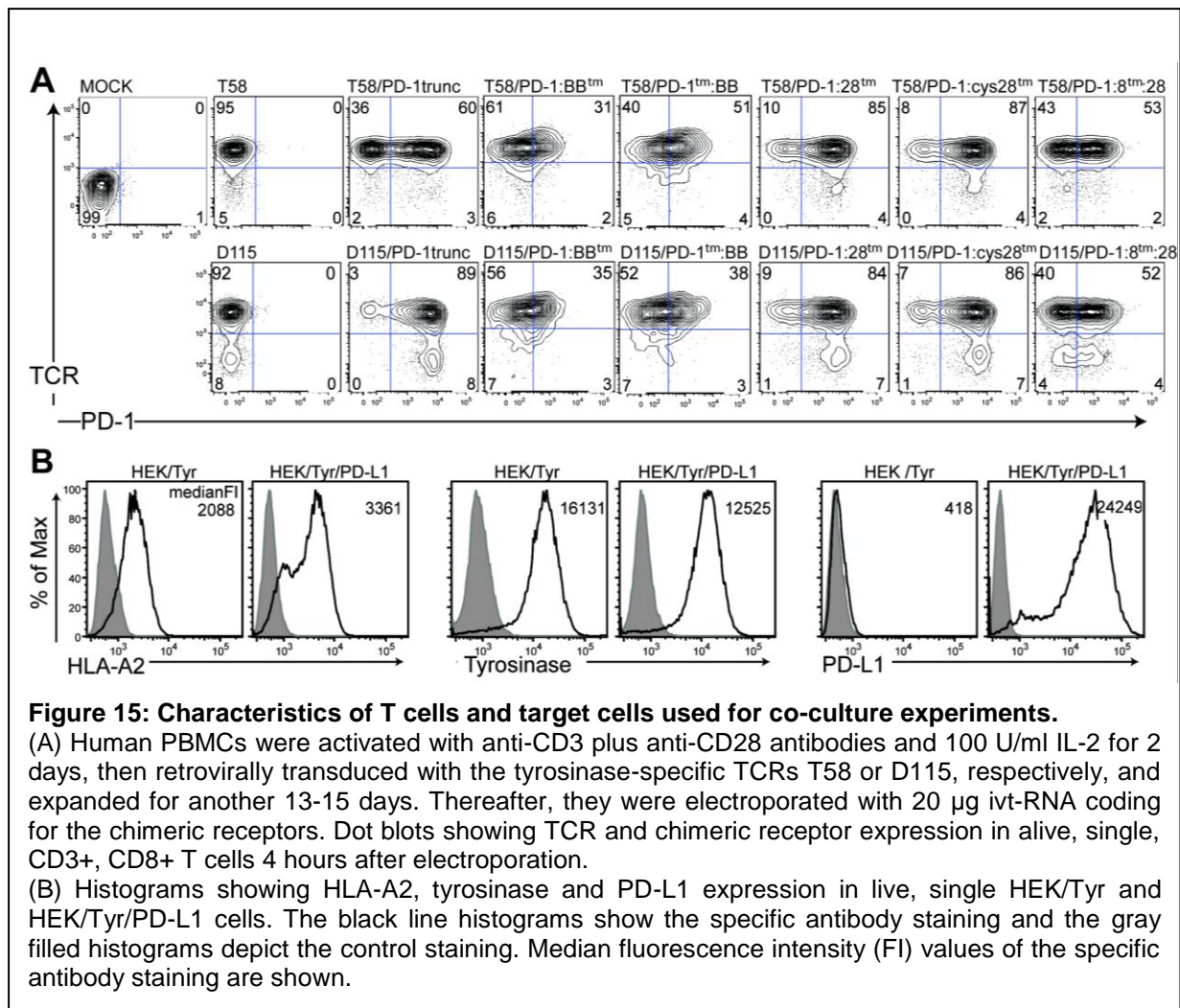
As all receptors containing the PD-1- or CD28-derived transmembrane domain were more efficient and more stably expressed compared to those with CD8 α - or 4-1BB-transmembrane domains, a PD-1:BB receptor was designed using the transmembrane domain of PD-1 (PD-1tm:BB). After electroporation, PD-1tm:BB was expressed by more CD8⁺ and CD4⁺ T cells compared to PD-1:BBtm ($p < 0.05$, figure 14) and the median FI of electroporated PD-1tm:BB T cells was also higher compared to PD-1:BBtm in both CD8⁺ and CD4⁺ T cells (difference reached significance for CD4⁺ T cells).



7.2 PD-1:28tm- and PD-1:cys28tm-engineering of T cells enhanced TCR-mediated IL-2 and IFN- γ secretion

To analyze the effect of the chimeric receptors on T cell function, TCR-induced cytokine secretion of human T cells was analyzed. In a first step, human T cells were transduced to stably express the HLA-A2-restricted tyrosinase-specific TCR-T58 or TCR-D115 (65). In a second step, chimeric co-stimulatory receptors were electroporated into T cells stably expressing the transduced TCR. Expression of chimeric co-stimulatory receptors and TCRs is shown in figure 15A. Chimeric receptor expression was similar for TCR-T58 and -D115 T cells.

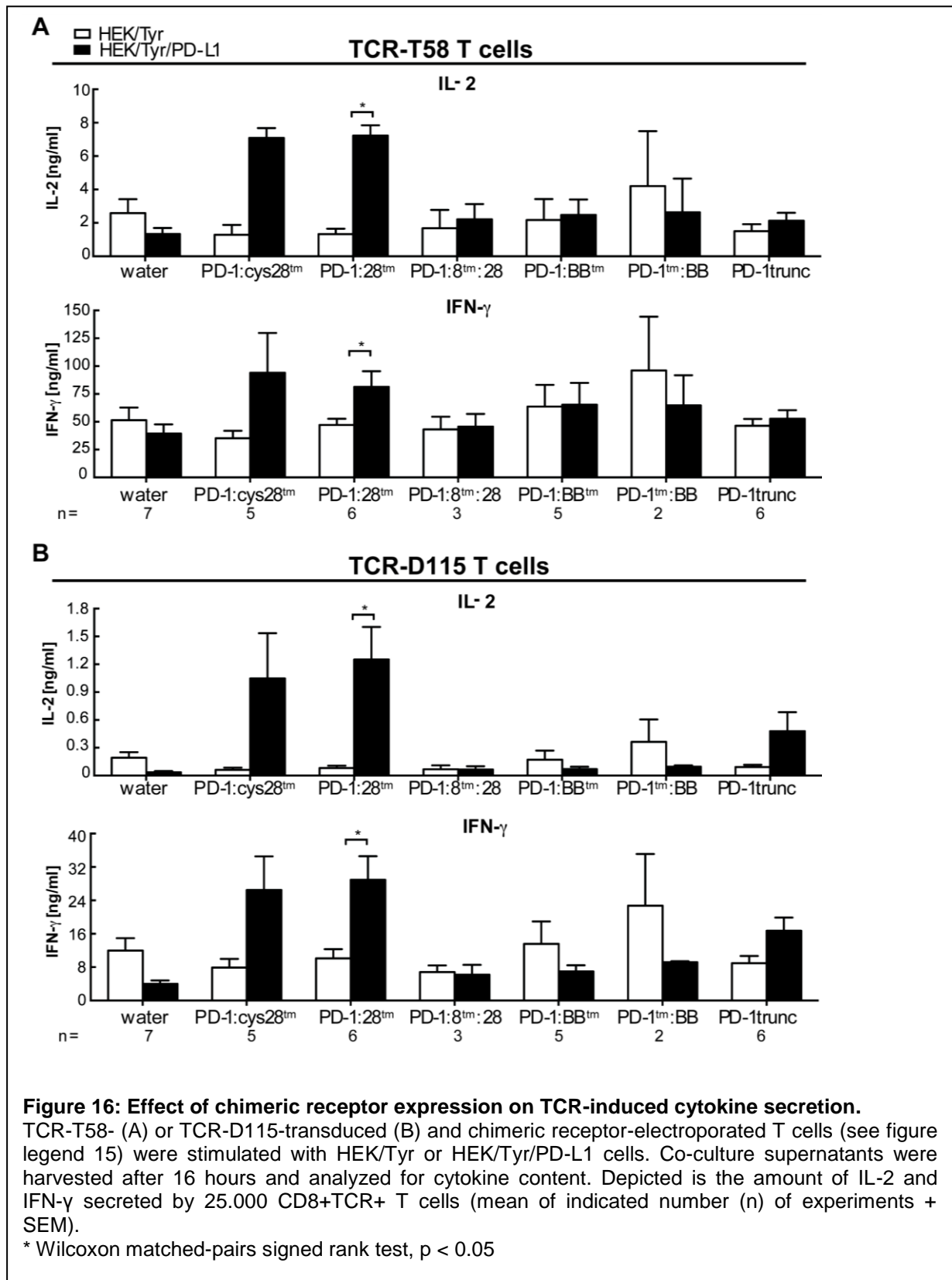
For T cell stimulation 2 target cells were used: HLA-A2+ HEK293 cells retrovirally transduced to stably express either the target antigen tyrosinase alone (HEK/Tyr) or HLA-A2+ HEK293 expressing tyrosinase and the PD-1 ligand, PD-L1 (HEK/Tyr/PD-L1). The transduced HEK293 cells were derived from single cell clones and selected for comparable HLA-A2 and tyrosinase expression (figure 15B). Stimulation with HEK/Tyr will elicit a TCR signal only, whereas stimulation with HEK/Tyr/PD-L1 induces the TCR plus a co-stimulatory signal if the T cells express a chimeric receptor. The proposed experimental outcome of co-culture was that T cells without chimeric receptors should secrete a similar amount of cytokines independent of the stimulator cell. T cells expressing a chimeric receptor could receive co-stimulation when stimulated with HEK/Tyr/PD-L1 and might secrete more cytokines compared to stimulation with HEK/Tyr.



To test this hypothesis, T cells and target cells were co-cultured at ratio of 1:2 for 24 hours and co-culture supernatants were analyzed for secreted IL-2 and IFN- γ .

As the percentages of TCR+ T cells varied between transductions (ranging from 28-97%) and the TCRs are functional in CD8+ T cells only, the amount of cytokine produced in each experiment was normalized to similar number (25,000) of TCR+CD8+ T cells, which was determined by flow cytometry before each experiment. As depicted in figure 16, TCR-T58- or TCR-D115 T cells electroporated with water secreted similar amounts of cytokines when stimulated with HEK/Tyr or HEK/Tyr/PD-L1 cells, as expected. TCR-T58 and TCR-D115 T cells expressing the chimeric receptors PD-1:28tm or PD-1:cys28tm secreted more IL-2 and IFN- γ when stimulated with HEK/Tyr/PD-L1 compared to stimulation with HEK/Tyr. The p-value was significant for PD-1:28tm with an observed increase of IL-2 secretion from 1.3 ng/ml to 7.2 ng/ml for TCR-T58 T cells and from 0.08 ng/ml to 1.3 ng/ml for TCR-

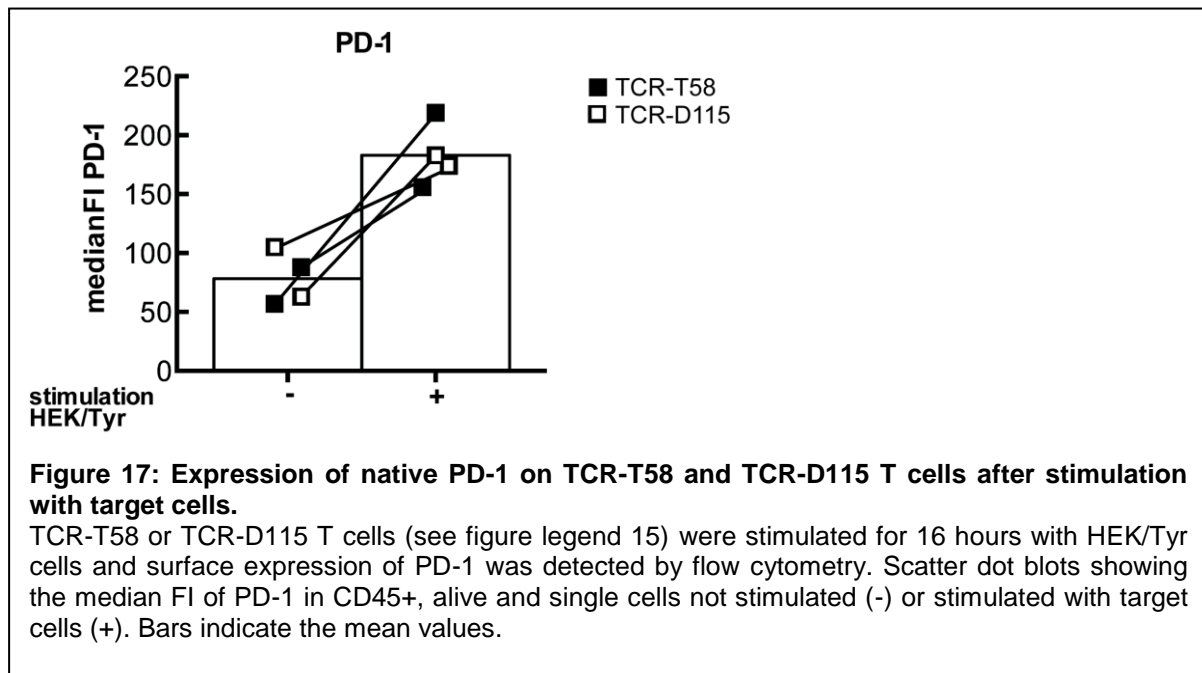
D115 T cells. The amount of secreted IFN- γ significantly increased from 47.2 ng/ml to 81.3 ng/ml (TCR-T58 T cells) and from 10.1 ng/ml to 28.9 ng/ml (TCR-D115 T cells). These results provide evidence that chimeric PD-1:28 receptors can indeed enhance T cell cytokine secretion.



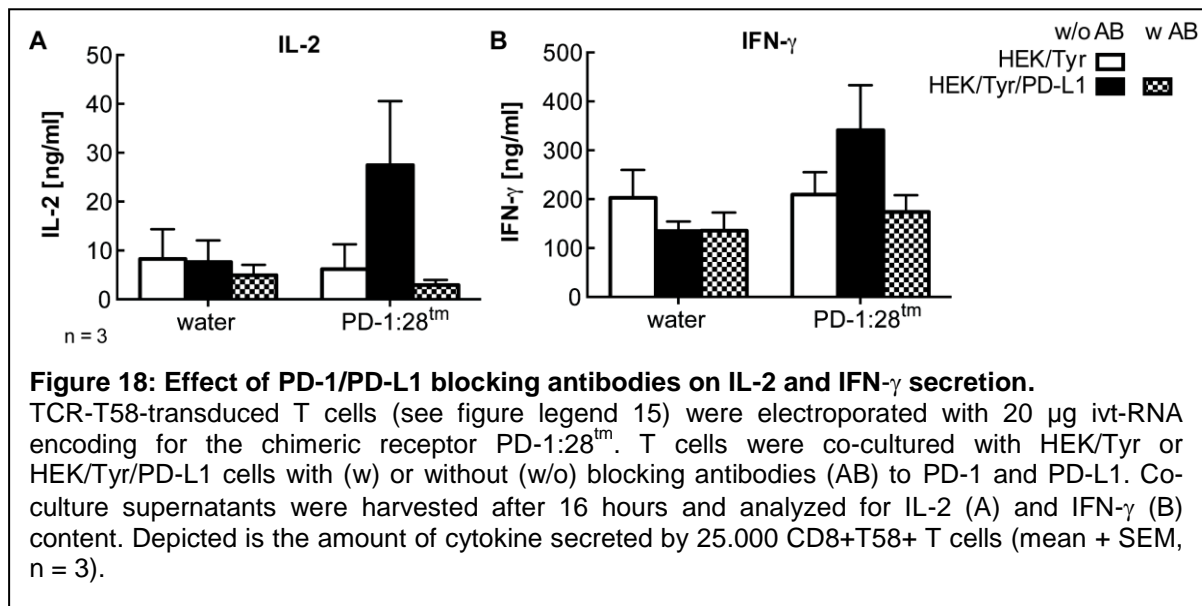
The PD-1:28 chimeric receptor containing the transmembrane domain of CD8 α showed no effect on IL-2 and IFN- γ production, for both TCRs tested. Since the other receptors with the CD28 signaling domain increased cytokine secretion, it can be speculated that the lack of an effect of PD-1:8tm:28 was due to low surface expression.

No effects were seen with the PD-1:BB receptors. That the 4-1BB co-stimulatory domain had no impact on T cells in this experimental system could be due to low receptor expression as seen for PD-1:8tm:28.

The expression of the truncated PD-1 receptor did not improve cytokine secretion of TCR-T58-transduced T cells when stimulated with HEK/Tyr/PD-L1. While, TCR-D115/PD-1trunc T cells secreted more cytokine under the same stimulation condition. As for an explanation, it was considered that the truncated PD-1 receptor, which has no signaling domain, might alleviate inhibitory effects mediated by the native PD-1 protein that is up-regulated during T cell stimulation. Indeed, TCR-T58 and TCR-D115 T cells up-regulated native PD-1 after stimulation to a similar extent (figure 17). As to why a benefit of PD-1trunc was observed only for TCR-D115 T cells might lie in the strength of the TCR signaling initiated from low- versus high-avidity TCRs, respectively (see section 7.4).



To provide evidence that the enhanced cytokine secretion of PD-1:28tm-engineered T cells was due to PD-1:28tm expression, blocking antibodies to PD-1 and PD-L1 were added to the co-culture. In presence of the blocking antibodies, the cytokine amounts in co-cultures with HEK/Tyr/PD-L1 cells were similar to those with HEK/Tyr cells (figure 18) indicating that the supporting effect was due to PD-1:28tm/PD-L1 interaction.



7.3 Ligation of PD-1:28tm and PD-1:cys28tm chimeric receptors increased TCR-mediated phosphorylation of extracellular signal regulated kinase and ribosomal protein S6

The observation that PD-1:28tm and PD-1:cys28tm expression by T cells enhanced TCR-mediated cytokine secretion led to the investigation of the underlying mechanism. To this end, TCR-T58-transduced T cells were electroporated with chimeric receptor ivt-RNA, stimulated with HEK/Tyr/PD-L1 cells and the phosphorylation of extracellular signal regulated kinase (ERK) and ribosomal protein S6 (RPS6), which are downstream targets of the CD28 and TCR signaling cascade, were analyzed by intracellular phospho-flow cytometry. The percentages of T cells with phosphorylated ERK and RPS6 were determined in CD8+ T cells, as the TCR-T58 is only functional in CD8+ T cells. For analysis of ERK activation, the intensity of

phosphorylated ERK (p-ERK) was additionally considered and used to derive a phospho index, which is defined as the percentage of p-ERK positive cells multiplied by the median fluorescence intensity of p-ERK positive cells.

As shown in figure 19, phosphorylation of both ERK and RPS6 was enhanced in PD-1:28tm T cells and PD-1:cys28tm T cells (yet significance was not reached as analyzed by Wilcoxon matched-pairs signed rank test). Compared to water electroporated cells, the phosphorylation of ERK was increased 4.4-fold in PD-1:28tm T cells and 43% stained positive for p-RPS6 compared to 33% of the water control.

For T cells expressing PD-1:cys28tm p-ERK increased 5.5-fold and 38% of T cells stained positive for p-RPS6.

Phosphorylation of ERK and RPS6 was not increased in PD-1trunc T cells when they were stimulated with HEK/Tyr/PD-L1 cells suggesting that the effect seen with the PD-1:28 receptors was due to the CD28 signaling domain.

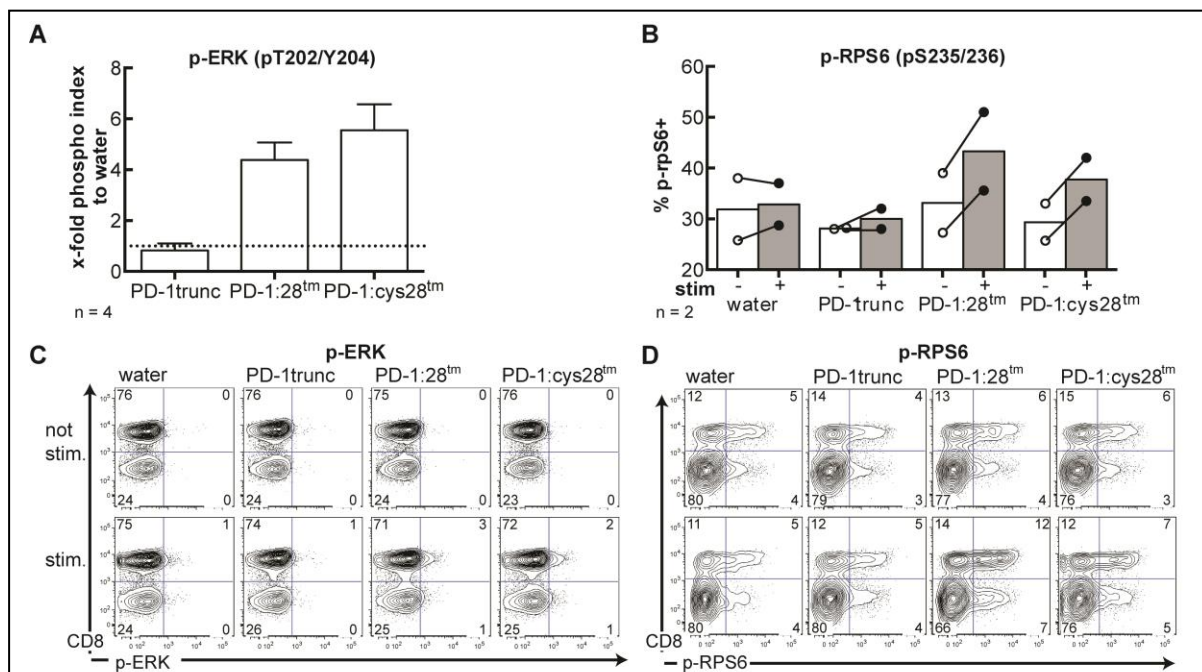


Figure 19: Effect of chimeric receptors on phosphorylation of ERK (pT202/Y204) and RPS6 (pS235/236).

TCR-T58 T cells (see figure legend 15) were electroporated with 20 μ g ivt-RNA coding for the chimeric receptors.

(A-D) T cells were stimulated with HEK/Tyr/PD-L1 cells. Phosphorylation of ERK and RPS6 was analyzed by intracellular phospho-flow cytometry.

(A) X-fold change of the ERK phospho index of CD8⁺ TCR-T58 T cells. ERK phospho index is defined as the percentage of p-ERK positive cells among CD8⁺ T cells multiplied by the MFI of p-ERK positive cells (mean + SEM, n = 4).

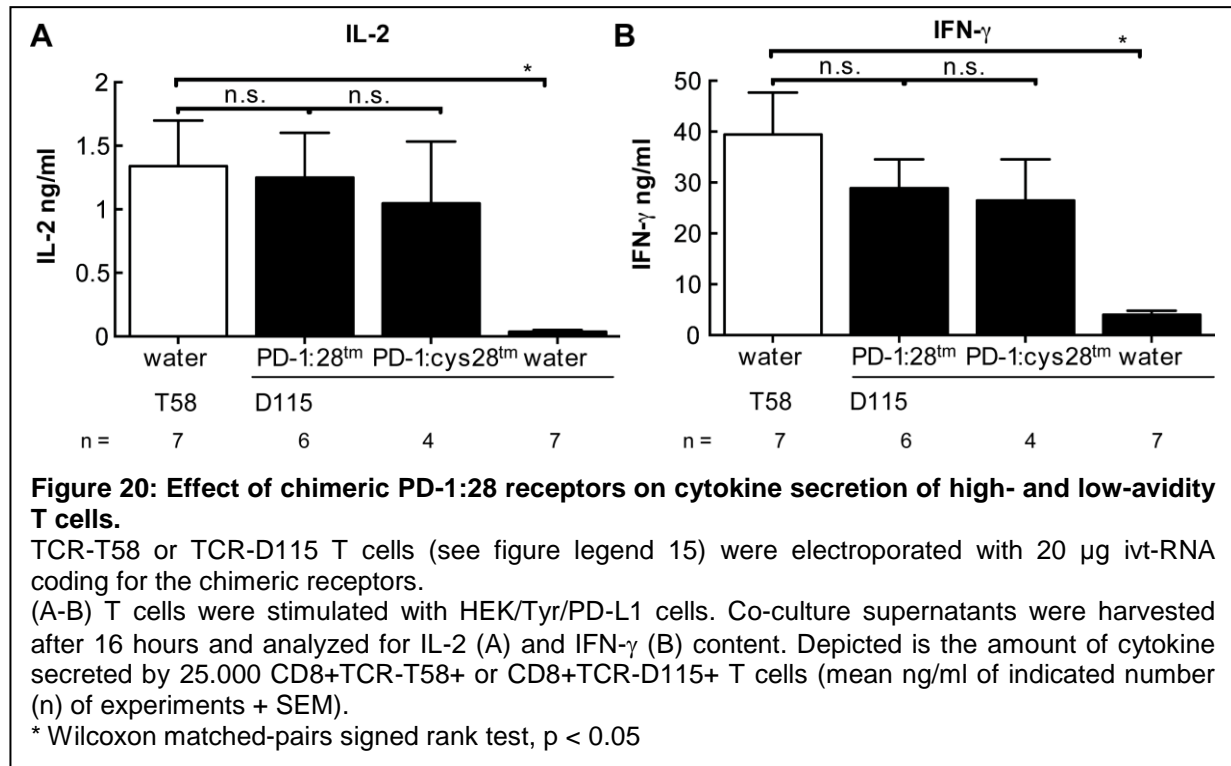
(B) Percentage of p-RPS6 positive CD8⁺ T cells in unstimulated (white bars) and HEK/Tyr/PD-L1 stimulated (grey bars) cells (mean, n = 2).

(C, D) Dot plots showing CD8 and p-ERK or p-RPS6 fluorescence intensity of T cells electroporated with water or chimeric receptor, either not stimulated or stimulated with HEK/Tyr/PD-L1 cells. Phosphorylation occurred in CD8⁺ T cells only, as the transgenic TCR is not functional in CD4⁺ T cells.

7.4 PD-1:28 receptors upgraded low-avidity T cells to approximate the cytokine response of high-avidity T cells

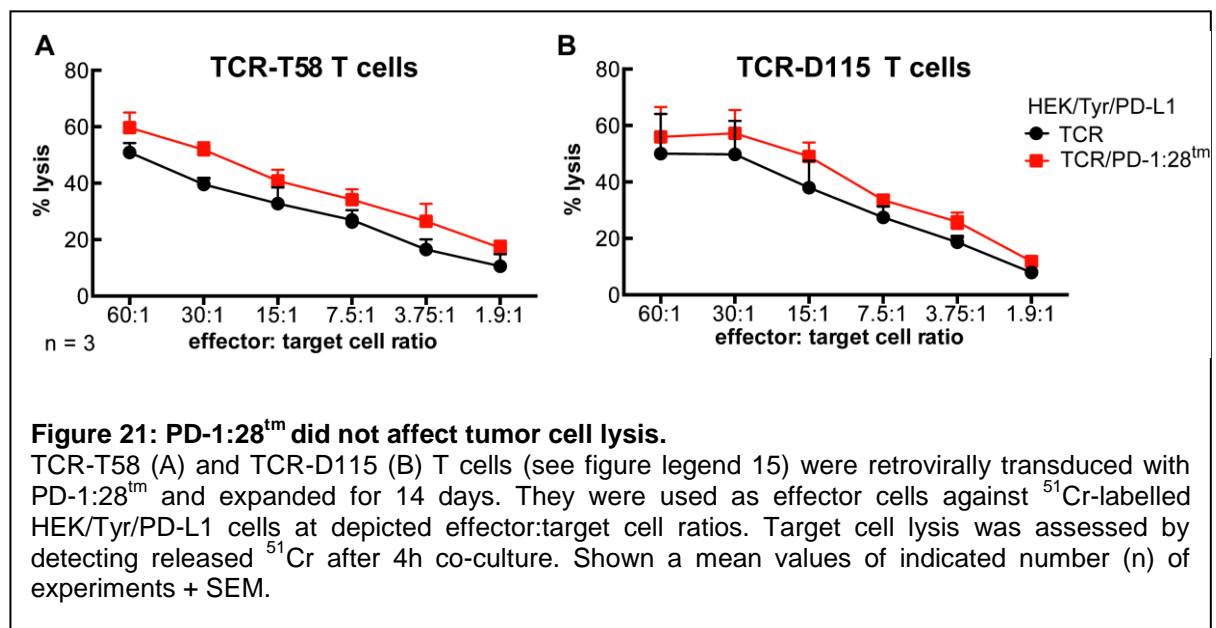
The TCRs T58 and D115 recognize the same tyrosinase epitope (AA 366-377) restricted by HLA-A*0201 but are of different affinity: TCR-T58 T cells showed a half maximal IFN- γ response at a tyrosinase peptide concentration of 10^{-9} M. TCR-D115 T cells required a peptide concentration of 10^{-7} M to induce the half maximal IFN- γ response (65). High-avidity T cells are considered superior in the anti-tumor response as in clinical trials adoptive therapy with high-avidity T cells yielded higher response rates compared to low-avidity T cells (59). However, high-avidity T cells are more likely to be tolerized in the tumor environment and to acquire negative regulatory functions (59). If the performance of low-avidity T cells can be improved their use in adoptive therapy might be advantageous.

Comparing the low-avidity TCR-D115 with its high-avidity counterpart TCR-T58 revealed that TCR-D115 T cells secreted significantly less IL-2 and IFN- γ ($p < 0.05$, figure 20) than TCR-T58 T cells when stimulated with the same target cell HEK/Tyr/PD-L1, despite similar levels of TCR expression (TCR-T58 T cells produced on average 1.3 ng/ml IL-2 and 39.4 ng/ml IFN- γ while TCR-D115 T cells 0.036 ng/ml IL-2 and 4 ng/ml IFN- γ). To determine whether chimeric PD-1:28 receptors will improve the function of low-avidity T cells, TCR-D115 T cells were engineered with PD-1:28tm and PD-1:cys28tm and stimulated with HEK/Tyr/PD-L1 cells. The cytokine secretion was compared to that of the high-avidity TCR-T58 T cells stimulated with the same target cell. TCR-D115 T cells expressing PD-1:28tm or PD-1:cys28tm secreted levels of IL-2 and IFN- γ close to those of the high-avidity TCR-T58 T cells. Thus, PD-1:28 receptors can approximate the response of low-avidity T cells to high-avidity T cells.



7.5 PD-1:28 receptors had no effect on tumor cell lysis

Besides cytokine secretion cytotoxicity is an important effector function for the anti-tumor response. As PD-1:28tm showed a beneficial effect on cytokine secretion and phosphorylation of ERK the effect on cytotoxicity was analyzed. TCR-T58- and TCR-D115-transduced T cells with or without PD-1:28tm were tested against ⁵¹Cr-labeled HEK/Tyr/PD-L1 cells at various effector to target cell ratios (figure 21). The observed lytic activity against HEK/Tyr/PD-L1 was overall similar with a marginal higher activity for T cells expressing PD-1:28tm.

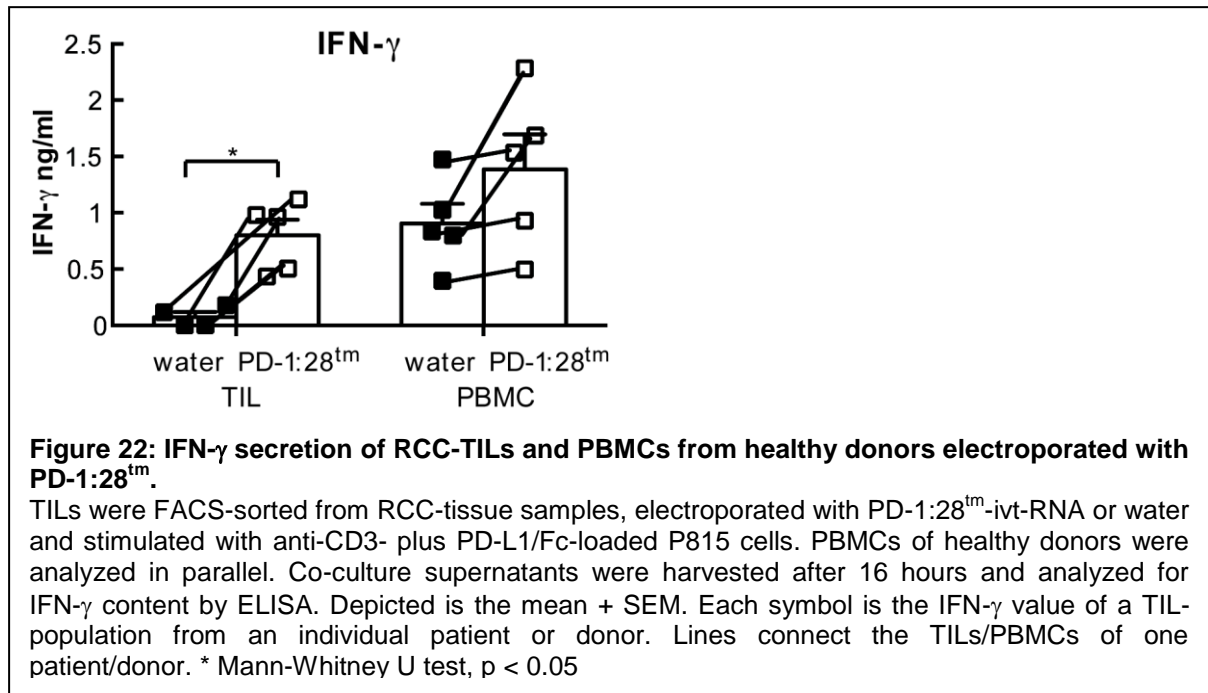


That PD-1:28tm did not significantly enhance lysis of target cells in vitro cannot exclude its potency to support tumor eradication. As shown by Milone et al. 2009 (32), although the CD19-directed CAR utilizing the 4-1BB signaling domain did not show a greater impact on T cell function than a CD19-CAR using CD3 ζ , the 4-1BB CD19-CAR showed superior anti-leukemic effect in vivo.

7.6 PD-1:28tm reinstated IFN- γ secretion in unresponsive tumor-infiltrating lymphocytes from human renal cell carcinoma

It was previously shown that tumor-infiltrating lymphocytes (TILs) isolated from human renal cell carcinoma (RCC) samples showed deficits in degranulation and IFN- γ secretion, in part due to insufficient activation of signaling molecules AKT, ERK and JNK (48). The deficits were reversible ex vivo, but required treatment with IL-2 or diacylglycerol kinase- α (DGK- α) inhibitor (48). As CD28 co-stimulation fosters activation of intracellular signaling molecules, including AKT, ERK and JNK, I thought to determine whether co-stimulation through PD-1:28tm can restore functionality in unresponsive TILs. To this end, sorted CD11c-CD3⁺/⁻ TILs from human RCC tissues were electroporated with PD-1:28tm or water. PBMCs from healthy donors were analyzed in parallel. TILs and PBMCs were stimulated with target cells that presented PD-L1. TILs were derived from different patients. Tumor or target cells with cognate pMHC were not available. Had they been available, they likely would have expressed varied pMHC and PD-L1 levels resulting in different signaling strength. This would obscure comparison and evaluation of PD-1:28tm-mediated effects. Therefore, a surrogate target cell was used for all TILs and PBMCs. This surrogate target was the P815 mastocytoma cell line loaded exogenously with anti-CD3 antibody and a PD-L1/Fc chimera, which bind to Fc receptors expressed by P815 cells.

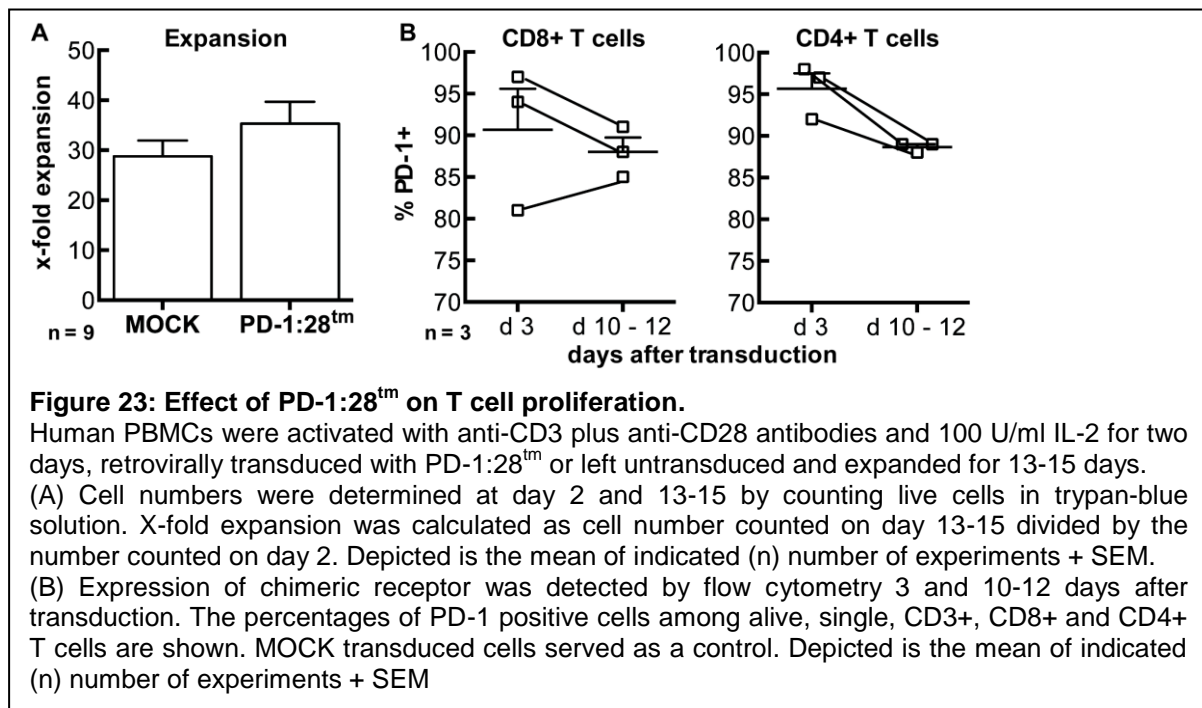
As shown in figure 22, TILs electroporated with water did not secrete IFN- γ upon stimulation. However, TILs electroporated with PD-1:28tm clearly produced IFN- γ at levels comparable to those of PBMCs from healthy donors. This provides evidence that stimulation through PD-1:28tm can reinstate functionality in T cells which had lost activity in the tumor microenvironment.



7.7 PD-1:28tm expressing T cells showed no aberrant cell expansion

CD28 stimulation can support T cell proliferation (5) and the super-agonistic anti-CD28 antibody TGN1412 led to hyperproliferation and cytokine storm in a phase I clinical trial (66). To assess the impact of PD-1:28 on T cell proliferation independent of TCR stimulation, T cells were transduced to stably express the PD-1:28tm receptor, which had shown the strongest effects in previous assays. PD-1:28tm T cells were expanded for 13-15 days and the increase in cell number was determined. As depicted in figure 23A, T cells expressing PD-1:28tm did not proliferate more than not-transduced T cells.

In addition to overall population expansion it was also determined whether the percentage of PD-1:28tm+ T cells in the population changed over expansion time. Therefore, the PD-1:28tm+ fraction was determined by flow cytometry using anti-PD-1 antibody. The percentage of PD-1:28tm expressing cells did not change during expansion indicating that PD-1:28tm expression did not lead to preferential proliferation of PD-1:28tm+ cells (figure 23B).

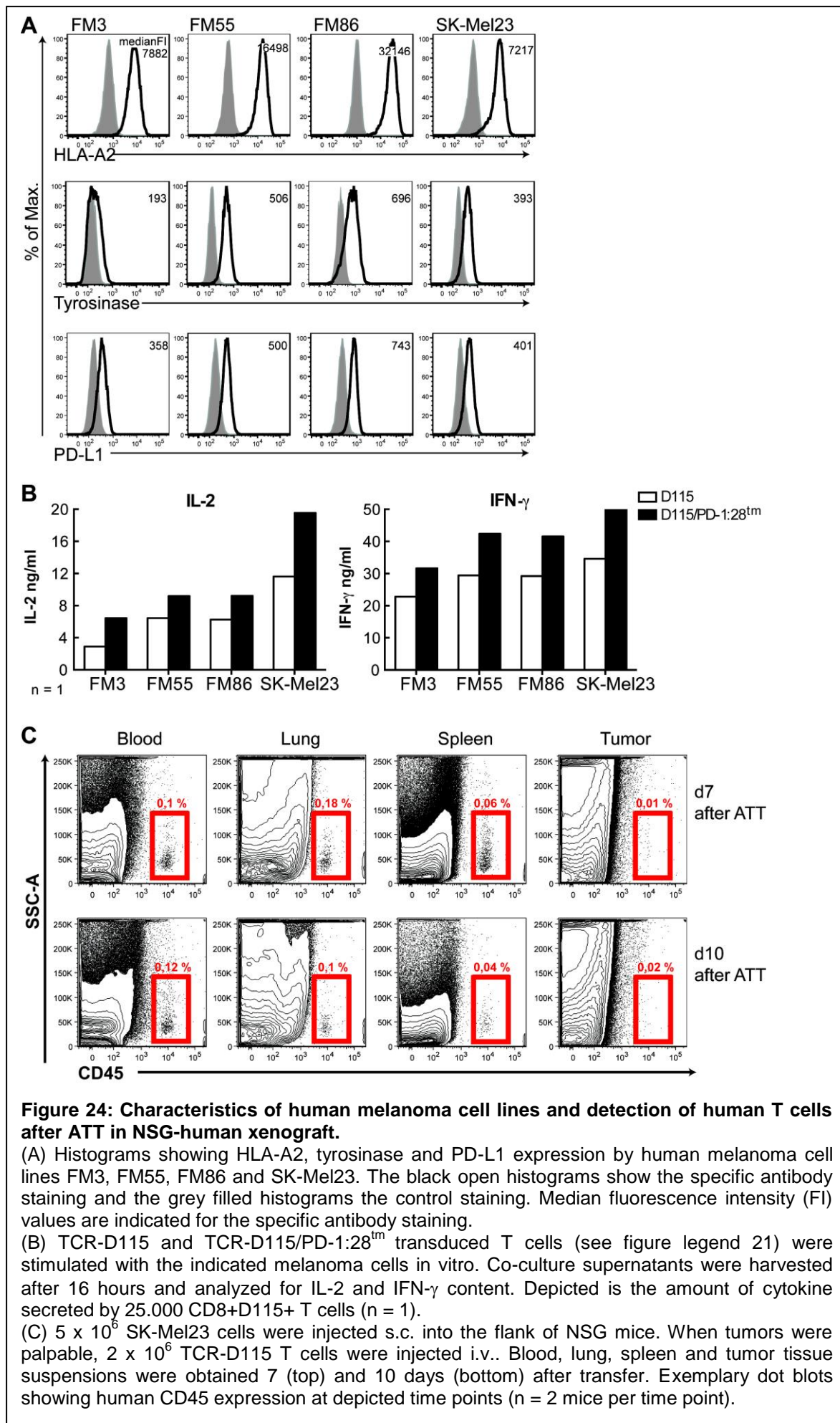


7.8 PD-1:28tm expression enhanced T cell proliferation in the microenvironment of a human melanoma xenograft

To study the effect of PD-1:28tm expression on T cells in vivo, a human melanoma xenograft mouse model was chosen, which involved the NSG mice carrying vascularized subcutaneous human melanoma tumors.

To select a melanoma cell line for the subcutaneous xenograft, 4 melanoma cell lines, FM3, FM55, FM86 and SK-Mel23, were compared for HLA-A2, tyrosinase and PD-L1 expression (figure 24A). FM3 had the lowest tyrosinase expression and evoked the lowest cytokine response by TCR-D115 and TCR-D115/PD-1:28tm T cells. SK-Mel23 evoked the strongest IL-2 response (figure 24B) by TCR-D115 and D115/PD-1:28tm T cells and was, therefore, chosen to be injected into NSG mice. The cytokine response of TCR-D115/PD-1:28tm T cells was higher compared to that of TCR-D115 T cells indicating that tumor cell-expressed PD-L1 can induce co-stimulation (figure 24B).

Five x 10⁶ SK-Mel23 cells were injected s.c. and after 15 days, when tumors were palpable, 2 x 10⁶ human TCR-D115 T cells were injected i.v.. Blood, lungs, spleens and tumors were analyzed 7 and 10 days after adoptive T cell transfer (ATT) for presence of transferred T cells by staining with an anti-human CD45 antibody. As depicted in figure 24C, transferred human T cells (CD45+) were detected in blood, lungs and spleens, while they were barely detected in tumor cell suspensions. No further analysis was attempted due to low cell yield of the transferred human T cells.



As human T cells apparently poorly migrated into the human xenograft when injected i.v., a second experiment was performed where T cells were injected directly into the tumors (figure 25A). Before injection TCR-D115 and TCR-D115/PD-1:28tm T cells (figure 25B) were labeled with CFSE to allow cell tracing and assessment of proliferation in vivo. When tumors reached a size of 802 mm³ (SEM ± 83), 6 x 10⁶ TCR-D115 or TCR-D115/PD-1:28tm T cells were injected i.t.. Tumors were harvested at 4 hours, 1, 2, 4, 6 and 10 days after ATT. Tumor suspensions were prepared and analyzed by flow cytometry. It was observed that TCR-D115 T cells were PD-1 negative before ATT but stained positive for PD-1 1 and 2 days after ATT, thus they up-regulated native PD-1 protein expression. After day 2 native PD-1 staining decreased but was never lost completely (figure 25C, E). This temporary expression of native PD-1 can be seen as a sign of T cell activation within the tumor microenvironment, which apparently lasted until day 2 after transfer. For TCR-D115/PD-1:28tm T cells, a temporary expression of native PD-1 is not discernable from the transgenic PD-1:28tm signal. However, a temporary increase in the median FI of PD-1 in TCR-D115/PD-1:28tm T cells was observed. Both TCR-D115 and TCR-D115/PD-1:28tm T cells showed down-regulation of CD8 with nearly complete loss at day 2 after ATT, again indicating activation (figure 25D, F). TCR-D115/PD-1:28tm T cells were starting to regain CD8 expression at day 4 while TCR-D115 T cells without PD-1:28tm stayed CD8 negative much longer with an indication of CD8 recovery at the latest time point analyzed (day 10).

Assessing the CFSE staining intensity revealed that at day 6 and 10 after ATT TCR-D115 T cells retained significantly more CFSE than TCR-D115/PD-1:28tm T cells ($p < 0.05$), thus they did not proliferate as much as TCR-D115/PD-1:28tm T cells, although they appeared to be activated in situ as judged by up-regulated PD-1 and down-regulated CD8 (figure 25G-H).

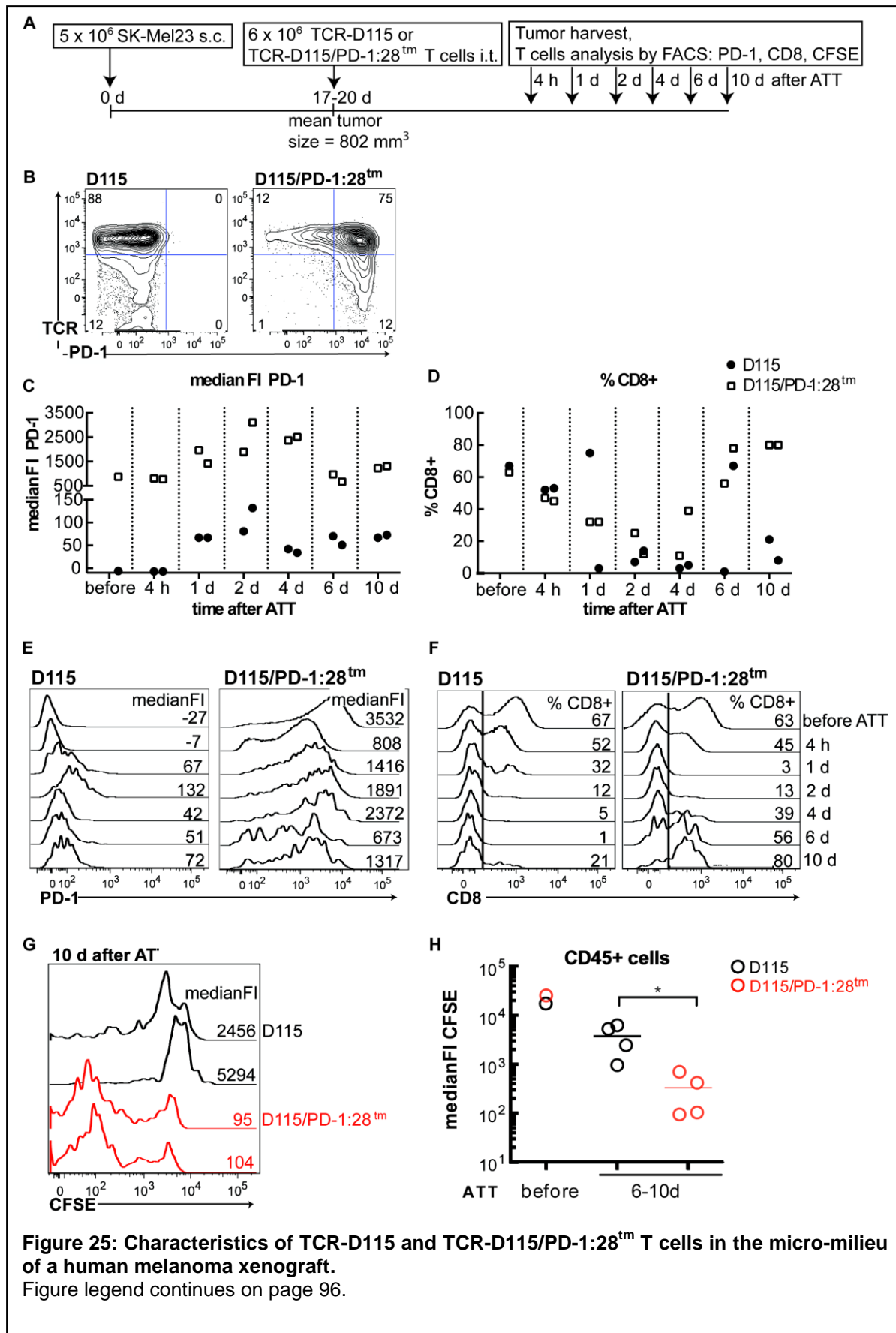


Figure 25: Characteristics of TCR-D115 and TCR-D115/PD-1:28tm T cells in the micro-milieu of a human melanoma xenograft.
 Figure legend continues on page 96.

Figure 25: Characteristics of TCR-D115 and TCR-D115/PD-1:28tm T cells in the micro-milieu of a human melanoma xenograft.

(A) Experimental outline: 5×10^6 human melanoma cells SK-Mel23 were injected s.c. into NSG mice. When tumors reached a size of $802 \text{ mm}^3 (\pm 83)$, 6×10^6 CFSE labeled TCR-D115 or TCR-D115/PD-1:28tm T cells were injected i.t. ($n = 2$ mice per T cell and time point). Tumors were harvested 4 hours, 1, 2, 4, 6 and 10 days after ATT and single cell suspensions were prepared for flow cytometry analysis of PD-1, CD8 and CFSE.

(B) Characteristics of T cells used for ATT: Human TCR-D115 T cells were activated with anti-CD3 plus anti-CD28 antibodies and 100 U/ml IL-2 for two days, retrovirally transduced with PD-1:28tm or MOCK and expanded for 14 days. Dot plots showing PD-1 and TCR expression in gated alive, single, CD3+, CD8+ T cells.

(C-F) Characteristics of T cells in the tumor microenvironment: Tumors were harvested on indicated time points after ATT, single cell suspensions were prepared and analyzed by flow cytometry. Scatter dot blots (C-D) and histograms (E-F) showing anti-human PD-1 (C, E) and CD8 (D, F) staining in gated human CD45+, alive and single cells.

(G) Histogram showing CFSE staining of gated human CD45+, alive and single TCR-D115 (black) and TCR-D115/PD-1:28tm T cells (red) in tumor suspension prepared 10 days after i.t. injection.

(H) Summary graph showing median FI of CFSE of gated human CD45+, alive and single TCR-D115 and -D115/PD-1:28tm T cells in tumor suspensions harvested before and 6 or 10 days after i.t. injection. * Mann-Whitney U test, $p < 0.05$

To analyze whether PD-1:28tm expression on T cells has an effect on tumor control, TCR-D115 or TCR-D115/PD-1:28tm T cells were injected into xenografts when tumors were palpable (mean \pm SEM = $78 \text{ mm}^3 \pm 5$) and tumor growth was measured over time. As depicted in figure 26A, i.t. injection of T cells with or without PD-1:28tm compared to PBS injection did not change tumor growth kinetics nor did it induce tumor shrinkage. Similarly, transfer of the high-avidity TCR-T58 T cells with or without PD-1:28tm did not show any effect on tumor growth (figure 26B).

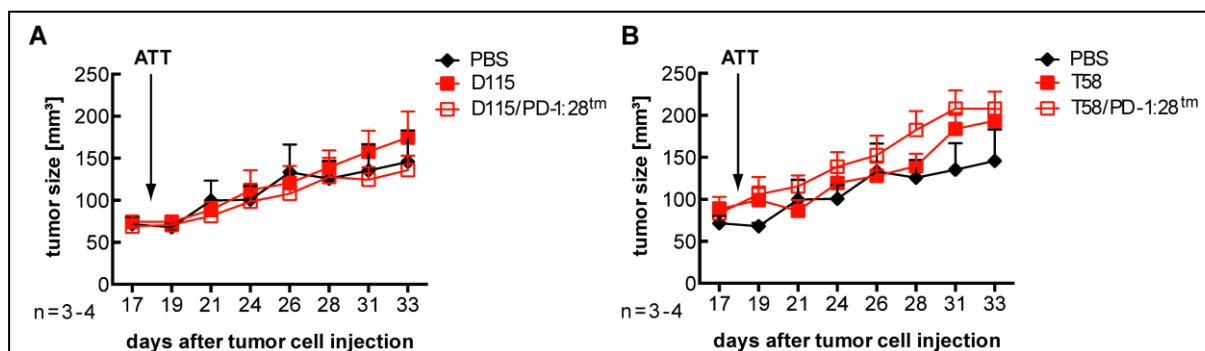


Figure 26: Growth kinetics of SK-Mel23 human melanoma xenograft in NSG mice receiving PBS or i.t. ATT.

5×10^6 SK-Mel23 cells were injected s.c. into NSG mice. When tumors were palpable (mean = 78 mm^3 , SEM ± 5), 6×10^6 TCR-D115 or TCR-D115/PD-1:28tm T cells (A, $n = 4$ mice per group), TCR-T58 or TCR-T58/PD-1:28tm T cells (B, $n = 4$ mice per group) or PBS ($n = 3$ mice) were injected i.t..

Tumor size (mean + SEM) was measured at indicated days after tumor cell injection.

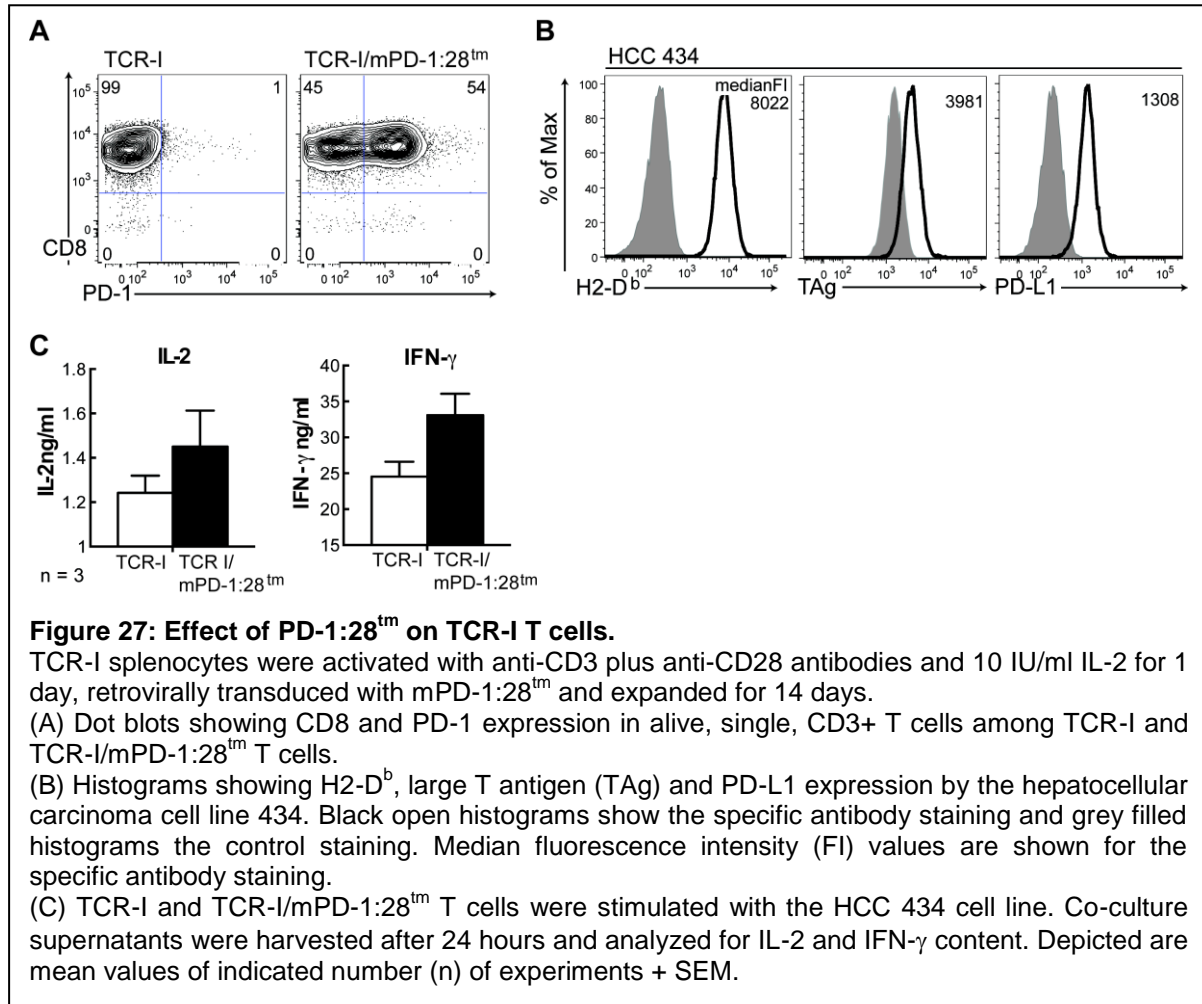
7.9 PD-1:28tm did not affect survival in an autochthonous hepatocellular carcinoma mouse model but suppressed Th2+Th17 polarization of TILs

The failure of PD-1:28tm to cause tumor shrinkage or delay tumor outgrowth in the human melanoma xenograft NSG mouse model might have been due to the xenogeneic nature of the NSG model. In the mouse background, human T cells cannot receive supportive cytokine signals nor can they follow chemokine gradients, as these mediators are mouse-derived. This will limit human T cell trafficking, survival as well as effector function. In addition, effector cytokines secreted by the human T cells, such as human IFN- γ , cannot affect the tumor vasculature, which is of murine origin, and, therefore, insensitive to the destructive effect of human IFN- γ .

Considering this, a fully murine model was chosen. The tumor model was the autochthonous hepatocellular carcinoma mouse model, LoxP-TAg, published by Willimsky et al. (60, 61). LoxP-TAg mice are transgenic for the oncogenic simian virus large T antigen (59), controlled by a stop cassette. Upon injection of adenoviruses coding for Cre recombinase (Ad.Cre) the stop cassette is deleted and TAg is expressed. Due to the hepatic tropism of adenoviruses TAg is predominantly activated in the liver and mice develop multinodular hepatocellular carcinoma (HCC) within 8-24 weeks after virus injection. In this model, the 3 phases of anti-tumor immune response, elimination-equilibrium-escape, can be observed (67). In the early phase of oncogenic activation tumor cells develop causing multiple malignant lesions in the liver. During this phase T cells are activated and eliminate most of the tumor cells. Then, around 6 weeks after oncogene activation, T cell exhaustion sets in and residual tumor cells grow out leading to death over a period of 8-35 weeks. Regarding the mechanism of immune escape, it is indicated that PD-1/PD-L1 interaction contributes to the immune escape since survival could be prolonged when anti-PD-L1 antibody was applied (61).

To analyze the effect of PD-1:28tm a murine construct (mPD-1:28tm) was generated and retrovirally transduced into LoxP-TAg mouse splenocytes (see below). Its capacity to enhance T cell function was assessed in vitro using splenocytes of TCR-I-transgenic mice. The TCR-I recognizes epitope I of TAg presented on murine H2-D^b. The HCC cell line 434, which expressed H2-D^b, TAg and PD-L1 (figure 27B), was used as a target to stimulate TCR-I T cells. TCR-I T cells were transduced with mPD-

1:28tm (figure 27A) and co-cultured with HCC 434 cells for 24 hours. As depicted in figure 27C, mPD-1:28tm enhanced the amount of secreted IL-2 and IFN- γ , thus seemed to be functionally expressed on TCR-I T cells.



The effect of mPD-1:28tm in vivo was addressed by transducing splenocytes of LoxP-TAg mice with mPD-1:28tm 15 weeks after initiation of oncogenesis and using them for ATT. According to published data (61), at this time point splenocytes should contain antigen specific T cells, which are exhausted and unable to control tumor outgrowth after the initial round of tumor cell killing. It was the question whether genetic engineering of these exhausted splenocytes with mPD-1:28tm could restore their function and enable them to control tumor outgrowth.

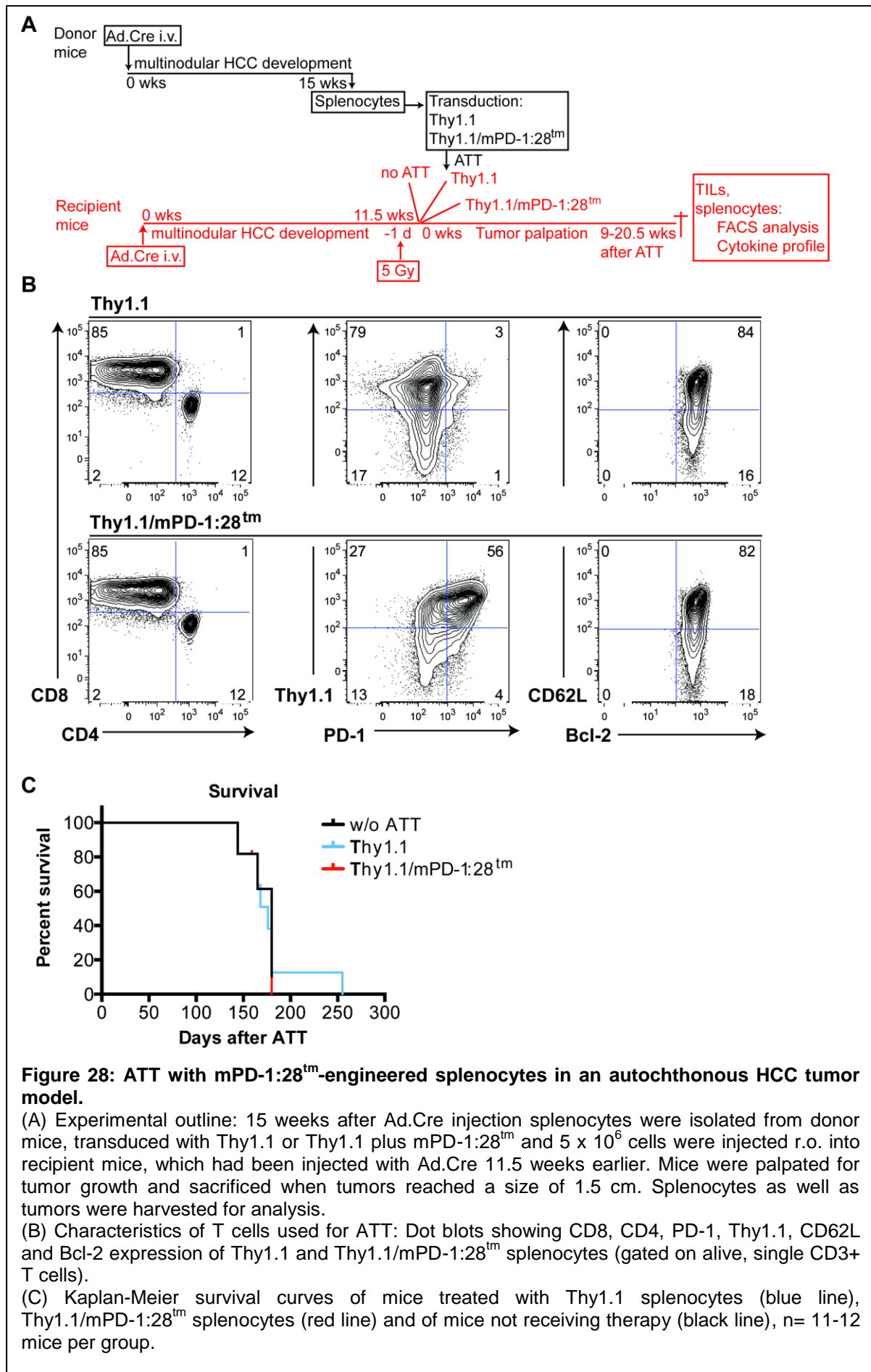
Before ATT splenocytes were transduced with Thy1.1 to allow tracing in vivo and one part of cells was additionally transduced with mPD-1:28tm. Transduced splenocytes were enriched for Thy1.1 positive cells using magnetic bead separation. Thy1.1 and

Thy1.1/mPD-1:28tm splenocytes expressed Thy1.1 to 81% and 83%, respectively. The transduction efficiency of mPD-1:28tm was 60%. The cell populations used for ATT were composed of 85% CD8⁺ T cells and 12% CD4⁺ T cells. CD62L was expressed by 84% and 82% of Thy1.1 and Thy1.1/mPD-1:28tm splenocytes, respectively. All T cells were 100% Bcl-2 positive and 84% of Thy1.1 and 82% of Thy1.1/mPD-1:28tm splenocytes expressed CD62L (figure 28B). Given the similar expression of Bcl-2 and CD62L it was assumed that Thy1.1 and Thy1.1/mPD-1:28tm splenocytes were in a similar state of differentiation.

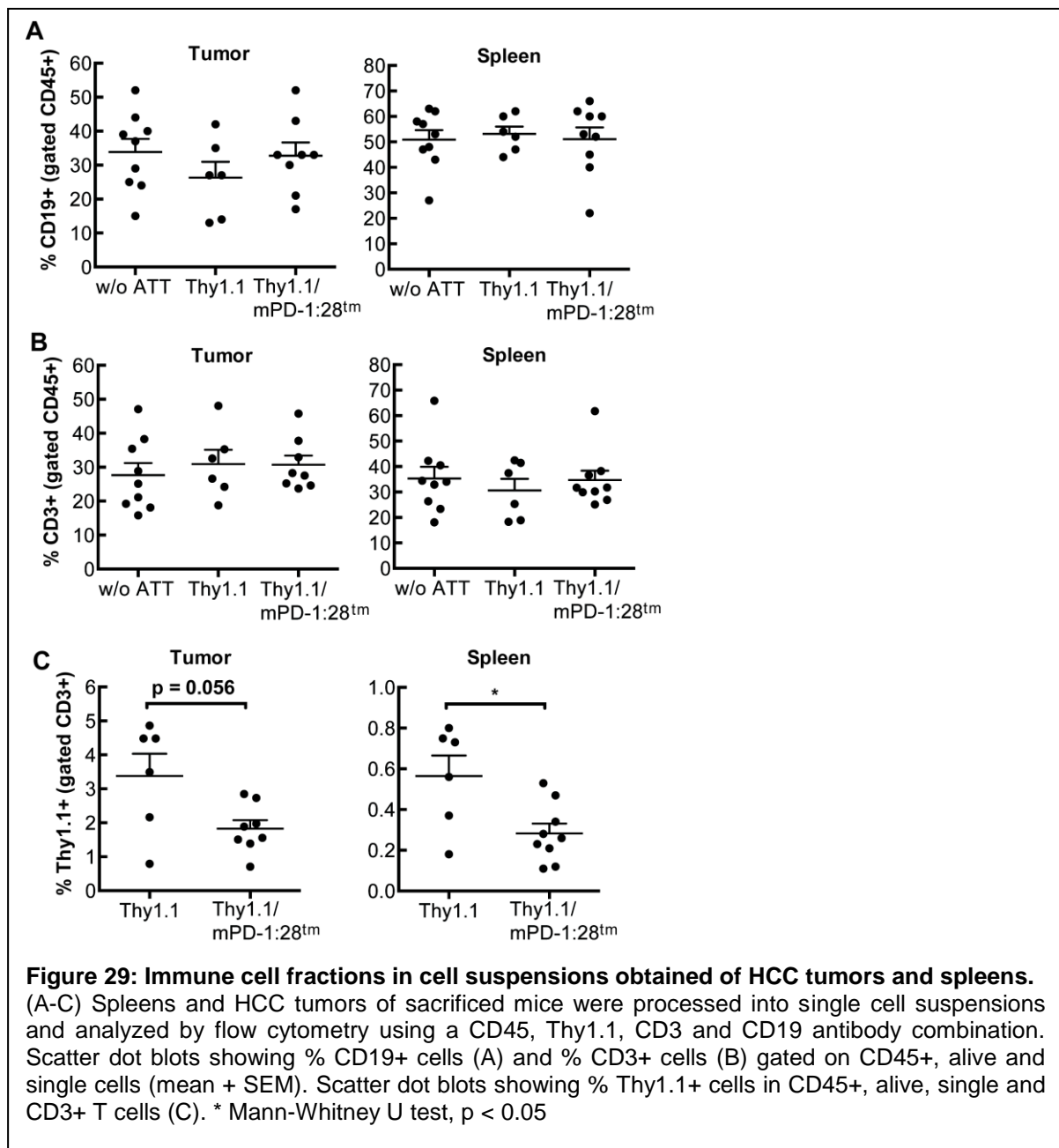
The ATT experiment involved 3 arms, each with 11-12 mice: i) no ATT, ii) ATT with Thy1.1 transduced splenocytes, iii) ATT with Thy1.1/mPD-1:28tm splenocytes (figure 28A). Blood was drawn at day 4, 7, 14 and 16 after ATT and analyzed for the presence of transferred T cells.

The blood analysis showed that Thy1.1⁺ cells were hardly detectable (0.01-0.6% of all cells) at day 4 after ATT and remained at the detection limit at day 7, 14 and 16 after ATT (not shown). Mice were observed for tumor growth by palpating the abdomen every second day. Mice were sacrificed when tumor size appeared to have reached a size of 1.5 cm or mice seemed to be in distress. After scarification HCC tumors and spleens were harvested and single cell suspensions prepared. TILs were separated from tumor cells and hepatocytes by Percoll density gradient centrifugation.

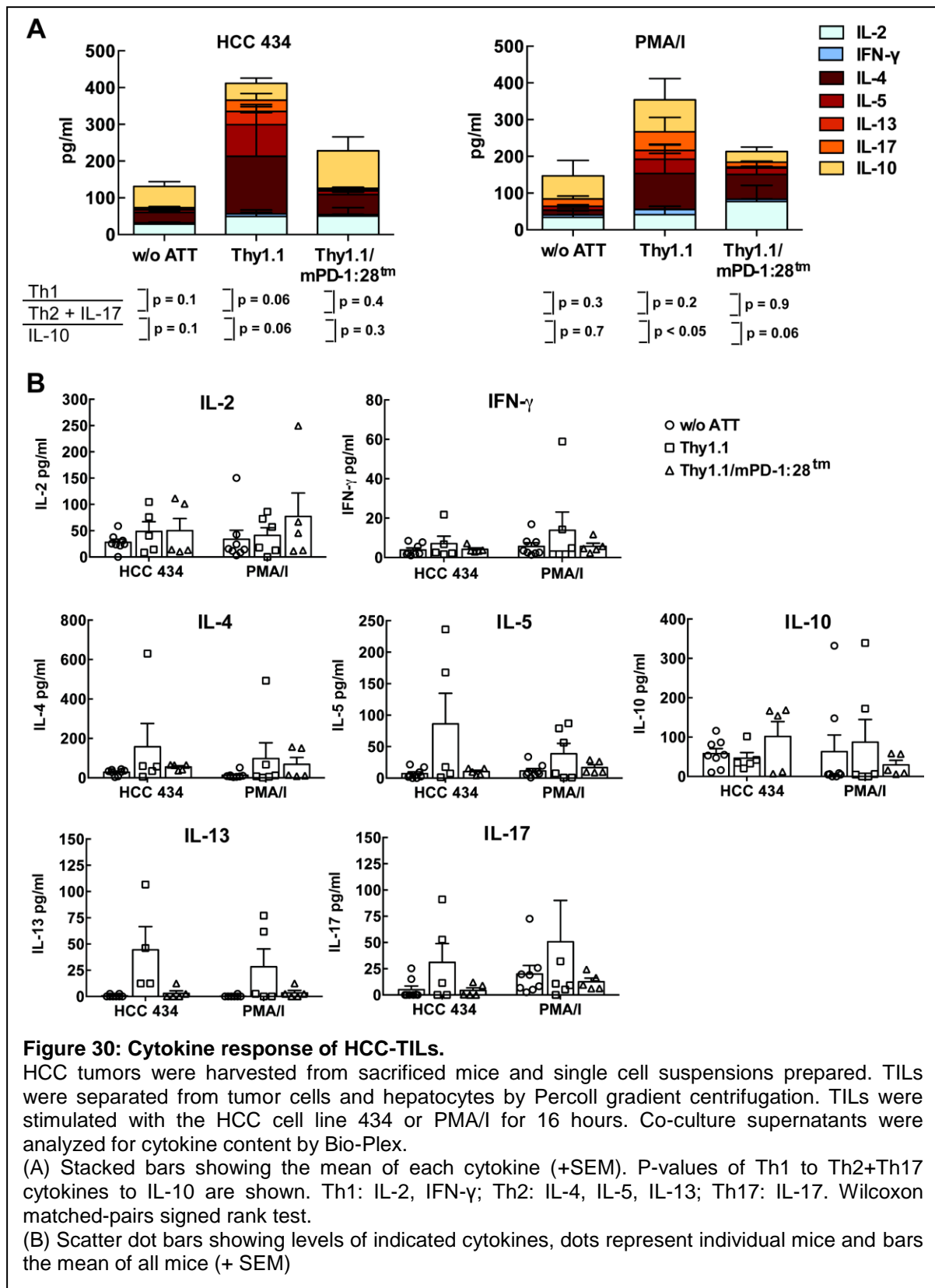
The cumulative survival curves (using Kaplan-Meier analysis) were similar for all 3 arms indicating that ATT using Thy1.1 and Thy1.1/mPD-1:28tm splenocytes had no effect on tumor growth (figure 28C).



Flow cytometry analysis was performed with TILs and splenocytes from sacrificed mice. The overall percentage of CD19+ B cells or CD3+ T cells in tumors or spleens were similar in all 3 treatment groups (figure 29A-B). Calculating the fraction of transferred T cells within the CD3+ T cells of spleens and tumors, i.e. the percentage of Thy1.1+ cells among all CD3+ T cells, revealed a higher percentage of Thy1.1+ cells in tissues of mice treated with Thy1.1 ATT (figure 29C). Among TILs on average 3.4% of CD3+ T cells from mice treated with Thy1.1 splenocytes stained positive for Thy1.1, while 1.8% stained Thy1.1 positive when mice received Thy1.1/mPD-1:28tm ATT. In spleens, 0.6% and 0.3% of CD3+ T cells stained positive for Thy1.1 when mice were treated with Thy1.1 or Thy1.1/mPD-1:28tm ATT, respectively.



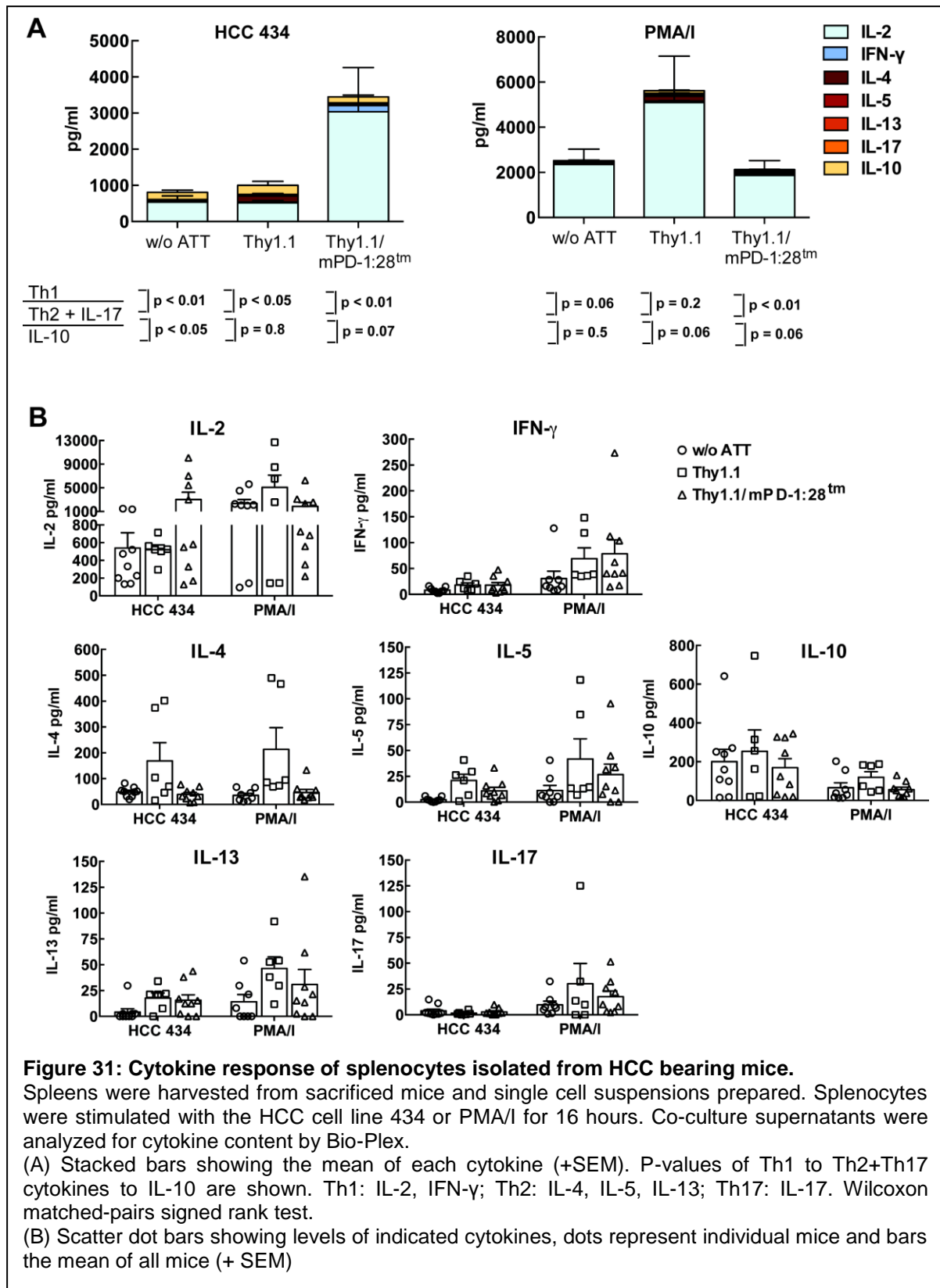
TILs and splenocytes were additionally analyzed for their responsiveness to stimulation and cytokine profile. Specifically, cytokines IFN- γ , IL-2, IL-4, IL-5, IL-10, IL-13 and IL-17 were analyzed using the Bio-Plex method to determine the Th1/Th2+IL-17/IL-10 polarization. For T cell stimulation the TILs and splenocytes were stimulated with the autologous HCC cell line 434, which expresses TAg and PD-L1. The observed cytokine secretion should predominantly result from stimulation of tumor antigen-specific T cells. In parallel, TILs and splenocytes were stimulated with PMA/I as it was considered possible that the tumor cell line might inhibit the T cell response due to its PD-L1 expression. The cytokine response observed after PMA/I stimulation results from all T cells independent of antigen-specificity and can be used to interpret the overall tissue-associated T cell polarization. The results for TILs and splenocytes are shown in figure 30 and 31. As a general note, the amount of cytokines produced by TILs was much lower than that of splenocytes regardless of stimulation with the HCC cell line 434 or PMA/I. Th1 cytokines secreted by TILs were similar in all treatment groups. TILs from mice having received Thy1.1 ATT produced more Th2 cytokines and also more IL-17 than TILs of mice from the Thy1.1/mPD-1:28tm ATT or no ATT arm. This finding was also observed when cells were stimulated with PMA/I indicating a reprogramming of TILs in tumors of the Thy1.1 ATT group. On the other hand, TILs of mice having received Thy1.1/mPD-1:28tm ATT secreted higher amounts of the regulatory cytokine IL-10. The secretion of IL-10 was more prominent when TILs were stimulated with the HCC cell line 434.



As indicated before, the cytokine response of splenocytes was higher compared to TILs and was dominated by IL-2 in all treatment groups (figure 31). When stimulated with the tumor cell line 434, splenocytes from the mPD-1:28tm ATT arm secreted clearly higher amounts of IL-2 and IFN- γ . In contrast to splenocytes of the Thy1.1 ATT treatment group, splenocytes of the mPD-1:28tm ATT and no ATT arm did not tend to secrete Th2 cytokines.

When splenocytes were stimulated with PMA/I, less IL-10 was observed compared to stimulation with the HCC cell line 434.

These findings indicate that ATT with mPD-1:28tm positive T cells might prevent the induction of Th2+IL-17 cytokines and retain the capacity to secrete high amounts of IL-2 upon stimulation with tumor cells.



8 DISCUSSION

Loss of function and poor persistence of T cells in the tumor environment are major hurdles for successful adoptive T cell therapy. Co-stimulation can enhance both T cell effector function and proliferation. In particular, it has been shown that co-stimulation can extend the duration and effectiveness of the cytotoxic response in an environment of high antigen load and can overcome TGF- β -mediated repression of T cell proliferation (53, 68). These are desirable and much needed characteristics for ATT that should help to augment the efficacy of ATT. However, a large proportion of human CD8⁺ effector T cells, in contrast to murine T cells, are CD28 negative (54) and most epithelial tumors do not express the co-stimulatory ligands CD80 or CD86 (55, 56). Thus, human T effector cells cannot receive the classical co-stimulatory signals in the tumor environment. With the advent of genetic engineering (69) the idea to equip T cells with desired characteristics is becoming reality. In this thesis, I explored the concept whether engineering of T cells with a chimeric co-signaling receptor consisting of the extracellular domain of PD-1 linked to an intracellular stimulatory domain could be a strategy to initialize co-stimulation in the tumor microenvironment. Facilitated co-stimulation through chimeric co-signaling receptors with the extracellular domain of PD-1 is conceptually attractive for cancer immunotherapy as the ligand for PD-1, PD-L1, is commonly expressed at high levels on solid tumor cells (57) and absent or poorly expressed by healthy tissue (70). Thus, activation of the co-signaling pathway from the PD-1:28 chimeric receptor will occur in the tumor milieu and T cells should receive co-stimulation when interacting with tumor cells thus at the time and place stimulation is required. In addition, the chimeric receptor should counterbalance the inhibitory effect of the native PD-1. Thereby, chimeric co-stimulatory receptors could turn tumor-mediated inhibition into activation. The field of chimeric immune receptors is currently best known for chimeric antigen receptors (CAR), which are highlights of cancer immunotherapy (16). Here, an antibody domain is fused via a hinge region to the TCR signaling domain of CD3 ζ and one of several co-signaling domains. T cells expressing a CAR are equipped with the recognition specificity of an antibody and activate T cell effector functions, such as cytotoxicity and cytokine secretion, when recognizing the target structure. A design linking the antibody specificity of CD19 to the co-signaling domain of 4-1BB

has caught attention due to remarkable clinical efficacy in patients with relapsed or refractory acute lymphoblastic leukemia patients (34). This clinical trial was the first to show tumor clearance concomitant with long-term persistence of the adoptively transferred CD19-CAR-T cells. It is speculated that this unique achievement was due to the 4-1BB signaling sequence of the CAR, although comparative side-by-side trials with otherwise identical chimeric receptors encoding the CD28 versus the 4-1BB co-signaling domain are only now being performed.

4-1BB is a co-stimulatory molecule for activated T cells that has been reported to increase CD4⁺ and CD8⁺ T effector function and to provide survival signals and expansion mainly for CD8⁺ T cells. Its particular value for cancer immunotherapy may lay in the capacity to sustain ongoing T cell responses as well as to enhance or rescue suboptimal immune responses (6, 10).

While it is still contentious which co-stimulatory signal or combination thereof might be optimal, the necessity of co-stimulation is without question, at least in the CAR field. Facilitated co-stimulation has not been explored for TCR-engineered CD8⁺ T cells that are being used in clinical trials with efficacies remaining behind expectation (37). Given the lack of CD28 expression on most human CD8⁺ T effector cells, facilitated co-stimulation could be a step towards improving efficacy.

8.1 Design influences chimeric receptor expression

In this dissertation, different chimeric co-signaling receptors were created utilizing the extracellular domain of PD-1 and the signaling domain of either CD28 or 4-1BB. One receptor design (PD-1:8tm:28) closely followed the domain arrangement of CARs, utilizing the CD8 hinge and transmembrane region to link the extracellular domain of PD-1 to the intracellular CD28 signaling domain. Hinge regions in CARs are meant to increase receptor flexibility and facilitate the binding of membrane-proximal epitopes (28). Surprisingly, the PD-1:8tm:28 chimeric protein was poorly expressed on the surface of T cells. The receptor did not accumulate intracellularly, thus excluding poor ER-Golgi transport. Rather, the translation efficacy of the ivt-RNA seemed limited for as yet unknown reasons. Similarly, poor expression, and, additionally, poor retention on the cell surface, was observed for the chimeric protein PD-1:BBtm, which

consists of the transmembrane domain and the intracellular signaling domain of 4-1BB. Here, the short surface presence might be due to features of the 4-1BB protein, which exhibits fast recycling when expressed under native conditions (7, 71). A new construct containing the transmembrane domain of PD-1 instead of 4-1BB (PD-1tm:BB) was created to address this hypothesis. Indeed, preliminary results suggest better surface expression and future experiments will be performed to study the kinetics and functionality of the chimeric receptor.

Regarding chimeric receptors containing the CD28 signaling domain, 2 variants were compared, PD-1:cys28tm and PD-1:28tm, whereby the former contained the CD28 membrane proximal sequence that encodes the cysteine at position AA 141. The native CD28 protein is expressed on the surface as a homodimer while PD-1 is a monomer. It was considered possible that the dimerization through the cysteine might be required for proper surface expression and CD28 signaling activity of a chimeric PD-1:28 receptor. Yet, there was no evidence for this proposition as PD-1:cys28tm and PD-1:28tm showed similar patterns for both expression and activity.

8.2 PD-1:28 chimeric receptors can enhance functionality of human T cells and restore tumor-inhibited TIL function

After it was shown that chimeric PD-1:cys28tm and PD-1:28tm receptors could be stably detected on the T cell surface it was assessed whether these receptors can enhance T cell function. Indeed, it could be demonstrated that T cells expressing the PD-1:cys28tm or PD-1:28tm receptor secreted more IFN- γ and IL-2 when stimulated with PD-L1 expressing target cells. The increased cytokine secretion will likely be beneficial for the anti-tumor response as both cytokines are important components for effective tumor control. IFN- γ can up-regulate MHC expression (72) and thereby increase the visibility of tumor cells for T cells. Furthermore, IFN- γ can foster infiltration of NK cells and macrophages by inducing the production of chemokines. In addition, IFN- γ can target tumor stroma and inhibit angiogenesis (73).

The beneficial effect on cytokine secretion was more profound for IL-2 than for IFN- γ . This is conceivable since the IL-2 promoter is a primary target of the CD28 co-stimulation pathway (5). Furthermore, as the activation threshold for IL-2 transcription is higher compared to IFN- γ , i.e. stronger TCR signals are required to elicit an IL-2

response (74) and IL-2 transcription may be more susceptible to CD28 co-stimulation than IFN- γ . Epigenetic alterations of the IL-2 promoter upon CD28 stimulation, such as reduced cytosine methylation and increased histone acetylation (75) could be underlying mechanisms for the effect of CD28 co-signaling receptors on IL-2 expression.

Regarding T cell effector activity, facilitated secretion of IL-2 by CD8⁺ T cells is particularly valuable as CD8⁺ T effector cells often do not produce IL-2 themselves but are dependent on IL-2 secreted by concurrently activated CD4⁺ T cells. Becoming independent of CD4⁺ T cell help is a major asset for effector CD8⁺ T cell function as many tumor cells are MHC class II negative (76) and thus cannot activate CD4⁺ T cells. IL-2 provision helps CD8⁺ T cell proliferation and might promote tumor localization (77).

Co-stimulation has a major impact on the T cell response by enhancing signaling cascades downstream of the TCR, such as increasing the activation level of the MAP kinase pathway including ERK. ERK is implicated in cytokine secretion and degranulation (1, 2). In addition, co-stimulation can enhance the mTOR pathway leading to RPS6 activation (5, 78). RPS6 supports proliferation and is involved in protein synthesis (4). Thus, through facilitating enhanced TCR signaling, PD-1:28 might overcome known deficits of TILs including reduced effector function and low perforin expression (48). Indeed I could demonstrate that T cells expressing chimeric PD-1:28tm or PD-1:cys28tm receptors elicited higher phosphorylation of ERK and RPS6 when stimulated with PD-L1⁺ target cells compared to T cells not expressing the chimeric receptors. Since it has been observed previously that blockade of ERK and AKT phosphorylation is one mechanism that causes loss of function of T cells in human renal cell carcinoma tissue (48), I hypothesized that co-stimulation might restore these deficits and allow TILs to regain function. Indeed, TILs engineered to express PD-1:28tm did secrete IFN- γ when stimulated with PD-L1⁺ target cells while the same TILs without PD-1:28tm did not secrete cytokine under the same stimulation conditions. In future experiments it will be analyzed whether gain of function is associated with de-blocking of the ERK and AKT signaling cascades. TILs are being used in adoptive T cell therapy of melanoma and RCC with clinical response rates of 56% and 11%, respectively (16, 79). Given the results of this thesis, it might be

interesting to explore whether genetic engineering of TILs before transfer might improve efficacy.

In addition to TILs, T cells genetically engineered to express a tumor-specific TCR are used in adoptive T cell therapy. High-avidity TCRs are desired as it is thought that they confer superior effector function compared to low-avidity TCRs (80, 81). Published studies indeed suggest that low-avidity T cells can remain ignorant of antigen expressing target cells and may not mount a successful tumor-specific response (82). Efforts are therefore taken to modify TCR sequences to increase their affinity for antigen recognition (25, 83). However, results with affinity-enhanced TCRs are controversial, demonstrating no or improved responses compared to low-avidity counterparts (21, 59). Moreover and of concern for clinical application are observed serious adverse effects with adoptively transferred T cells expressing affinity-enhanced TCRs (26, 27). These adverse reactivities are attributed to the genetically altered TCR sequence that created unpredicted reactivity to new target structures expressed by vital organs. Less risk of autoimmunity is expected with naturally occurring TCRs as they have been thoroughly selected by the thymus and are under peripheral control mechanisms. However, as a drawback of thymic selection, those TCRs participating in the anti-tumor response are of intermediate to low avidity (84). Genetic engineering with PD-1:28 receptors appears to be an interesting strategy that allows utilizing low-avidity T cells isolated from cancer patients, as it has been shown that expression of PD-1:28 receptors enhanced the cytokine response of low-avidity T cells to levels comparable to high-avidity T cells.

Transgenic expression of a chimeric co-stimulatory receptor does not alter the TCR sequence and thus will not change the T cell specificity. Therefore, the occurrence of unpredicted off-target recognition is not to be expected. Co-stimulation by enhancing the TCR signaling cascade might, however, lower the threshold for T cell activation, thus T cells expressing the chimeric co-stimulatory receptor might respond to cells with lower levels of cognate pMHC. This might be advantageous as tumor cells often down-regulate MHC I molecules, antigens and molecules of the antigen-presentation pathway (85, 86). Future experiments will address this question.

Co-inhibition strongly opposes an effective antitumor response. Counteracting co-inhibitory signals will be of value and enhance the function of anti-tumor immune responses. The importance of blocking co-inhibition is convincingly documented in

several clinical trials achieving tumor regression in advanced stages of several tumor entities when blocking the PD-1/PD-L1 axis with therapeutic antibodies (43). Opposing co-inhibition might be an additional mode of action of PD-1:28 receptors as they can dilute native PD-1 signals. It is shown in this thesis that low-avidity T cells in particular might benefit from ameliorating co-inhibition as PD-1trunc, with no signaling capacity, enhanced cytokine secretion of low-avidity TCR-D115 T cells but not of high-avidity TCR-T58 T cells. The difference between the two T cells regarding the effect of PD-1trunc was not explained by different levels of native PD-1 expression. In the literature it is suggested that low-avidity TCRs activate the TCR signaling cascade less efficiently (22). Inhibitory signals, or their attenuation have a stronger impact as compared to situations of strong TCR signaling.

In summary, it was shown that PD-1:28 chimeric receptors not only activated the co-stimulatory pathway resulting in enhanced TCR signaling and effector function but additionally opposed native PD-1. These are strong assets of chimeric co-signaling receptors and may help ameliorating a major hurdle of efficient antitumor function in PD-L1+ tumor milieus.

8.3 In vivo studies support the therapeutic potential of the PD-1:28 receptor

Co-stimulation also supports TCR-independent programs, such as survival, cell cycle progression and maintenance of lytic proteins (5, 53), all of which are particularly valuable in a challenging environment.

To analyze the effect of PD-1:28tm on T cell function in a tumor environment I performed adoptive T cell therapy experiments using several mouse models. The first model was a human melanoma xenograft model that allowed utilizing human T cells expressing the human tyrosinase-specific TCR-D115 and the human PD-1:28tm construct. Despite several shortcomings of the xenograft system (detailed below) it was clearly observed that TCR-D115 T cells expressing PD-1:28tm proliferated better in the tumor milieu than TCR-D115 T cells without PD-1:28tm. This observation suggests that PD-1:28tm has the potential to increase the persistence of adoptively transferred T cells in the tumor milieu.

Additional evidence for a better performance of T cells expressing the PD-1:28tm receptor may be deduced from the observation that TCR-D115/PD-1:28tm T cells re-expressed CD8 faster, while TCR-D115 T cells without PD-1:28tm remained CD8 negative over the observation time of 10 days. CD8 down-regulation indicates activation but CD8 re-expression is required for the T cell to be again responsive to stimulation (87). Cytotoxic CD8⁺ T cells with down-regulated CD8 expression are reported to have higher levels of cleaved caspase-3 and may, therefore, be more prone to cell death (88).

While stronger proliferation and CD8 regain of TCR-D115/PD-1:28tm T cells in the tumor milieu suggests that PD-1:28tm can provide support to T cells, there was no evidence that this translated into better tumor control.

There are many explanations: One is the incompatibility of chemokines and cytokines important for lymphocyte migration. Indeed, the adoptively transferred human T cells were not found in the tumor when injected intravenously, while they could be detected in blood, lung and spleen. To circumvent this problem, i.t. injection was chosen.

T cells were injected only once, which may not have been sufficient. Data from human clinical trials (89) and murine studies (90) provide evidence that multiple infusions of tumor-reactive T cells are more effective than a single infusion.

As it was the aim to address whether PD-1:28tm can provide T cells with the capacity to persist and maintain effective tumor-directed functionality, no human cytokines were co-administered. Thus, T cells might have experienced cytokine deprivation. Literature data suggests that it is necessary to destroy the tumor stroma, i.e. vasculature and carcinoma-associated fibroblasts (CAFs), to achieve tumor shrinkage (91, 92). To this end, the activity of IFN- γ is required (49), which can be produced when T cells are activated by antigen recognition.

In a xenograft model, the transferred T cells are of human origin and secrete human IFN- γ , while the tumor stroma is of murine origin. The incompatibility of human cytokines and murine stroma may be another reason why tumor shrinkage was not achieved despite signs of T cell activation.

Given the outlined limitations of xenograft models an autochthonous HCC model was selected. This model was established by Gerald Willimsky and involved induction of the oncogenic process by activating SV40 large T antigen (TAg) through the Lox-Cre-system (60, 61). Many characteristics of this model suggested that it might be

close to human cancer. The tumor is not transplanted but develops through activation of an oncogene and the course of tumor progression is slow, spanning up to 35 weeks from initiating the oncogenic process until death from tumor load. An initial phase of immune cell activation with clearance of tumor burden is followed by T cell exhaustion with indication of PD-1 involvement and loss of tumor control (61).

A fully murine tumor model required the generation of a murine PD-1:28tm (mPD-1:28tm) construct. This mPD-1:28tm receptor showed a beneficial effect on T cell cytokine secretion in vitro. As for tumor antigen-specific T cells to be engineered with mPD-1:28tm and used for ATT several options were available: TCR-transgenic T cells recognizing epitopes of the tumor antigen TAg or naturally induced TAg-specific T cells such as TILs from the HCC tumor or splenocytes, which would equal PBL in the human situation. With each T cell population different questions could be addressed regarding effect of mPD-1:28tm expression. These are prevention or reversal of acquired deficits and impact on the performance of T cells with a single or mixed specificity. In a first approach, TCR-transgenic T cells recognizing a TAg epitope were selected for ATT. Four epitopes (I-IV) are known for TAg. For epitope I (SAINNYAQKL) there is a transgenic mouse strain available that expresses the epitope I-directed TCR-I together with renilla luciferase, allowing trafficking of T cells after ATT via bioluminescence imaging (93), which appeared attractive. However, after transfer TCR-I T cells were not detectable at day 3 and 7. There is evidence in the literature that TCR-I T cells do not persist in vivo and may be tolerized in the periphery (94). This may be due to the high stability of epitope I/H2-D^b pMHC (95), which may cause TCR-I T cell deletion (96).

In a second experiment, naturally induced anti-tumor T cells were used. Based on published results (61) from 12 weeks on after tumor induction, exhausted T cells should be found in the spleen. Those splenocytes have been shown to be effective in ATT with additional improvement by anti-PD-L1 treatment (61). In this thesis, mPD-1:28tm-transduced splenocytes were used for ATT and survival compared to ATT without mPD-1:28tm and no ATT. Although no effect was observed on tumor growth, mPD-1:28tm ATT showed a positive effect on T cell cytokine polarization. Most notable was the prevention of Th2 polarization in the tumor milieu. Th2 cytokines and IL-17 are associated with metastasis (97), liver cirrhosis (98), increased tumor vascularization (99) and proliferation of cancer cells (100). In addition to less Th2 cytokines, more IL-10 was observed in ATT with mPD-1:28tm. IL-10 can have

conflicting effects such as suppression of anti-tumor immunity but also enhancement of cytotoxicity of and IFN- γ secretion by CD8⁺ T cells, thereby controlling tumor growth (101, 102). The suppression of Th2 by mPD-1:28tm ATT could be explained by the observation that native PD-1 signaling inhibits secretion of Th1 but not Th2 cytokines (58) and that PD-1 blockade can suppress Th2 polarization (103). When transferred T cells express mPD-1:28tm, the inhibitory effect of native PD-1 can be counterbalanced by the chimeric receptor and thus a Th2 polarization can be prevented.

Several possibilities are considered that may explain the failure to achieve tumor rejection. In this experiment, ATT in general, independent of mPD-1:28tm, did not show any effect over no ATT. One explanation might be that the splenocytes used for ATT lacked or contained only few tumor-reactive T cells or/and T cells were irreversibly inhibited.

Moreover, the observation that transferred T cells could not be detected in the blood after injection supports the hypothesis that they did not persist. ATT was given as a single dose without administration of cytokines. However, injection of cytokines might have supported the persistence of transferred T cells. Injection of IL-2 might help T cell persistence as observed for human TILs (104) and its administration along transfer of autologous TILs is a standard protocol in the clinical setting (16). Moreover, administration of IL-7 and IL-15 as mediators of T cell proliferation and function might be beneficial. They might preferentially support memory T cells and thereby enhance long-lasting responses (105).

The third option using TILs from HCC could not be explored within the time frame of this thesis.

There is no model system perfectly matching the tumor milieu of human cancer patients. In the currently available models the potential impact of the PD-1:28tm receptor might have been obscured. As the human immune system is different from the murine one (106), data observed with the help of a mouse model system cannot be transferred straightforward to the human situation. The observation that murine T cells are almost 100% CD28 positive and that they do not lose CD28 expression with age or in the course of chronic disease is completely different to the human situation where only 50% of CD8⁺ T cells express CD28 and there is a down-regulation of CD28 (107). Thus, it seems likely that murine and human T cells do not

share the same necessity of facilitated co-stimulation. The differences of human and murine immunity can only be circumvented by engraftment of NSG mice with human hematopoietic stem cells. This would allow the recruitment of engrafted leukocytes and might enhance migration of transferred cells to the tumor site. The means for this model were not available but this experimental setup might reveal the complete therapeutic potential of PD-1:28tm engineered T cell therapy.

8.4 Outlook

Co-stimulation and co-inhibition have a major impact on quality and quantity of immune responses. With a chimeric co-stimulatory receptor I hypothesized that both quality and quantity can be addressed and support be provided to T cells used for adoptive therapy of human cancer. Many of the observed effects of PD-1:28, including enhanced TCR signaling, stronger cytokine production, up-grading of low-avidity T cells, restored function of TILs isolated from human RCC, better proliferation of T cells in the tumor milieu of a xenograft model and suppression of tumor-inflicted Th2 polarization in a model of murine HCC hint at its therapeutic potential.

Although tumor shrinkage could not be detected in the analyzed models, the results still suggest that a PD-1:28 receptor might improve adoptive T cell therapy. Given the complexity of tumor immune escape mechanisms it is, however, not to be expected that PD-1:28 as a stand-alone intervention will enable tumor rejection. Rather combination of strategies targeting different escape mechanisms is likely necessary to achieve an optimal result (108). In this regard, a combination of PD-1:28tm engineered T cells or TILs and IL-2 to support T cell persistence may be beneficial. Blockade of additional inhibitory signals could add to the beneficial effect of PD-1:28tm facilitated co-stimulation, such as blocking antibodies to CTLA-4 could further increase TCR signaling and thereby strengthen T cell functionality.

9 ABBREVIATIONS

7-AAD	7-Aminoactinomycin
A	Alanine
A488, A647, A700	Alexa 488, 647, 700
Ad.Cre	Adenovirus coding for Cre recombinase
ATT	Adoptive T cell therapy
Akt (= PKB)	Protein kinase B
APC	Allophycyanin; antigen presenting cell
APC-Cy7	Allophycyanin – Cyanine 7
APC-eF780	Allophycyanin – eFluor 780
Ca	Calcium
CAR	Chimeric antigen receptor
CD	Cluster of differentiation
C region	Constant region
D	Aspartic acid
DAG	Diacylglycerol
DGK- α	Diacylglycerol kinase- α
DGK-I	Inhibitor of DGK- α
DC(s)	Dendritic cell(s)
DMEM	Dulbecco's modified eagle medium
DMSO	Dimethyl sulfoxide
DNA	Deoxyribonucleic acid
E	Glutamic acid
EDTA	Ethylenediaminetetraacetic acid
ERK	Extracellular signal related kinase
F	Phenylalanine
FACS	Fluorescence activated cell sorting
FCS	Fetal calf serum
FITC	Fluorescein isothiocyanate
FSC-A, -H	Forward side scatter-area, -height
G	Glutamine
Gy	Gray
H	Histidine
HBSS	Hank's buffered salt solution
HEK 293 cells	Human embryonic kidney 293 cells
Hepes	4-(2-Hydroxyethyl)-1-piperazine-ethanesulfonic acid

HS	Human serum
ICAM-1	Intercellular adhesion molecule-1
IFN- γ	Interferon-gamma
Ig	Immunoglobulin
IL	Interleukin
ITAM	Immunoreceptor tyrosine-based activation motif
ITK	Interleukin-2 inducible T cell kinase
IP ₃	Inositol-1,4,5-trisphosphate
IU	International units
i.v.	intravenously
JNK	C-Jun N-terminal kinase
K	Lysine
kDa	Kilo Dalton
L	Lysine
LAT	Linker for activation of T cells
Lck	Leukocyte C-terminal sarcoma kinase
LCMV	Lymphocytic Choriomeningitis Virus
LTR	Long terminal repeat(s)
M	Methionine
MAPK	Mitogen activated protein kinase
MDSCs	Myeloid-derived suppressor cells
MESV	murine embryonic stem cell virus
MFI	Median fluorescence intensity
MHC	Major histocompatibility complex
MLV	Mouse leukaemia virus
MPSV	Murine myeloproliferative sarcoma virus
N	Asparagine
NFAT	Nuclear factor of activated T cells
NF κ B	Nuclear factor of kappa light polypeptide gene enhancer in B cells
NK cell	Natural killer cell
P	Proline; phosphorylated
PB	Pacific blue
PBL	Peripheral blood lymphocyte(s)
PBMC	Peripheral blood mononuclear cell(s)
PBS	Phosphate buffered saline
PD-1	Programmed cell death protein-1
PE	Phycoerythrin
PE-Cy7	Phycoerythrin – Cyanine 7
PFA	Paraformaldehyde

PH domain	Pleckstrin homology domain
PI3K	Phosphatidylinositol-4-phosphate 3-kinase
PIP ₂	Phosphatidylinositol-3,4-bisphosphate
PIP ₃	Phosphatidylinositol-3,4,5-trisphosphate
PKC- θ	Protein kinase C-theta
PLC- γ	Phospholipase C-gamma
pMHC	Peptide MHC
Q	Glutamine
R	Arginine
RCC	Renal cell carcinoma
r.o.	retroorbitally
RPMI	Roswell Park Memorial Institute
RPS6	40S ribosomal protein S6
S	Serine
s.c.	subcutaneously
SEM	Standard error of the mean
SLP-76	SH2 domain-containing leukocyte protein of 76 kDa
Src kinase	Sarcoma kinase
SSC-A	Sideward scatter-area
T	Threonine
TAg	Simian virus large T antigen
TCR	T cell receptor
TGF- β	Transforming growth factor-beta
TIL(s)	Tumor infiltrating lymphocyte(s)
TNF- α	Tumor necrosis factor-alpha
U	Units
V region	Variable region
Y	Tyrosine
ZAP-70	CD3zeta associated protein of 70 kDa

10 REFERENCES

1. Ken Murphy PT, Mark Walport. 2008. *Janeway's Immunobiology*: Garland Science Taylor & Francis Group
2. Radoja S, Frey AB, Vukmanovic S. 2006. T-cell receptor signaling events triggering granule exocytosis. *Crit Rev Immunol* **26**: 265-90
3. Takata H, Naruto T, Takiguchi M. 2012. Functional heterogeneity of human effector CD8+ T cells. *Blood* **119**: 1390-8
4. Sulic S, Panic L, Barkic M, Mercep M, Uzelac M, et al. 2005. Inactivation of S6 ribosomal protein gene in T lymphocytes activates a p53-dependent checkpoint response. *Genes Dev* **19**: 3070-82
5. Boomer JS, Green JM. 2010. An enigmatic tail of CD28 signaling. *Cold Spring Harb Perspect Biol* **2**: a002436
6. Cheuk AT, Mufti GJ, Guinn BA. 2004. Role of 4-1BB:4-1BB ligand in cancer immunotherapy. *Cancer Gene Ther* **11**: 215-26
7. Dawicki W, Watts TH. 2004. Expression and function of 4-1BB during CD4 versus CD8 T cell responses in vivo. *Eur J Immunol* **34**: 743-51
8. Arch RH, Thompson CB. 1998. 4-1BB and Ox40 are members of a tumor necrosis factor (TNF)-nerve growth factor receptor subfamily that bind TNF receptor-associated factors and activate nuclear factor kappaB. *Mol Cell Biol* **18**: 558-65
9. Nam KO, Kang H, Shin SM, Cho KH, Kwon B, et al. 2005. Cross-linking of 4-1BB activates TCR-signaling pathways in CD8+ T lymphocytes. *J Immunol* **174**: 1898-905
10. Watts TH. 2005. TNF/TNFR family members in costimulation of T cell responses. *Annu Rev Immunol* **23**: 23-68
11. Dudley ME, Wunderlich JR, Shelton TE, Even J, Rosenberg SA. 2003. Generation of tumor-infiltrating lymphocyte cultures for use in adoptive transfer therapy for melanoma patients. *J Immunother* **26**: 332-42
12. Rosenberg SA, Yang JC, Sherry RM, Kammula US, Hughes MS, et al. 2011. Durable complete responses in heavily pretreated patients with metastatic melanoma using T-cell transfer immunotherapy. *Clin Cancer Res* **17**: 4550-7
13. Schwartzentruber DJ, Hom SS, Dadmarz R, White DE, Yannelli JR, et al. 1994. In vitro predictors of therapeutic response in melanoma patients

- receiving tumor-infiltrating lymphocytes and interleukin-2. *J Clin Oncol* **12**: 1475-83
14. Dudley ME, Yang JC, Sherry R, Hughes MS, Royal R, et al. 2008. Adoptive cell therapy for patients with metastatic melanoma: evaluation of intensive myeloablative chemoradiation preparative regimens. *J Clin Oncol* **26**: 5233-9
 15. Wu R, Forget MA, Chacon J, Bernatchez C, Haymaker C, et al. 2012. Adoptive T-cell therapy using autologous tumor-infiltrating lymphocytes for metastatic melanoma: current status and future outlook. *Cancer J* **18**: 160-75
 16. Rosenberg SA, Restifo NP. 2015. Adoptive cell transfer as personalized immunotherapy for human cancer. *Science* **348**: 62-8
 17. Morgan RA, Dudley ME, Wunderlich JR, Hughes MS, Yang JC, et al. 2006. Cancer regression in patients after transfer of genetically engineered lymphocytes. *Science* **314**: 126-9
 18. Dudley ME, Wunderlich JR, Yang JC, Sherry RM, Topalian SL, et al. 2005. Adoptive cell transfer therapy following non-myeloablative but lymphodepleting chemotherapy for the treatment of patients with refractory metastatic melanoma. *J Clin Oncol* **23**: 2346-57
 19. Vigano S, Utzschneider DT, Perreau M, Pantaleo G, Zehn D, et al. 2012. Functional avidity: a measure to predict the efficacy of effector T cells? *Clin Dev Immunol* **2012**: 153863
 20. Labrecque N, Whitfield LS, Obst R, Waltzinger C, Benoist C, et al. 2001. How much TCR does a T cell need? *Immunity* **15**: 71-82
 21. Johnson LA, Morgan RA, Dudley ME, Cassard L, Yang JC, et al. 2009. Gene therapy with human and mouse T-cell receptors mediates cancer regression and targets normal tissues expressing cognate antigen. *Blood* **114**: 535-46
 22. Zhong S, Malecek K, Johnson LA, Yu Z, Vega-Saenz de Miera E, et al. 2013. T-cell receptor affinity and avidity defines antitumor response and autoimmunity in T-cell immunotherapy. *Proc Natl Acad Sci U S A* **110**: 6973-8
 23. Jenkins MR, Tsun A, Stinchcombe JC, Griffiths GM. 2009. The strength of T cell receptor signal controls the polarization of cytotoxic machinery to the immunological synapse. *Immunity* **31**: 621-31
 24. McMahan RH, McWilliams JA, Jordan KR, Dow SW, Wilson DB, et al. 2006. Relating TCR-peptide-MHC affinity to immunogenicity for the design of tumor vaccines. *J Clin Invest* **116**: 2543-51
 25. Chinnasamy N, Wargo JA, Yu Z, Rao M, Frankel TL, et al. 2011. A TCR targeting the HLA-A*0201-restricted epitope of MAGE-A3 recognizes multiple

- epitopes of the MAGE-A antigen superfamily in several types of cancer. *J Immunol* **186**: 685-96
26. Morgan RA, Chinnasamy N, Abate-Daga D, Gros A, Robbins PF, et al. 2013. Cancer regression and neurological toxicity following anti-MAGE-A3 TCR gene therapy. *J Immunother* **36**: 133-51
 27. Linette GP, Stadtmauer EA, Maus MV, Rapoport AP, Levine BL, et al. 2013. Cardiovascular toxicity and titin cross-reactivity of affinity-enhanced T cells in myeloma and melanoma. *Blood* **122**: 863-71
 28. Shirasu N, Kuroki M. 2012. Functional design of chimeric T-cell antigen receptors for adoptive immunotherapy of cancer: architecture and outcomes. *Anticancer Res* **32**: 2377-83
 29. Cartellieri M, Bachmann M, Feldmann A, Bippes C, Stamova S, et al. 2010. Chimeric antigen receptor-engineered T cells for immunotherapy of cancer. *J Biomed Biotechnol* **2010**: 956304
 30. Hombach A, Hombach AA, Abken H. 2010. Adoptive immunotherapy with genetically engineered T cells: modification of the IgG1 Fc 'spacer' domain in the extracellular moiety of chimeric antigen receptors avoids 'off-target' activation and unintended initiation of an innate immune response. *Gene Ther* **17**: 1206-13
 31. Carpenito C, Milone MC, Hassan R, Simonet JC, Lakhai M, et al. 2009. Control of large, established tumor xenografts with genetically retargeted human T cells containing CD28 and CD137 domains. *Proc Natl Acad Sci U S A* **106**: 3360-5
 32. Milone MC, Fish JD, Carpenito C, Carroll RG, Binder GK, et al. 2009. Chimeric receptors containing CD137 signal transduction domains mediate enhanced survival of T cells and increased antileukemic efficacy in vivo. *Mol Ther* **17**: 1453-64
 33. Kochenderfer JN, Dudley ME, Feldman SA, Wilson WH, Spaner DE, et al. 2012. B-cell depletion and remissions of malignancy along with cytokine-associated toxicity in a clinical trial of anti-CD19 chimeric-antigen-receptor-transduced T cells. *Blood* **119**: 2709-20
 34. Maude SL, Frey N, Shaw PA, Aplenc R, Barrett DM, et al. 2014. Chimeric antigen receptor T cells for sustained remissions in leukemia. *N Engl J Med* **371**: 1507-17
 35. Morgan RA, Yang JC, Kitano M, Dudley ME, Laurencot CM, et al. 2010. Case report of a serious adverse event following the administration of T cells transduced with a chimeric antigen receptor recognizing ERBB2. *Mol Ther* **18**: 843-51

36. Lamers CH, Sleijfer S, van Steenbergen S, van Elzaker P, van Krimpen B, et al. 2013. Treatment of metastatic renal cell carcinoma with CAIX CAR-engineered T cells: clinical evaluation and management of on-target toxicity. *Mol Ther* **21**: 904-12
37. Kershaw MH, Westwood JA, Slaney CY, Darcy PK. 2014. Clinical application of genetically modified T cells in cancer therapy. *Clin Transl Immunology* **3**: e16
38. Gabrilovich DI, Nagaraj S. 2009. Myeloid-derived suppressor cells as regulators of the immune system. *Nat Rev Immunol* **9**: 162-74
39. Wherry EJ. 2011. T cell exhaustion. *Nat Immunol* **12**: 492-9
40. Pauken KE, Wherry EJ. 2015. Overcoming T cell exhaustion in infection and cancer. *Trends Immunol* **36**: 265-76
41. Baitsch L, Baumgaertner P, Devevre E, Raghav SK, Legat A, et al. 2011. Exhaustion of tumor-specific CD8(+) T cells in metastases from melanoma patients. *J Clin Invest* **121**: 2350-60
42. Wu K, Kryczek I, Chen L, Zou W, Welling TH. 2009. Kupffer cell suppression of CD8+ T cells in human hepatocellular carcinoma is mediated by B7-H1/programmed death-1 interactions. *Cancer Res* **69**: 8067-75
43. Topalian SL, Hodi FS, Brahmer JR, Gettinger SN, Smith DC, et al. 2012. Safety, activity, and immune correlates of anti-PD-1 antibody in cancer. *N Engl J Med* **366**: 2443-54
44. Schwartz RH. 2003. T cell anergy. *Annu Rev Immunol* **21**: 305-34
45. Greenwald RJ, Boussiotis VA, Lorschach RB, Abbas AK, Sharpe AH. 2001. CTLA-4 regulates induction of anergy in vivo. *Immunity* **14**: 145-55
46. Zheng Y, Zha Y, Gajewski TF. 2008. Molecular regulation of T-cell anergy. *EMBO Rep* **9**: 50-5
47. Zheng Y, Zha Y, Driessens G, Locke F, Gajewski TF. 2012. Transcriptional regulator early growth response gene 2 (Egr2) is required for T cell anergy in vitro and in vivo. *J Exp Med* **209**: 2157-63
48. Prinz PU, Mendler AN, Masouris I, Durner L, Oberneder R, et al. 2012. High DGK-alpha and disabled MAPK pathways cause dysfunction of human tumor-infiltrating CD8+ T cells that is reversible by pharmacologic intervention. *J Immunol* **188**: 5990-6000

49. Qin Z, Blankenstein T. 2000. CD4+ T cell--mediated tumor rejection involves inhibition of angiogenesis that is dependent on IFN gamma receptor expression by nonhematopoietic cells. *Immunity* **12**: 677-86
50. Briesemeister D, Sommermeyer D, Loddenkemper C, Loew R, Uckert W, et al. 2011. Tumor rejection by local interferon gamma induction in established tumors is associated with blood vessel destruction and necrosis. *Int J Cancer* **128**: 371-8
51. Mendler AN, Hu B, Prinz PU, Kreutz M, Gottfried E, et al. 2012. Tumor lactic acidosis suppresses CTL function by inhibition of p38 and JNK/c-Jun activation. *Int J Cancer* **131**: 633-40
52. Burkholder B, Huang RY, Burgess R, Luo S, Jones VS, et al. 2014. Tumor-induced perturbations of cytokines and immune cell networks. *Biochim Biophys Acta* **1845**: 182-201
53. Krummel MF, Heath WR, Allison J. 1999. Differential coupling of second signals for cytotoxicity and proliferation in CD8+ T cell effectors: amplification of the lytic potential by B7. *J Immunol* **163**: 2999-3006
54. Weng NP, Akbar AN, Goronzy J. 2009. CD28(-) T cells: their role in the age-associated decline of immune function. *Trends Immunol* **30**: 306-12
55. Chong H, Hutchinson G, Hart IR, Vile RG. 1996. Expression of co-stimulatory molecules by tumor cells decreases tumorigenicity but may also reduce systemic antitumor immunity. *Hum Gene Ther* **7**: 1771-9
56. Tirapu I, Huarte E, Guiducci C, Arina A, Zaratiegui M, et al. 2006. Low surface expression of B7-1 (CD80) is an immunoescape mechanism of colon carcinoma. *Cancer Res* **66**: 2442-50
57. Afreen S, Dermime S. 2014. The immunoinhibitory B7-H1 molecule as a potential target in cancer: killing many birds with one stone. *Hematol Oncol Stem Cell Ther* **7**: 1-17
58. Li J, Jie HB, Lei Y, Gildener-Leapman N, Trivedi S, et al. 2015. PD-1/SHP-2 inhibits Tc1/Th1 phenotypic responses and the activation of T cells in the tumor microenvironment. *Cancer Res* **75**: 508-18
59. Hurwitz AA, Cuss SM, Stagliano KE, Zhu Z. 2014. T cell avidity and tumor immunity: problems and solutions. *Cancer Microenviron* **7**: 1-9
60. Willimsky G, Blankenstein T. 2005. Sporadic immunogenic tumours avoid destruction by inducing T-cell tolerance. *Nature* **437**: 141-6

61. Willimsky G, Schmidt K, Loddenkemper C, Gellermann J, Blankenstein T. 2013. Virus-induced hepatocellular carcinomas cause antigen-specific local tolerance. *J Clin Invest* **123**: 1032-43
62. Prosser ME, Brown CE, Shami AF, Forman SJ, Jensen MC. 2012. Tumor PD-L1 co-stimulates primary human CD8(+) cytotoxic T cells modified to express a PD1:CD28 chimeric receptor. *Mol Immunol* **51**: 263-72
63. Ankri C, Shamalov K, Horovitz-Fried M, Mauer S, Cohen CJ. 2013. Human T cells engineered to express a programmed death 1/28 costimulatory retargeting molecule display enhanced antitumor activity. *J Immunol* **191**: 4121-9
64. Croft M. 2003. Costimulation of T cells by OX40, 4-1BB, and CD27. *Cytokine Growth Factor Rev* **14**: 265-73
65. Wilde S, Sommermeyer D, Frankenberger B, Schiemann M, Milosevic S, et al. 2009. Dendritic cells pulsed with RNA encoding allogeneic MHC and antigen induce T cells with superior antitumor activity and higher TCR functional avidity. *Blood* **114**: 2131-9
66. Suntharalingam G, Perry MR, Ward S, Brett SJ, Castello-Cortes A, et al. 2006. Cytokine storm in a phase 1 trial of the anti-CD28 monoclonal antibody TGN1412. *N Engl J Med* **355**: 1018-28
67. Dunn GP, Old LJ, Schreiber RD. 2004. The immunobiology of cancer immunosurveillance and immunoediting. *Immunity* **21**: 137-48
68. Koehler H, Kofler D, Hombach A, Abken H. 2007. CD28 costimulation overcomes transforming growth factor-beta-mediated repression of proliferation of redirected human CD4+ and CD8+ T cells in an antitumor cell attack. *Cancer Res* **67**: 2265-73
69. Uckert W, Becker C, Gladow M, Klein D, Kammertoens T, et al. 2000. Efficient gene transfer into primary human CD8+ T lymphocytes by MuLV-10A1 retrovirus pseudotype. *Hum Gene Ther* **11**: 1005-14
70. Okazaki T, Honjo T. 2007. PD-1 and PD-1 ligands: from discovery to clinical application. *Int Immunol* **19**: 813-24
71. Sica G, Chen L. 1999. Biochemical and immunological characteristics of 4-1BB (CD137) receptor and ligand and potential applications in cancer therapy. *Arch Immunol Ther Exp (Warsz)* **47**: 275-9
72. Boehm U, Klamp T, Groot M, Howard JC. 1997. Cellular responses to interferon-gamma. *Annu Rev Immunol* **15**: 749-95

73. Blohm U, Potthoff D, van der Kogel AJ, Pircher H. 2006. Solid tumors "melt" from the inside after successful CD8 T cell attack. *Eur J Immunol* **36**: 468-77
74. Itoh Y, Germain RN. 1997. Single cell analysis reveals regulated hierarchical T cell antigen receptor signaling thresholds and intraclonal heterogeneity for individual cytokine responses of CD4+ T cells. *J Exp Med* **186**: 757-66
75. Thomas RM, Gao L, Wells AD. 2005. Signals from CD28 induce stable epigenetic modification of the IL-2 promoter. *J Immunol* **174**: 4639-46
76. Thibodeau J, Bourgeois-Daigneault MC, Lapointe R. 2012. Targeting the MHC Class II antigen presentation pathway in cancer immunotherapy. *Oncoimmunology* **1**: 908-16
77. Huang H, Hao S, Li F, Ye Z, Yang J, et al. 2007. CD4+ Th1 cells promote CD8+ Tc1 cell survival, memory response, tumor localization and therapy by targeted delivery of interleukin 2 via acquired pMHC I complexes. *Immunology* **120**: 148-59
78. Salmond RJ, Emery J, Okkenhaug K, Zamoyska R. 2009. MAPK, phosphatidylinositol 3-kinase, and mammalian target of rapamycin pathways converge at the level of ribosomal protein S6 phosphorylation to control metabolic signaling in CD8 T cells. *J Immunol* **183**: 7388-97
79. Figlin RA, Thompson JA, Bukowski RM, Vogelzang NJ, Novick AC, et al. 1999. Multicenter, randomized, phase III trial of CD8(+) tumor-infiltrating lymphocytes in combination with recombinant interleukin-2 in metastatic renal cell carcinoma. *J Clin Oncol* **17**: 2521-9
80. Speiser DE, Kyburz D, Stubi U, Hengartner H, Zinkernagel RM. 1992. Discrepancy between in vitro measurable and in vivo virus neutralizing cytotoxic T cell reactivities. Low T cell receptor specificity and avidity sufficient for in vitro proliferation or cytotoxicity to peptide-coated target cells but not for in vivo protection. *J Immunol* **149**: 972-80
81. Alexander-Miller MA, Leggatt GR, Berzofsky JA. 1996. Selective expansion of high- or low-avidity cytotoxic T lymphocytes and efficacy for adoptive immunotherapy. *Proc Natl Acad Sci U S A* **93**: 4102-7
82. Lyman MA, Nugent CT, Marquardt KL, Biggs JA, Pamer EG, et al. 2005. The fate of low affinity tumor-specific CD8+ T cells in tumor-bearing mice. *J Immunol* **174**: 2563-72
83. Robbins PF, Li YF, El-Gamil M, Zhao Y, Wargo JA, et al. 2008. Single and dual amino acid substitutions in TCR CDRs can enhance antigen-specific T cell functions. *J Immunol* **180**: 6116-31

84. Aleksic M, Liddy N, Molloy PE, Pumphrey N, Vuidepot A, et al. 2012. Different affinity windows for virus and cancer-specific T-cell receptors: implications for therapeutic strategies. *Eur J Immunol* **42**: 3174-9
85. Johnsen AK, Templeton DJ, Sy M, Harding CV. 1999. Deficiency of transporter for antigen presentation (TAP) in tumor cells allows evasion of immune surveillance and increases tumorigenesis. *J Immunol* **163**: 4224-31
86. Igney FH, Krammer PH. 2002. Immune escape of tumors: apoptosis resistance and tumor counterattack. *J Leukoc Biol* **71**: 907-20
87. Xiao Z, Mescher MF, Jameson SC. 2007. Detuning CD8 T cells: down-regulation of CD8 expression, tetramer binding, and response during CTL activation. *J Exp Med* **204**: 2667-77
88. Yan J, Sabbaj S, Bansal A, Amatya N, Shacka JJ, et al. 2013. HIV-specific CD8+ T cells from elite controllers are primed for survival. *J Virol* **87**: 5170-81
89. Mackensen A, Meidenbauer N, Vogl S, Laumer M, Berger J, et al. 2006. Phase I study of adoptive T-cell therapy using antigen-specific CD8+ T cells for the treatment of patients with metastatic melanoma. *J Clin Oncol* **24**: 5060-9
90. Kalos M, June CH. 2013. Adoptive T cell transfer for cancer immunotherapy in the era of synthetic biology. *Immunity* **39**: 49-60
91. Ribatti D, Vacca A, Dammacco F. 1999. The role of the vascular phase in solid tumor growth: a historical review. *Neoplasia* **1**: 293-302
92. Kakarla S, Song XT, Gottschalk S. 2012. Cancer-associated fibroblasts as targets for immunotherapy. *Immunotherapy* **4**: 1129-38
93. Charo J, Perez C, Buschow C, Jukica A, Czeh M, et al. 2011. Visualizing the dynamic of adoptively transferred T cells during the rejection of large established tumors. *Eur J Immunol* **41**: 3187-97
94. Otahal P, Schell TD, Hutchinson SC, Knowles BB, Tevethia SS. 2006. Early immunization induces persistent tumor-infiltrating CD8+ T cells against an immunodominant epitope and promotes lifelong control of pancreatic tumor progression in SV40 tumor antigen transgenic mice. *J Immunol* **177**: 3089-99
95. Fu TM, Mylin LM, Schell TD, Bacik I, Russ G, et al. 1998. An endoplasmic reticulum-targeting signal sequence enhances the immunogenicity of an immunorecessive simian virus 40 large T antigen cytotoxic T-lymphocyte epitope. *J Virol* **72**: 1469-81

96. Engels B, Chervin AS, Sant AJ, Kranz DM, Schreiber H. 2012. Long-term persistence of CD4(+) but rapid disappearance of CD8(+) T cells expressing an MHC class I-restricted TCR of nanomolar affinity. *Mol Ther* **20**: 652-60
97. Budhu A, Wang XW. 2006. The role of cytokines in hepatocellular carcinoma. *J Leukoc Biol* **80**: 1197-213
98. de Lalla C, Galli G, Aldrighetti L, Romeo R, Mariani M, et al. 2004. Production of profibrotic cytokines by invariant NKT cells characterizes cirrhosis progression in chronic viral hepatitis. *J Immunol* **173**: 1417-25
99. Gu FM, Li QL, Gao Q, Jiang JH, Zhu K, et al. 2011. IL-17 induces AKT-dependent IL-6/JAK2/STAT3 activation and tumor progression in hepatocellular carcinoma. *Mol Cancer* **10**: 150
100. Cochaud S, Giustiniani J, Thomas C, Laprevotte E, Garbar C, et al. 2013. IL-17A is produced by breast cancer TILs and promotes chemoresistance and proliferation through ERK1/2. *Sci Rep* **3**: 3456
101. Mocellin S, Marincola FM, Young HA. 2005. Interleukin-10 and the immune response against cancer: a counterpoint. *J Leukoc Biol* **78**: 1043-51
102. Mumm JB, Emmerich J, Zhang X, Chan I, Wu L, et al. 2011. IL-10 elicits IFN γ -dependent tumor immune surveillance. *Cancer Cell* **20**: 781-96
103. Dulos J, Carven GJ, van Boxtel SJ, Evers S, Driessen-Engels LJ, et al. 2012. PD-1 blockade augments Th1 and Th17 and suppresses Th2 responses in peripheral blood from patients with prostate and advanced melanoma cancer. *J Immunother* **35**: 169-78
104. Yee C, Thompson JA, Byrd D, Riddell SR, Roche P, et al. 2002. Adoptive T cell therapy using antigen-specific CD8+ T cell clones for the treatment of patients with metastatic melanoma: in vivo persistence, migration, and antitumor effect of transferred T cells. *Proc Natl Acad Sci U S A* **99**: 16168-73
105. Ku CC, Murakami M, Sakamoto A, Kappler J, Marrack P. 2000. Control of homeostasis of CD8+ memory T cells by opposing cytokines. *Science* **288**: 675-8
106. Mestas J, Hughes CC. 2004. Of mice and not men: differences between mouse and human immunology. *J Immunol* **172**: 2731-8
107. Riley JL, June CH. 2005. The CD28 family: a T-cell rheostat for therapeutic control of T-cell activation. *Blood* **105**: 13-21
108. Chen DS, Mellman I. 2013. Oncology meets immunology: the cancer-immunity cycle. *Immunity* **39**: 1-10

ACKNOWLEDGEMENTS

I am thankful to everyone who supported me during my thesis.

First and foremost many thanks to my supervisor Prof. Dr. Elfriede Nößner. I owe her the opportunity to work on this exciting project. Her input and advice moved this project forward. I am also very thankful for her support during the writing of this thesis.

I wish to thank Prof. Dr. Dolores J. Schendel and Prof. Dr. Ralph Mocikat for the opportunity to work at the Institute of Molecular Immunology.

I am very thankful to my colleagues. Especially to Anna Brandl who has been a tremendous help. Thank you for your assistance.

I wish to thank Jan Schmollinger, Nadine Hömberg, Adam Slusarski as well as Michael Hagemann, Sabine Schlink and all members of the animal facility for their support during the in vivo experiments.

I send many thanks to Matthias Leisegang and Kordelia Hummel for their help and assistance as well as for making me feel very welcome during my research stays in Berlin.

I am thankful to Susanne Wilde for generating the TCRs T58 and D115 and allowing me to utilize them during my thesis. I send my thanks to Gerald Willimsky for the opportunity to test my construct in his mouse model.

My thanks go to all blood donors and patients.

So many thanks to Petra Prinz, Anna Mendler, Anna Brandl, Luis Olguin, Doro Brech, Ilias Masouris, Julia Schnappinger, Stephan Weisz, all Bachelor and Master students and all colleagues at the IMI not only for creating such a great, unique atmosphere at work but also for time we spent together after hours.

Thank you Julia for believing in me and for keeping me motivated.

I am so very thankful to my parents. Without your support, love and belief in me during the last 27 years I would not be where and who I am today.

CURRICULUM VITAE

PERSONAL DETAILS

Name: Ramona Schlenker
Date of birth: 11.02.1988
Nationality: German
E-Mail: ramonaschlenker@aol.com

DOCTORAL STUDIES

Sept 2011 – May 2015 Doctoral studies to obtain the degree Dr. rer. nat. at the Faculty of Medicine, Ludwig-Maximilians-University Munich carried out at the Helmholtz Center Munich, Institute of Molecular Immunology
Title: Chimeric co-stimulatory receptors as a strategy to improve the performance of T cells in the tumor environment

Sept 2012 – Jan 2015 Spokesperson of the PhD students' graduate programme of the SFB-TR36 (Principles and Applications of Adoptive T Cell Therapy)

EDUCATION

Sept 2009 – May 2011 Master of Science Biomedicine (grade: 1,1 (excellent))
Julius-Maximilians-University Würzburg, Germany
Master thesis: "Strategies to improve the functional response of effector T lymphocytes in the tumor milieu"

Oct 2006 – June 2009 Bachelor of Science Biomedicine (grade: 1,6 (very good))
Julius-Maximilians-University Würzburg, Germany
Bachelor thesis: "Expression of CD34+ progenitors on Notch-ligand expressing stromal cells"

Sept 1998 – May 2006 Gymnasium Fridericianum Rudolstadt, Germany (A level, grade:1,0 (excellent))

PUBLICATIONS

Noessner E, Brech D, Mendler AN, Masouris I, Schlenker R, Prinz PU. Intratumoral alterations of dendritic-cell differentiation and CD8(+) T-cell anergy are immune escape mechanisms of clear cell renal cell carcinoma. *Oncoimmunology* 2012, **1(8)**: 1451-1453.

Data of this thesis have been published and presented as follows:

Society for Immunotherapy of Cancer (SITC) Meeting 2014, poster presentation: “Turning tumor inhibition into activation: Engineering T cells with chimeric signaling receptors”

Tumor Immunology meets Oncology X Workshop, 2014, talk: “Turning tumor inhibition into activation: Engineering T cells with chimeric signaling receptors”

AFFIDAVIT

Schlenker, Ramona

I hereby declare that the submitted thesis, entitled

“Chimeric co-stimulatory receptors as a strategy to improve the performance of
T cells in the tumor environment
Turning PD-1-mediated inhibition into activation”

is my own work. I have only used the sources indicated and have not made unauthorized use of services of a third party. Where the work of others has been quoted or reproduced, the source is always given.

I further declare that the submitted thesis or parts thereof have not been presented as part of an examination degree to any other university.

Munich, 20.11.2015

Place, date

Signature doctoral candidate